Erosion processes and bed level maintenance strategies in the tide influenced branches of the Rhine-Meuse delta

T.C. Smits

Delft University of Technology

Faculty of Civil Engineering and Geosciences

Section Hydraulic Engineering

A thesis submitted for the degree of

Master of Science

December 2011

Graduation Committee

Prof. Dr. Ir. H.J. De Vriend
Delft University of Technology
Section Hydraulic Engineering

Dr. Ir. C.J. Sloff
Delft University of Technology
Section Hydraulic Engineering

Dr. Ir. E. Mosselman
Delft University of Technology
Section Hydraulic Engineering

Dr. G.J. Weltje
Delft University of Technology
Section Applied Geology

Photo on the title page: https://beeldbank.rws.nl, Rijkswaterstaat.

Abstract

Due to the closure of the Haringvliet in 1970 as part of the Delta works and the opening of the Beerdam in 1997, the course of the tidal flow in the Rhine-Meuse delta has changed. The tidal flow from and towards the Haringvliet is now completely taking place through the branches that connect the Haringvliet with the Nieuwe Maas and Nieuwe Waterweg. This causes these branches to erode by the increase of the tidal prism. The erosion problems occur in the central parts of the Rhine-Meuse delta, which, amongst other rivers, includes the rivers Spui, Oude Maas, Noord and Dordtsche Kil. The presence of sand, clay and peat layers in the branches causes the erosion mechanism to be rather complex. The alternation of sand and clay layers in the area causes the erosion to be non-uniformly distributed, resulting in deep local scour holes. The goal of this research is to determine an adequate maintenance strategy for the problem area. In order to do so the erosion processes are modelled in an existing Delft3D model.

In this study, the morphodynamics in a depth averaged model, covering the Dordtsche Kil and a part of the Oude Maas, are calibrated in such a way that it quantitatively fits the existing long term erosion trend and that the qualitative processes of scour in the model simulations comply with the erosion occurring in reality. This is achieved by implementing multiple sediment layers simulating a bed topography where clay layers and local sand packages alternate.

Subsequently modelling a variety of possible maintenance strategies has shown that several effective strategies are possible to deal with the erosion problems. Two strategies are suggested regarding the shortage of sediment in the system. The best way to deal with the local scour problems is to prevent further scouring of existing holes by fixation with riprap. Continuous nourishment in scour holes prevents the holes from scouring any further and moreover provides a solution for the long-term problem due to the fact that outflowing sediment diffuses and spreads out over the whole length of the river. A disadvantage of this strategy is the future obligation of continuous maintenance and monitoring for the whole Rhine-Meuse delta. The uncontrolled character of this stragey can also cause navigation nuisance.

The other type of maintenance strategies considered is the reduction of erosive flow in the system. A situation where the Haringvliet gates are always opened, even during high tide, leads to a remarkable reduction in erosion. The scour holes still undergo erosion, but at a slower rate, and the erosion of the clay layer decreases to a negligible amount. A combination

of fixing scour holes and opening the Haringvliet gates is also considered, which solves the problem for long-term erosion and the local scour, but comes at a high cost to implement. Besides in the Oude Maas, the erosion in the Spui branch is also alarmingly severe. In order to reduce erosion in this river branch, an option is to close it off. This causes the flow velocity in the Oude Maas to increase with approximately 10% and to reduce the flow velocity in the river Spui by half.

It is strongly recommended to investigate the effects and possibilities of opening the Haringvliet sluices further. Also, the model that has been used now is a depth averaged model (2DH) and cannot capture all the effects that occur. Research with a 3D model could help to understand local scour problems better for possible similar situations in the future. Further research should also be done with the extension of the Delft3D model to the Spui river, the downstream part of the Oude Maas and the Noord. Since the numerical model can become (even more) extensive with the implementations of 3 more domains, much more insight in the problems can be obtained with the interaction of the different eroding branches in a Delft3D model.

Preface

This document constitutes the final thesis report to accomplish the Master of Science degree in Hydraulic Engineering at Delft University of Technology, Faculty of Civil Engineering and Geosciences. The subject of this graduation work is the erosion processes and maintenance strategies in the tide influenced branches of the Rhine-Meuse delta. The study was carried out at Deltares under the supervision of Kees Sloff and Erik Mosselman.

I would like to acknowledge all the people who made my graduation and study possible.

First of all I would like to thank my thesis committee for their support, interest and enthousiasm from the beginning to the very end of my graduation work. I thank Erik Mosselman and Kees Sloff for their daily supervision and openness to questions and a helping hand. I furthermore would like to thank Huib de Vriend and Gert Jan Weltje for their valuable input during meetings. I would like to thank Deltares for providing me with a workplace and all other necessary support in order to make this graduation successful. I also thank Rijkswaterstaat for their interest in my work, in particular Arie van Gelder, Ary van Spijk and Arie Broekhuizen for their enthusiasm and feedback.

Secondly, I'd like to thank my fellow students at Deltares, who made the working environment a very pleasant one. The nice atmosphere during lunches, coffee breaks and graduation drinks have helped to make this graduation a great period to look back on. I would especially like to thank ir. Frank Melman and ir. Sander Post with whom I spent a lot of time studying and having fun, from the last year of the bachelor program up till our joint time at Deltares. I would also like to thank all other fellow students with whom I have worked together pleasantly for the last six years.

Last but not least, I would like to thank my family and friends for all their support during my study. I thank my parents for their support, both financially and morally, and their infinite interest in my study. On the same note I would also like to thank my brother and friends their encouragement. A special word of thanks goes out to Alina Blasquez, who has been very interested and supportive from the beginning until the end of this graduation work.

Tom Smits,
Delft, December 2011

Contents

List of Figures and Tables **xi**

List of Symbols **xv**

1 Introduction **1**

1.1 Problem definition 1

1.2 The Rhine-Meuse delta 1

1.3 Erosion processes 3

1.4 Objectives 4

1.5 Outline 5

2 Approach **7**

2.1 The numerical model 7

2.2 Model calibration 7

2.3 Modelling maintenance strategies 8

3 Numerical model setup **9**

3.1 Introduction 9

3.2 Model approach 9

3.2.1 SOBEK model 9

3.2.2 Delft3D Model 11

3.3 Hydrodynamics 13

3.3.1 General equations 13

3.3.2 Computational stability 13

3.3.3 Roughness 15

3.3.4 Boundary conditions 15

3.4 Morphology 16

3.4.1 Introduction 16

3.4.2 Sediment distribution 16

3.4.3 Sediment layers 17

3.4.4 Fixed layers 19

4 Model calibration **21**
4.1 Introduction . . . 21
4.2 Sediment transport . . . 21
4.2.1 Cohesive sediment transport . . . 21
4.2.2 Non-cohesive sediment transport . . . 22
4.2.3 Choice of formula . . . 24
4.3 Scour holes . . . 26
4.3.1 Introduction . . . 26
4.3.2 Transverse bed slope effects . . . 26
4.3.3 Effects of varying bed slope parameters . . . 27
4.4 Effect of higher and lower discharges . . . 28
4.4.1 Introduction . . . 28
4.4.2 High and low discharges . . . 28
4.4.3 Effects of sea level rise . . . 31
4.4.4 Effects of an extreme flood wave . . . 33
4.5 Conclusion . . . 34

5 Maintenance strategies **37**
5.1 Introduction: Haringvliet sluices 'ajar' . . . 37
5.2 Important findings in the calibrated model . . . 37
5.3 Strategies for shortage of sediment . . . 37
5.3.1 Filling erosion holes with sand . . . 37
5.3.2 Fixed scour holes . . . 40
5.3.3 Dredging and dumping strategically . . . 40
5.4 Strategies to reduce erosive flow . . . 45
5.4.1 Open the Haringvliet sluice gates . . . 45
5.4.2 Fixed scour holes and opened Haringvliet sluice gates . . . 46
5.4.3 Closing of the Spui branch . . . 47
5.5 Economic consideration . . . 48
5.6 Influence of sea level rise . . . 50
5.7 Conclusions . . . 52

6 Discussion **55**

7 Conclusions and Recommendations **59**
7.1 Conclusions . . . 59
7.2 Recommendations . . . 61

References **63**

Appendix **65**

A Sediment data **65**

A.1 Start-up 65

A.2 Sediment distribution 66

A.3 Bed level development 67

B Boundary conditions **69**

B.1 Upstream boundaries 69

B.2 Downstream boundaries for varying discharges 70

B.3 Downstream boundaries for different measures 72

C Delft3D Schematizations **73**

C.1 Flow computations 73

C.1.1 Introduction 73

C.1.2 Equations 73

C.1.3 Numerical aspects 74

C.1.4 Grid 74

C.1.5 Domain and boundaries 76

C.2 Morphology 76

C.2.1 Sediment fractions 76

C.2.2 Sedimentation and erosion 77

C.2.3 Sediment transport formulas 78

C.2.4 Morphological time scale factor 80

D SOBEK **83**

D.1 SOBEK-RE 83

D.2 Domain 84

D.3 Boundaries 85

D.4 Structures 86

List of Figures and Tables

Figures

1.1 The Rhine-Meuse delta (Sloff et al., 2001) 2
1.2 Erosion process 3

3.1 Domain of the Sobek model and the area corresponding to the Delft3D model 10
3.2 Observed data and schematised discharge distribution. 11
3.3 The five domains of the Delft3D model. 12
3.4 A part of the numerical grid. 14
3.5 Sediment distribution in the Oude Maas. 17
3.6 Implementation of bed level data into the model for the Oude Maas. 18
3.7 Implementation of bed level data into the model for the Dordtsche Kil. 18

4.1 Maximum shear stress over the river (top) and time series of shear stress on an arbitrary location in the river (bottom). 22
4.2 Modelled erosion rate of the Oude Maas compared to the measured rate for 3 $\cdot 10^{-6}$ kg/(m^2·s) 22
4.3 Classification of sediment transport (Jansen et al, 1994). 23
4.4 Cumulative erosion (-) and sedimentation (+) for Van Rijn 2007 (left) and Van Rijn 1993 (right). 24
4.5 Cumulative erosion (-) and sedimentation (+) for Engelund Hansen (top) and Van Rijn 1993 (bottom). 25
4.6 Scour hole near the junction of the Oude Maas and the Dordtsche Kil. 28
4.7 Four year development of the scour hole for different parameters. 28
4.8 Cumulative erosion (-) and sedimentation (+) in the Oude Maas under low (top), average (centre) and high (bottom) discharge conditions. 29
4.9 Cumulative erosion (-) and sedimentation (+) in the Dordtsche Kil under low (left), average (centre) and high (right) discharge conditions. 30
4.10 Flow velocity (top), sediment transport (centre) and cumulative sediment transport (bottom) in the Dordtsche Kil under low, average and high discharge conditions. 31
4.11 Cumulative erosion (-) and sedimentation (+) in the Dordtsche Kil for the case with one metre sea level rise (left) and the average case and (right). 32

4.12 The biggest difference between normal situation (top) and the situation with sea level rise (bottom) is the larger scour hole in the situation with sea level rise. 32
4.13 Flow velocity, sediment transport and cumulative sediment transport in the Dordtsche Kil for the average case and the case with one metre sea level rise. 33
4.14 Scour hole development in case of an extreme flood wave. 34
4.15 Cumulative sedimentation and erosion (m) in the Oude Maas. 35
4.16 Cumulative sedimentation (+) and erosion (-) for the Dordtsche Kil before (left) and after (right) implementing multiple sediment layers. 36

5.1 Depths larger than 14 m below NAP. 38
5.2 Initial nourishment, and the migration after 1, 2 and 3 years. 39
5.3 Erosion and sedimentation pattern for the situation where every breach in the clay layer is covered with riprap. 41
5.4 The 4 year simulation of continuously nourishing 250.000 m^3 of sediment. . . 42
5.5 Initially dumped sediment and the migration after 1, 2 and 3 years for continuous nourishing. 42
5.6 The results after a 4 year simulation of yearly nourishing in the Oude Maas up to 14 m below NAP. 43
5.7 Initially dumped sediment and the migration after 1, 2 and 3 years for yearly nourishing up to 14 m below NAP. 44
5.8 Comparison of the erosion and sedimentation for the situation when the Haringvliet gates are open (top) and the current situation (bottom). 45
5.9 Comparison of the erosion and sedimentation for the situation when the Haringvliet gates are open, without fixating the scour holes (top) and with fixed scour holes (bottom) 46
5.10 Comparison of the erosion and sedimentation for the situation when the river Spui is closed off (top) and the current situation (bottom). 47
5.11 The impact on flow velocities due to the closure of the river Spui from the North side. 48
5.12 Cumulative sedimentation and erosion pattern in the Oude Maas in the situation where the Haringvliet gates are open, under the condition of a normal sea level (top) and 1 metre sea level rise (bottom). 50
5.13 Cumulative sedimentation and erosion pattern in the Dordtsche Kil in the situation where the Haringvliet gates are open, under the condition of a normal sea level (left) and 1 metre sea level rise (right). 51

A.1 Distribution of sediment fractions for the single mixed layer morphodynamic model. 65
A.2 Sediment distribution in the Dordsche Kil along the river axis. 66
A.3 Sediment distribution in the Dordsche Kil along the river axis. 66
A.4 Bed level development on the river axis of the Oude Maas from 2006-2009. . 67

B.1 Upstream boundary for the extreme situation, high discharge, average discharge and low discharge. 69
B.2 Downstream boundary for the high discharge, average discharge and low discharge. 70
B.3 Downstream boundary for the extreme situation and the average situation. . 71
B.4 Change in downstream boundary due to 1 meter sea level rise. 71
B.5 Boundary conditions for opened Haringvliet gates. 72
B.6 Boundary conditions for a closed off Spui rive.r 72

C.1 Staggered grid with computational control volume. 75
C.2 Grid cell in the staggered grid. 75
C.3 Grid with grid enclosure and boundary location. 75
C.4 Selection of the reference (kmx)layer (left) and schematic arrangement of flux bottom boundary condition (right). 77
C.5 Schematic representation of the implementation of the morphological factor in the Delft3D flow computations. 81

D.1 Domain of the Rhine-Meuse delta SOBEK model. 84
D.2 Upstream discharges in the SOBEK model for the low, average and high discharge scenario. 85
D.3 Upstream discharges in the SOBEK model for the Haringvliet and the Nieuwe Waterweg boundary. 85

Tables

1.1 Riverbed development 1990-2000 3

3.1 Averaged discharge bins 10
3.2 Description of the domains in the numerical model 12

4.1 Different sets of parameters corresponding to equation 4.9 27

5.1 Amount of sediment needed for a once-per-year nourishment 43

List of Symbols

Symbol Description [SI-unit]

a	Van Rijn's reference height [m]
A	Cross-sectional area of flow [m^2]
A	Tuning parameter in the simplified Van Rijn alluvial roughness formulation [-]
A_{sh}	Tuning parameter for transverse bedslope effects [-]
b	Degree of nonlinearity of sediment transport model [-]
B	Tuning parameter in the simplified Van Rijn alluvial roughness formulation [-]
B_{sh}	Tuning parameter for transverse bedslope effects [-]
c	Celerity [m/s]
c_a	Sediment concentration at reference level [-]
c_b	Average sediment concentration in the near bottom computational layer [-]
C	Chézy Coefficient [$m^{1/2}$/s]
C_{sh}	Tuning parameter for transverse bedslope effects [-]
D	Deposition flux [kg/(m^2· s)]
D^*	Dimensionless particle size [m]
D_{50}	Median particle size [m]
D_{90}	Particle size such that 90% is smaller [m]
D_i	Mean particle size of sediment fraction i [m]
D_m	Median particle size [m]
D_{sh}	Tuning parameter for transverse bedslope effects [-]
$DPSED$	Depth of sediment available at the bed [m]
E	Erosion flux [kg/(m^2· s)]
f'_c	Grain friction coefficient due to current [-]
f_{FIXFAC}	Upwind fixed layer proximity factor [-]
f_{silt}	Silt factor [-]
$f(\theta)$	Dimensionless function for bed slope effects [-]
F	Integration factor [-]
g	Gravitational acceleration [m/s^2]
h	Water depth [m]
k	White Colebrook parameter [m]
k_s	Bed form height [m]
L	Sediment migration distance [m]
M	User defined erosion parameter [kg/(m^2· s)]
M_e	Mobility parameter [-]
p_{mud}	Fraction of mud [-]
q_s	Sediment transport per unit with [m^2/s]
Q	Discharge [m^3/s]
R	Hydraulic radius [m]
S	Total transport [m^3/s]
S_b	Bed load transport [m^3/s]
S_b^*	Bed load transport [m^3/s]

S_d	Deposition function [-]
S_e	Erosion function [-]
S_s	Suspended load transport [m^3/s]
t	Time [s]
T	Dimensionless bed shear parameter [-]
$THRESH$	User-defined erosion threshold [m]
u	Flow velocity [m/s]
U	Depth-averaged velocity in x-direction [m/s]
$\overline{U}$	Mean cross-sectional flow velocity [m/s]
U_*	Shear velocity [m/s]
U_{cr}	Critical flow velocity [m/s]
U_δ	Instantaneous current velocity [m/s]
V	Depth-averaged velocity in y-direction [m/s]
w_s	Fall velocity [m/s]
x	Horizontal co-ordinate [m]
y	Horizontal co-ordinate [m]
z_b	Bed level [m]

α	Correction coefficient for non-uniform flow [-]
γ	Calibration coefficient [-]
δ	Thickness of the viscous sublayer [m]
Δ	Relative density of the bed material [-]
Δt	Computational time step [s]
Δx	Computational spacial step [m]
Δy	Computational spacial step [m]
ϵ_p	Porosity of the bed material [-]
η	Calibration exponent [-]
θ	Shields parameter [-]
ν	Kinematic viscosity of the water [m^2/s]
ρ_s	Density of bed material [kg/m^3]
τ_b'	Effective bed-shear stress [N/m^2]
$\tau_{b,cr}$	Critical bed shear stress [N/m^2]
τ_{cw}	Maximum bed shear stress [N/m^2]
$\tau_{cw,d}$	User defined critical erosion shear stress [N/m^2]
$\tau_{cw,e}$	User defined critical deposition shear stress [N/m^2]
ϕ_S	Original direction of sediment transport [-]
ϕ_T	Final direction of sediment transport [-]

1 Introduction

1.1 Problem definition

The Rhine-Meuse delta has been eroding heavily since 1970, mainly caused by the increase in tidal flow in the area. Moreover, the alternation of sand and clay layers in the area causes the erosion to be non-uniformly distributed. This results in deep local scour holes. It is important to investigate where and when these scour holes can occur, and which processes occur during this development. The development of the scour holes in time and space, and the influence of a deep scour hole on the flow and local sediment transport in the river are also of importance. It is necessary to understand the degree of stability of the fixed layers and the influence of the scour holes on the stability. It is also interesting to investigate what happens when the sea level rises. A higher sea level causes the flow profile of the branches to increase, which could accelerate the erosion in the branches. The rather complex and alarming development of these scour holes demands a long term strategy for the large scale erosion problems in the area, caused by the increase in tidal flow. This strategy should be separated from the procedure for the stabilisation of existing local scour holes.

1.2 The Rhine-Meuse delta

The Rhine-Meuse delta (Rijn-Maasmonding) has been a much-discussed area for a long time in Dutch history, especially in the 20^{th} century. The first thing that comes to mind is of course the disastrous North Sea flood of 1953, but already before this flood the insufficient height of the existing dikes in the South-West of the Netherlands was a known problem. After the planning and construction of the Delta works, the Rhine-Meuse delta was also the first system of rivers subjected to hydraulic computations using the analog computer Deltar, based on the publication 'Electrische nabootsing der getijden' (Electrical simulation of tides) by Johan van Veen[1] (1946). The design for this computer was based on his research on the analogy between water and electricity.

Over the last 50 years the Rhine-Meuse delta, especially its western part, is more and more characterised by busy shipping traffic and surrounded by industry. Due to the important shipping routes, this sedimentation area by nature is regulated by dredging activities. Now, due to the closure of the Haringvliet in 1970 as part of the Delta works and the opening of the Beerdam in 1997, the course of the tidal flow in the Rhine-Meuse delta has changed. The tidal flow from and towards the Haringvliet is now completely occuring through the branches

[1] Johan van Veen was also the first person warning about the risks of a flood in several publications since 1937. Under the pseudonym 'Dr. Cassandra' he was able to create awareness about politically sensitive issues. The plan of blocking the estuary mouths in January of 1953 however, came too late, just several days before the major flood. In 1962, he revealed the true identity of Dr. Cassandra.

that connect the Haringvliet with the Nieuwe Maas and Nieuwe Waterweg. This causes these branches to erode by the increase of the tidal prism. This tendency to erode is not likely to change in the future, since the tidal prism will only increase by the increase of the cross sections of the branches. Moreover, due to alternating fixed layers and easily erodible parts in the riverbeds, the erosion of the branches is not uniformly distributed over the river. The erosion of the easily erodible layers causes deep local scour holes. It is this strong local erosion that endangers the stability of banks and structures most.

The erosion problems occur in the central parts of the Rhine-Meuse delta, which includes the rivers Spui, Oude Maas, Noord and Dordtsche Kil. Figure 1.1 shows the geography of the area of interest, taken from the earlier research on Spui, Oude Maas and Noord (Sloff et al., 2011). The area is characterised by a significant influence of tidal flow and subsoil with layers of peat and clay. The sections that follow elaborate on the important characteristics of the different branches in this area.

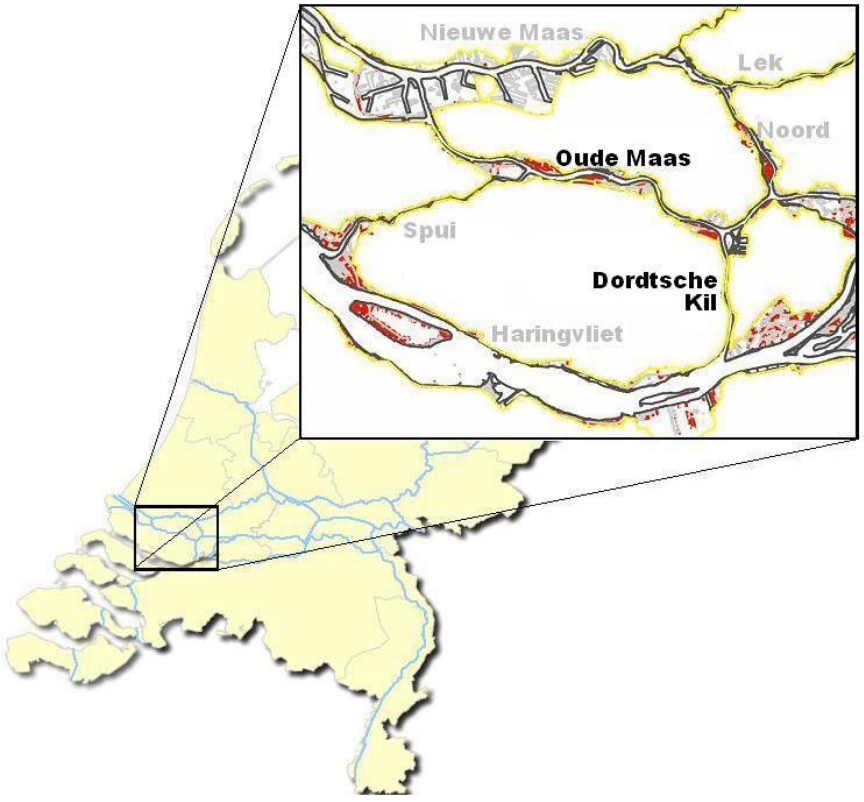

Figure 1.1: The Rhine-Meuse delta (Sloff et al., 2001)

1.3 Erosion processes

In order to gain insight in the future development of the riverbeds, it is useful to analyse the historical development of the riverbeds from bed measurements. Table 1.1 shows the developments for the Noord, Spui and Oude Maas in the years 1990 through 2000 (Snippen et al., 2005). These results clearly show that the riverbeds have eroded rapidly (2-8 cm/year) in this period. The study on Spui, Oude Maas and Noord (Sloff et al., 2011) also describes the morphological changes of the branches for a more recent period in more detail. These data can also be used as a start-up for this research.

Table 1.1: Riverbed development 1990-2000: negative values indicate erosion, positive values indicate sedimentation (Snippen et al., 2005)

Branch	**Load [cm/y]**	**Dredging [cm/y]**	**Mud [cm/y]**	**Sand [cm/y]**
Noord	-2.9	-1.2	-3.4	1.7
Oude Maas East (km 976-980)	0.0	-2.3	-3.7	6.0
Oude Maas Middle (km 981-995)	-4.5	-0.4	-3.3	-0.8
Oude Maas West (km 995-1006)	-8.2	-0.1	-7.9	-0.2
Spui	-1.8	0.0	-1.5	-0.3
Dordtsche Kil	-6.2	-2.1	1.8	-6.0

The presence of sand, clay and peat layers in the branches causes the erosion mechanism to be rather complex. It is this strong local erosion that endangers the stability of banks, structures and storm surge barriers. Clay and peat layers erode at a much smaller rate than sand layers. At locations where parts of sand layers are exposed, there will be strong local erosion that causes deep scour holes, which endanger the stability of banks, structures and storm surge barriers. This interaction between sand and clay is shown in figure 1.2.

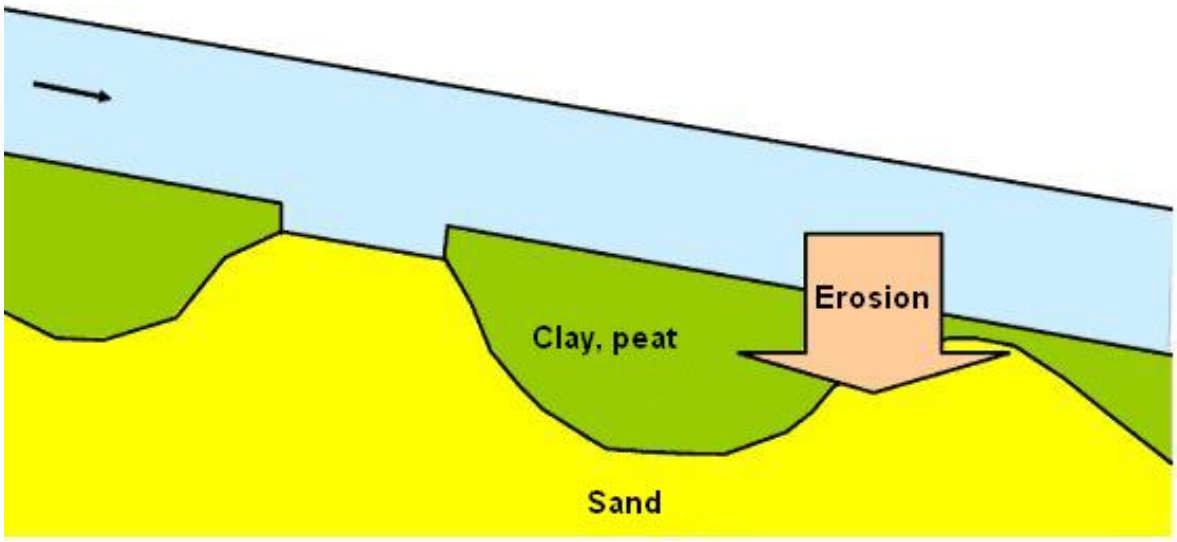

Figure 1.2: Erosion process

Not only have sand and clay different erodibilities, they also erode according to different mechanisms. Sand erodes by the pick-up of grains from the bed, governed by the relation between particle size and critical Shields value. The latter boils down to a critical shear stress value τ in a range of approximately $0.15 - 0.30$ N/m^2. Clay can erode in two different ways:

- The gradual erosion of the clay layer surface on particle level
- Erosion by sliding or tearing loose of lumps of clay near a forming scour hole

The gradual erosion of the clay layer surface has a critical shear stress of the fairly soft consolidated clay layers that is considered equal to 1.8 N/m^2, whereas the deeper hard consolidated layers have a much higher critical shear stress up to 15.8 N/m^2 (Sloff et al., 2011).

1.4 Objectives

The ultimate goal in this research is:

To determine an adequate maintenance strategy for the problem area, including a solution for both the long-term erosion and the strong local erosion that causes the deep scour scour holes.

There will be several preliminary targets to be met on the way.

- Create a multi-layered model to capture the effects of sediment erosion between and under clay layers and determine whether a 2DH model with multiple sediment layers if sufficient for investigating local scour, more specifically regarding a bed topography where clay layers and local sand packages alternate.
- Calibrate the morphodynamics in an available Delft3D model in such a way that the erosion in the Oude Maas is of the right order of magnitude. With this model, which covers the area of interest, the morphodynamic behaviour can be simulated in order to gain insight into the processes at hand.
- Investigate and possibly optimise the behaviour of the model around scour holes using this multi-layered model. It is unknown how well Delft3D can capture the whole process of scour, since this Delft3D model is not able to model all the occurring processes.
- Define and subsequently model suitable maintenance strategies for the project area in the Delft3D model.

1.5 Outline

After this introduction chapter including the necessary background information and goals of this study, chapter 2 treats the approach of this study. Chapter 3 elaborates on the existing numerical model of the area of interest, and the setup of the numerical model in this study. Chapter 4 continues with the fine-tuning of the model to the particular problem and the behaviour of the model under different upstream and downstream boundary conditions, whereas in chapter 5 the possible maintenance strategies are investigated using the calibrated numerical mode. The report ends with the discussion (chapter 6) and the conclusions and recommendations (chapter 7).

2 Approach

2.1 The numerical model

The first part of this study is to reproduce the processes that occur in the area of interest. The bed characteristics in the area should be implemented in the model using available data. Hereto, it is also important to specify the layered bed structure, since this is of key importance for this particular problem. In this research, a Delft3D model of a part of the area of interest (which is described in chapter 3) is used in order to simulate the important processes that are present in the area. The Delft3D model was previously used in a study by Giri (2010) for a morphological analysis of the Dordtsche Kil. In this study, low, medium and high flows with a tidal boundary were computed using a SOBEK model (Linden and Van Zetten, 2001) for the hydrodynamic simulation. Based on SOBEK simulation results and observations, the boundary conditions for Delft3D were deduced.

2.2 Model calibration

After this has been modelled satisfactorily, the transport of sediment should be optimised. A different transport formula can result in a different sedimentation/erosion-pattern. It is necessary to find the transport formulation that fits this specific problem best. Giri (2010) used the transport formula of Van Rijn (2007a,b), but the model should be tested for other transport formulas, like the Engelund Hansen formula, as well. After that, there will be a focus on the local scour holes, to investigate if it is possible to simulate the behaviour of sediment transport and flow around the scour holes accurately. Finally, the model is tested for different scenarios, i.e. different flow conditions. For these different conditions, the SOBEK model is used to compute the boundary conditions for the Delft3D model. Besides the average flow conditions, situations with high and low upstream discharges will be computed, as well as a situation with a high downstream water level boundary, to simulate the effects of sea level rise.

2.3 Modelling maintenance strategies

After a satisfactory simulation of the relevant processes, quantification in time and space of the occurring erosion problems should be possible, after which an adequate maintenance strategy can be formulated. Possible measures are the dredging and dumping of sediment to restore the eroding parts of the river system and stabilizing the scour holes and unstable banks that come into existence. But more preferable are proactive measures, such as nourishment of sediment to prevent the formation of scour holes, changing the line of flow in the river system or a different management of the Haringvliet gates in order to change the tidal flow in the Rijn-Maas delta. These proactive measurements are also simulated in the Delft3D model in order to gain insight into the effect of the different measures.

3 Numerical model setup

3.1 Introduction

This research consists of simulating the important processes that are present in the area, and subsequently determining an adequate maintenance strategy for the area. The processes are simulated with an existing numerical model. The approach to this model is described in the next section, after which the hydrodynamics are described in section 3.3. The model also needs to be adjusted in a sense that the morphology in the model had not been calibrated yet. Section 3.4 describes how multiple sediment fractions for clay and sand are implemented in this model to schematise the problem at hand.

3.2 Model approach

Almost all the computations in this study have been made using an available Delft3D model for the area of interest. However, in order to make use of this model, preliminary hydrodynamic calculations have been carried out using a much larger one-dimensional SOBEK model. In this way, the downstream boundary conditions in the Delft3D model can be extracted from the 1D model using the water level at the corresponding locations.

3.2.1 SOBEK model

Giri (2010) computed low, medium and high flows with a tidal boundary were computed using a SOBEK model for the hydrodynamic simulation. Based on SOBEK simulation results and observations, the boundary conditions for Delft3D can be deduced. Following time-series boundary conditions were extracted from the SOBEK model and measurement station records:

- Upstream boundary at Boven Merwede: Observed discharge at Tiel.
- Downstream boundary at North branch (in Oude Maas)
- Downstream boundary at South branch (in Hollandse Diep)
- Downstream boundary at Noord River entrance [2]
- Discharge extraction/insertion from/into Nieuwe Merwede near the confluence with Amer River

[2]Three options were used in the study by Giri (2010), namely discharge boundary, water level boundary and discharge extraction/insertion. A water level boundary proved to be the most accurate. All data were deduced from the SOBEK simulation results.

3. NUMERICAL MODEL SETUP

The SOBEK simulations were made for a range of constant upstream discharges (at Tiel, Lith and Hagestein). The range of constant discharges for each upstream boundary was deduced from observed data during 1997−2009. For this purpose, Giri sorted all collected observed data of the upstream boundary 'Tiel' and averaged them for four different ranges, illustrated in table 3.1.

Table 3.1: Averaged discharge bins

Range	Average
900 - 1100 m^3/s	998 m^3/s
1500 - 1700 m^3/s	1590 m^3/s
3800 - 4200 m^3/s	3980 m^3/s
4500 - 5500 m^3/s	4897 m^3/s

These discharges at Tiel in the SOBEK model are used as the upstream discharges at the Boven Merwede in the first domain of the Delft3D model. Giri (2010) used only the top three average discharges from table 3.1 were used to schematise the observed discharge. This is illustrated in figure 3.2. From the SOBEK calculations, boundary conditions are derived for the downstream locations in the Delft3D model. Figure 3.1 shows the full domain of the SOBEK model, with its downstream boundary all the way down at the North sea, and the location of the Delft3D downstream boundaries in the SOBEK model.

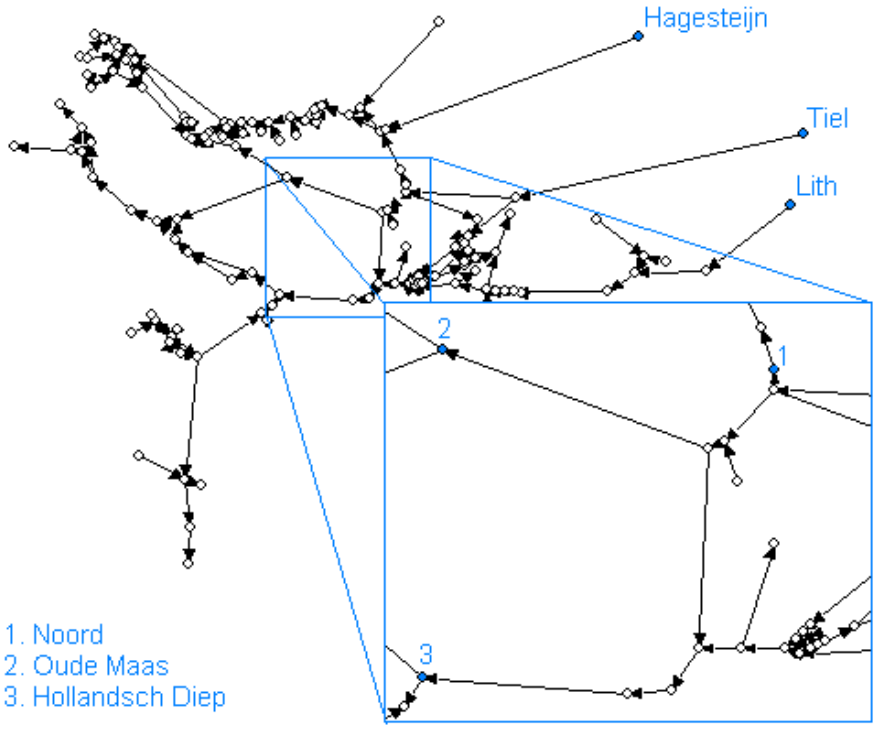

Figure 3.1: Domain of the Sobek model and the area corresponding to the Delft3D model

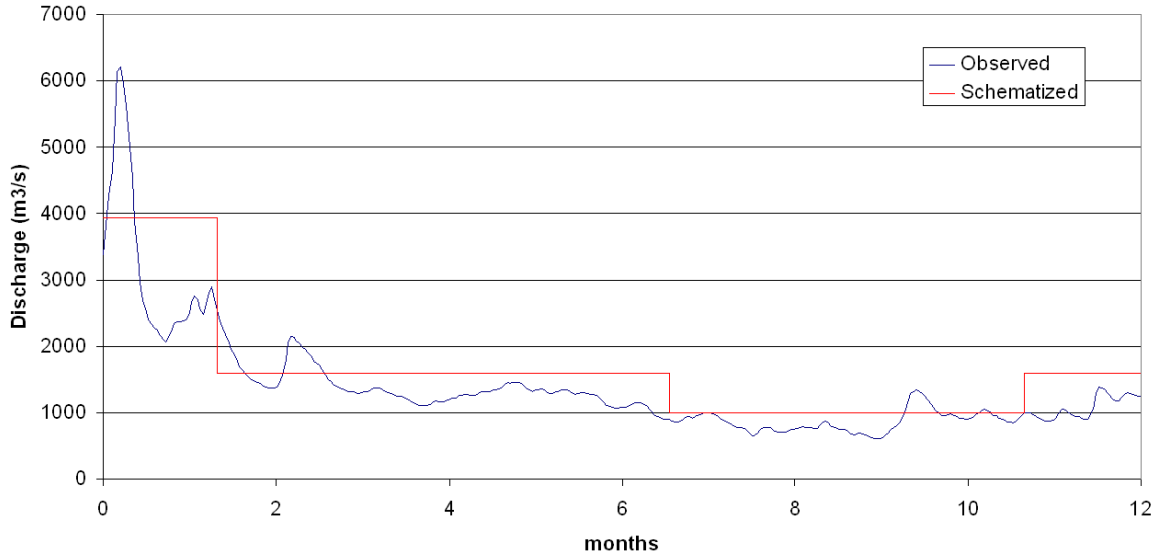

Figure 3.2: Observed data and schematised discharge distribution.

The Sobek model is used to create boundary conditions for all the different situations in this model. Appendix B contains an overview of the different boundary conditions, whereas appendix D describes the SOBEK model in greater detail.

3.2.2 Delft3D Model

For a part of the area of interest, an existing Delft3D model is available. The Delft3D model was previously used in a study by Giri (2010) for a morphological analysis of the Dordtsche Kil. In this study, the hydrodynamic performance of the new model was satisfactory, but for the branches other than the Dordtsche Kil, the morphodynamic behaviour of the model had not been calibrated yet.

The Delft3D model in the study by Giri (2010) has been decomposed into 5 different domains. Domain decomposition is a technique in which a model is divided into several smaller models. Domain decomposition allows local grid refinement, without the necessity of refining the whole model. This allows accurate modelling without excessive computation times. Another advantage of domain decomposition is the model flexibility, on which more is elaborated in appendix C. The complete model consists of three domains of the Merwede branches and newly connected fourth and fifth domains (figure 3.3).

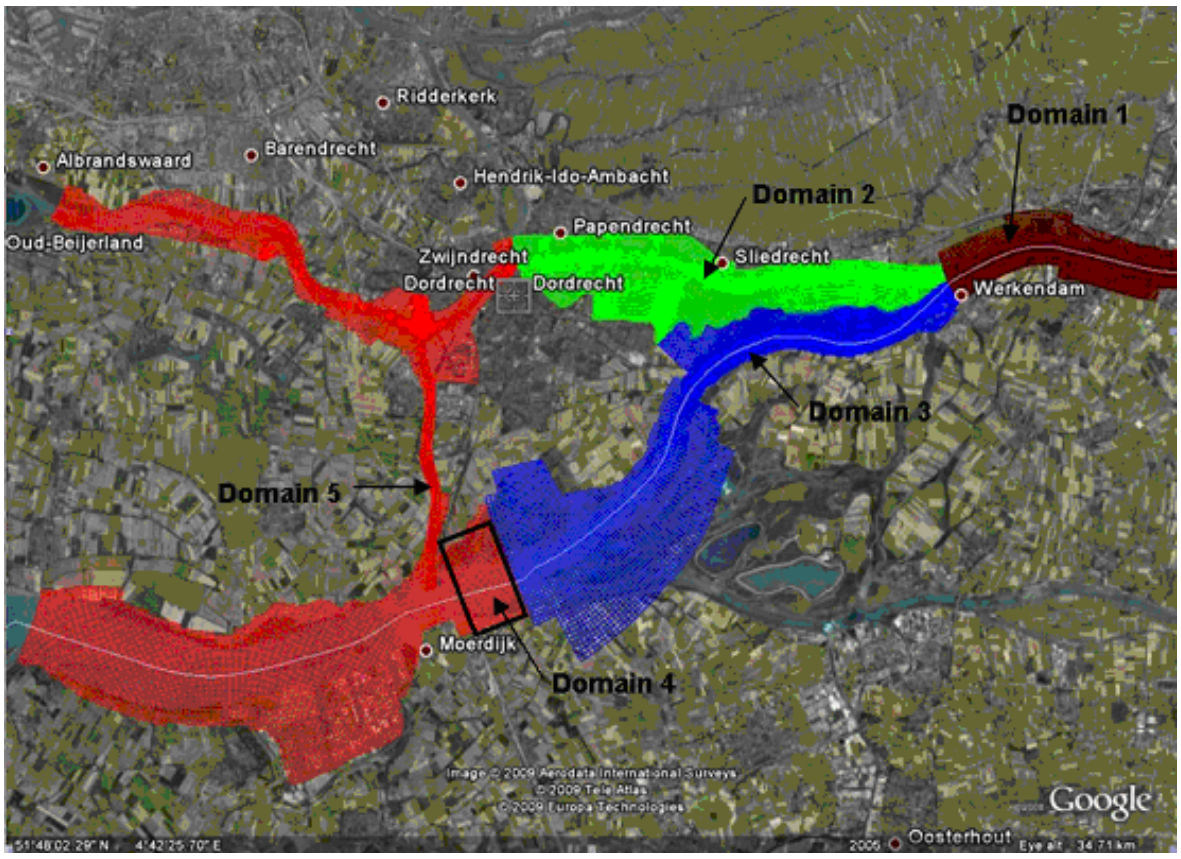

Figure 3.3: The five domains of the Delft3D model.

The domains represent a bifurcation at the end of the Boven Merwede, known as the 'Kop van de Oude Wiel', followed by two river branches (Beneden Merwede − Oude Maas in the North and Nieuwe Merwede − Hollandsch Diep in the South), interconnected by the Dordtsche Kil in the fifth domain. This fifth domain contains the area of interest for this study, in particular the branches Oude Maas and Dordtsche Kil. There is one upstream boundary at the beginning of domain 1 and three downstream boundaries in domain 5, which will be further elaborated in section 3.3.4. An overview of the domains from figure 3.3 is given in table 3.2.

Table 3.2: Description of the domains the numerical model

Domain 1	Boven Merwede
Domain 2	Beneden Merwede
Domain 3	Nieuwe Merwede
Domain 4	Connection Nieuwe Merwede to Hollandsch Diep
Domain 5	Hollands Diep, Dordtsche Kil and Oude Maas

3.3 Hydrodynamics

According to the study by Giri (2010), the model gives a reasonably accurate description of the flow in the Rhine-Meuse Delta so that hydrodynamic calibration and validation is unnecessary. This section will describe the important subjects for the hydrodynamic model.

3.3.1 General equations

The 2D movement of water is described by three shallow water equations, one for conservation of mass (3.1) and two for conservation of momentum (3.2 and 3.3). These equations are the basics for the hydrodynamics in (systems of) rivers, and are often referred to as the 2D St. Venant equations. These are the equations that Delft3D solves in order to model a river.

$$\frac{\partial \zeta}{\partial t} + \frac{\partial [hU]}{\partial x} + \frac{\partial [hV]}{\partial y} = 0 \tag{3.1}$$

$$\frac{\partial U}{\partial t} + U\frac{\partial U}{\partial x} + V\frac{\partial U}{\partial y} = fV + \nu_H \left[\frac{\partial^2 U}{\partial x^2} + \frac{\partial^2 U}{\partial y^2}\right] - \frac{gU\sqrt{U^2+V^2}}{hC^2} \tag{3.2}$$

$$\frac{\partial V}{\partial t} + U\frac{\partial V}{\partial x} + V\frac{\partial V}{\partial y} = fU + \nu_H \left[\frac{\partial^2 V}{\partial x^2} + \frac{\partial^2 V}{\partial y^2}\right] - \frac{gV\sqrt{U^2+V^2}}{hC^2} \tag{3.3}$$

where,

h	=	Water depth
U	=	Depth-averaged velocity in x direction
V	=	Depth-averaged velocity in y direction
z_b	=	mean cross-sectional bottom level
g	=	Gravitational acceleration
f	=	Coriolis parameter
ν_H	=	Horizontal eddy viscosity
C	=	Chézy coefficient
t	=	Time
x	=	Horizontal co-ordinate
y	=	Horizontal co-ordinate

3.3.2 Computational stability

In a numerical flow model such as this, there are certain limitations to the size of the computational time steps. A well known condition for this so-called computational stability is the CFL-condition (or limit to the Courant number):

$$\sigma = \max\left(\frac{U\Delta t}{\Delta x}, \frac{V\Delta t}{\Delta y}\right) < 1 \tag{3.4}$$

where:

U	=	Depth-averaged velocity in x direction
V	=	Depth-averaged velocity in y direction
Δt	=	Computational time step
Δx, Δy	=	Computational spatial step

The grids cells in the model have a length (in the direction of flow) varying somewhere between 30 and 200 metres and the flow velocity can exceed 1 m/s, which means that the set time step of 24 seconds should satisfy the condition. Moreover, due to the semi-implicit computational scheme within Delft3D, Courant numbers larger than 1 are possible. Increasing the time step should therefore be an interesting possibility, since it reduces the computational time. However, testing a time-step of 48 seconds (twice the time step used) gives inaccurate results for bed level changes. Appendix C also describes the computational scheme of Delft3D. Figure 3.4 shows a part of the computational grid in domain 5. It can be seen that some of the grid cells have a length to width ratio of around 5. Although this is not desirable, it is acceptable as long as the flow is always more or less in the longitudinal direction of the grid cell. Moreover, this is a good way to acquire a more refined grid over the width of the river.

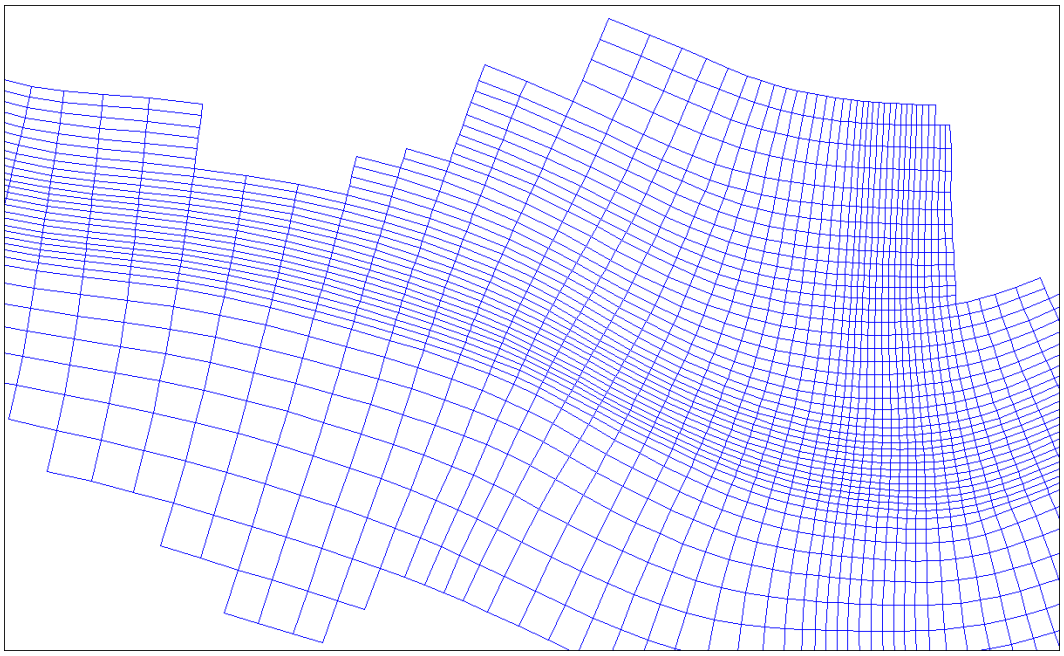

Figure 3.4: A part of the numerical grid.

3.3.3 Roughness

The roughness of the riverbed is an important factor in hydraulic computations. In this model, the roughness is given by a trachytope[3] definition file. The trachytope functionality allows for the usage of different types of roughness formulations at different locations within the computational domain. The trachytope definition file in this model uses three area classes and a linear class. The area classes 'simple trachytope' and 'alluvial trachytope' are used mostly and described below.

White Colebrook (Simple trachytope):
A simple trachytope class to determine the Chézy value according to the White-Colebrook formula:

$$C = 18log\left(\frac{12R}{k + \frac{1}{3.5}\delta}\right) \tag{3.5}$$

Simplified to the following equation for a hydraulic rough riverbed:

$$C = 18log\left(\frac{12R}{k}\right) \quad \text{for } k >> \delta \tag{3.6}$$

In this formula, R is the hydraulic radius, and k is the roughness height given in the definition file.

Simplified Van Rijn (Alluvial trachytope):
This alluvial roughness formula is a simplified version of the Van Rijn (1984c) alluvial roughness predictor.

$$k = Ah^{0.7}\left(1 - e^{-Bh^{-0.3}}\right) \tag{3.7}$$

In which A and B are tuning parameters given in the definition file, and h is the flow depth.

The third area class is a vegetation trachytope according to Klopstra et al. (1997) and the linear class is trachytope to simulate hedges or piers. For the description of the corresponding formulations will be referred to the Delft3D-FLOW User Manual (Deltares, 2010).

3.3.4 Boundary conditions

The full Delft3D model has one upstream boundary at the Boven Merwede (domain 1) and three downstream boundaries at the Oude Maas, Noord and Hollands Diep (all in domain 5). To determine the boundary conditions, a SOBEK model is used with three upstream discharge boundaries at Tiel, Lith and Hagestein respectively and tidal boundaries at Haringvliet and Hoek van Holland. From this model, a time-series discharge boundary was deduced for the Boven-Merwede boundary and three time-series water levels for the downstream boundaries. For the morphological computation, an averaged discharge (deduced from the time-series)

[3] After the Greek word τραχύτης for roughness

was used at the upstream boundary (see Appendix B). Also, the discharge coming from the Amer River has been taken into account in the domain of the Nieuwe Merwede as time-series of discharge insertion/extraction (see Appendix B), deduced from the SOBEK model as well (Giri, 2010). As mentioned before, the hydrodynamic performance of this model was satisfactory, but for the branches other than the Dordtsche Kil, the morphodynamic behaviour of the model had not been calibrated yet.

3.4 Morphology

3.4.1 Introduction

For morphological computations, sediment fractions are specified in each of the domains based on available sediment data (Appendix A), but the model only updates the bed level in the fifth domain to save computation time. This section elaborates on the morphology in this domain, where erodible layers have been specified, using (a combination of) several sediment fractions, as well as fixed layers (see section 3.4.4). Furthermore, the equilibrium boundary condition for suspended sediment transport has been used as equilibrium concentration at inflow boundaries.

3.4.2 Sediment distribution

In order to simulate the erosion processes, the sediment characteristics in the Delft3D model should be specified in such a way that the model is able to simulate the erosion problems described in chapter 1. Based on available data, Giri (2010) divided the sediment into 3 log-normally distributed sediment classes, clay (<63 µm), fine sand (63 - 200 µm) and coarse sand (200 - 1000 µm) and defined the fraction content for the different Merwede domains and for three different parts of the domain that includes Dordtsche Kil, Hollands Diep and Oude Maas (see appendix A). From the study of Stouthamer and De Haas (2011) on the erodibility of the riverbeds in the area of interest, it can be deduced that for the non-cohesive fractions (fine sand and coarse sand), the median grain size in the Holocene sand layers is around 175 µm. For the Pleistocene layer a median grain size of approximately 350 µm or slightly higher[4] can be assumed.

For the Oude Maas and Dordtsche Kil, two different sediment distributions are implemented in this model. Figure 3.5 shows the log-normal distribution of the sediment fractions for each branch. To save computation time, only 2 sediment fractions altogether are implemented in the Delft3D model, the fine fraction in the Oude Maas with a median grain size of 175 µm, and the coarse fraction of the Dordtsche Kil (600 µm), which are the finest and most coarse fraction in the model. The sediment fractions lying in between are modelled by a mixture of these two fractions, which is a good approximation of the distributions defined in figure 3.5.

[4]Sloff et al. (2011) state that there are reasons to believe that the grains are somewhat coarser than 350 µm.

For the cohesive sediment fraction (clay) the critical shear force determines the occurrence of

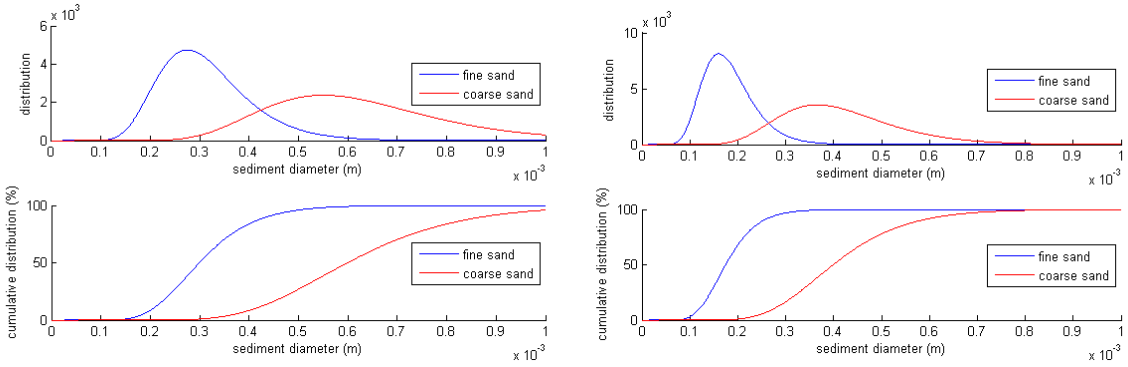

Figure 3.5: Sediment distribution in the Oude Maas.

erosion. In this case the critical shear for gradual erosion of the clay layer surface is considered to be 1.8 N/m^2 (Stouthamer and De Haas, 2011).

3.4.3 Sediment layers

Instead of using a mixed layer for the movable parts of the area, containing the 3 types of sediment according to the defined fraction content, graded layers are implemented in the model in order to simulate the effect of for instance clay layers on top of sand layers that have been 'breached'. For this purpose an initial bed composition file is implemented, which allows for a specification of the initial composition of multiple layers in the bed, as opposed to the vertically homogeneous bed composition in the initial model. The initial bed composition file consists of multiple thickness files, which indicate the thickness of each layer on each grid cell in the model. In this way, the most complex bed compositions can be modelled effectively.

Figures 3.6 and 3.7 show the layered composition of the bed in the Delft3D model compared to the available data. For the Dordtsche Kil, an approximate sketch of riverbed characteristics along the Dordtsche Kil (Giri, 2010) was used to create an initial bed composition, whereas for the Oude Maas a longitudinal section of the subsoil (Stouthamer and De Haas, 2011) was used. This lithological profile is based on bore data from the TNO-DINO database.

In this case of different sediment fractions, the sizes influence each other by means of hiding and exposure: Fine sediments are hidden by coarse sediments and are thereby partly shielded from the main flow, whereas the coarser sediments are more exposed than they would be among sediments of the same size. This effect is taken into account by increasing the effective critical shear stress for fine sediments while lowering it for coarse sediments. This adjustment can be carried out using a multiplicative factor ξ. This however is not taken into account in this model.

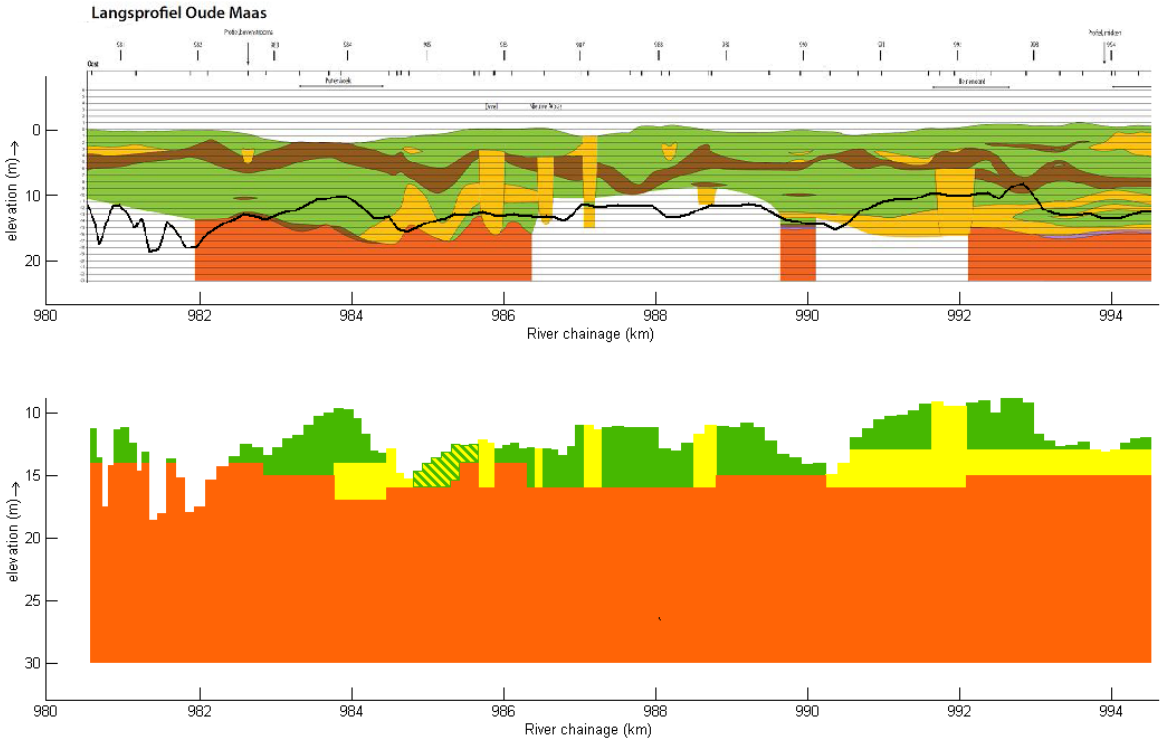

Figure 3.6: Implementation of bed level data into the model for the Oude Maas.

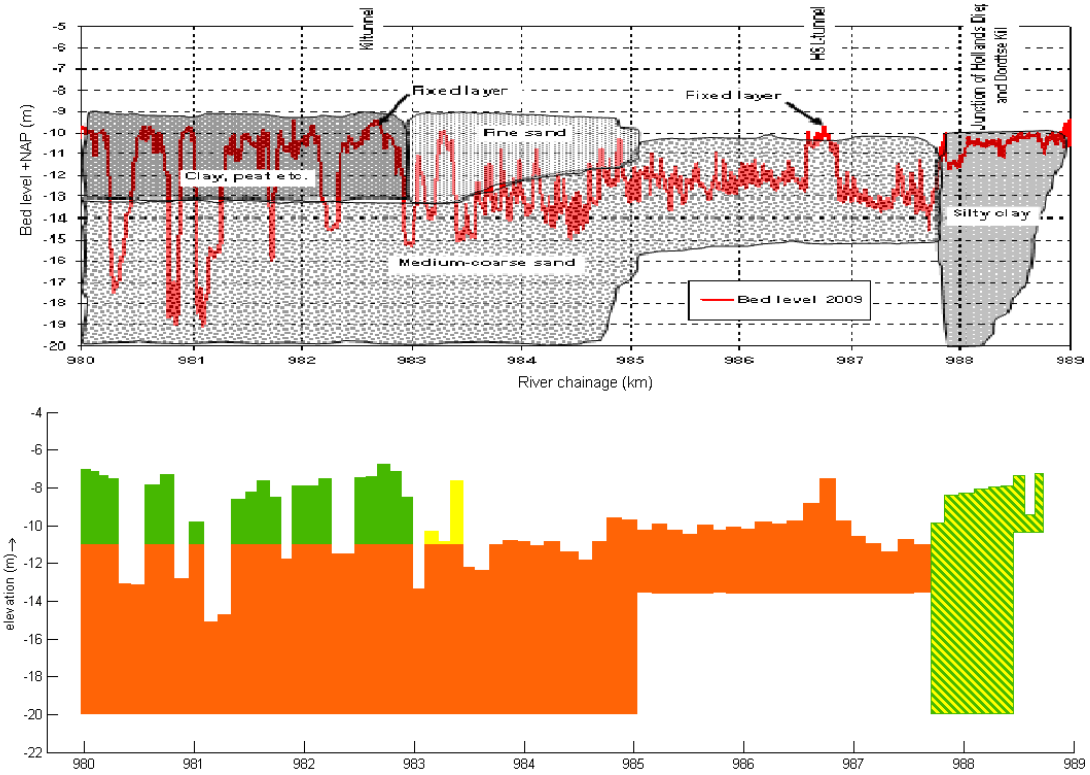

Figure 3.7: Implementation of bed level data into the model for the Dordtsche Kil.

3.4.4 Fixed layers

There are a number of fixed or non-erodible layers at for tunnels of the Dordtsche Kil and the Oude Maas that can be identified analysing the geotechnical data. Fixed layers can be implemented in two different ways. The first way is to reduce the sediment layers to zero, or to a certain depth below which there is no sediment transport possible. When all sediment layers are set to a depth of 0 metres at a certain location, no sediment transport is possible at all. In the research by Giri (2010), the slowly eroding clay layer was defined as a fixed layer and the more erodible parts as a vertically uniform mixture of sediments. In this research, only the few locations where for example a tunnel is located underneath the river is modelled as non-erodible.

Another way to define a fixed layer is to assign a threshold value for reducing sediment transport locally. If the quantity of sediment available is less than the threshold then the magnitude of the calculated bed-load transport vector is reduced as follows:

$$S_b^* = f_{FIXFAC} S_b \tag{3.8}$$

Where:

S_b	= Magnitude of the bed-load transport vector
S_b^*	= Magnitude of the reduced bed-load transport vector
f_{FIXFAC}	= upwind fixed layer proximity factor: $f_{FIXFAC} = \frac{DPSED}{THRESH}$
$DPSED$	= depth of sediment available at the bed
$THRESH$	= user-defined erosion threshold

In this way a layer can be fixed to a certain depth, where the sediment transport decreases as the bed level draws near the depth where the fixed layer is located.

4 Model calibration

4.1 Introduction

After the setup of the model in the previous chapter, a calibration can be carried out. Section 4.2 elaborates on the calibration of sediment transport, where the transport of cohesive sediment is calibrated and the best transport formula for non-cohesive sediment is chosen. Section 4.3 describes the calibration of the local erosion in the form of scour holes. Besides the calibration, a sensitivity analysis was carried out on the effect of varying upstream and downstream discharges is investigated, described in ection 4.4.

4.2 Sediment transport

4.2.1 Cohesive sediment transport

For cohesive sediment fractions (mud), the fluxes between the water phase and the bed are calculated with the Partheniades-Krone formulations (Partheniades, 1965):

$$E = M \cdot S_e = M \cdot \left(\frac{\tau_{cw}}{\tau_{cr,e}} - 1 \right) \quad \text{for} \quad \tau_{cw} > \tau_{cr,e} \tag{4.1}$$

$$D = w_s \cdot c_b \cdot S_d = w_s \cdot c_b \cdot \left(1 - \frac{\tau_{cw}}{\tau_{cr,d}} \right) \quad \text{for} \quad \tau_{cw} < \tau_{cr,d} \tag{4.2}$$

In this formulation, $\tau_{cw,e}$ and $\tau_{cw,d}$ represent the critical shear stress for erosion and deposition respectively. For this area the critical shear stress is 1.8 N/m^2 (Sloff et al., 2011), so that $\tau_{cw,e}$ is set to 1.8 N/m^2. For the deposition of sediment there is no data available. Setting $\tau_{cw,d}$ to 1.8 N/m^2 results into erosion of the clay fraction when the shear stress is below 1.8 N/m^2 and deposition of cohesive sediment when the shear stress is higher that 1.8 N/m^2. This is illustrated in figure 4.1 where both the maximum shear stress over the Oude Maas is shown and a time series of the shear stress for an arbitrary point in the river.
The erosion parameter M is used for calibrating the rate of erosion, and eventually set to a value of $3 \cdot 10^{-6}$ kg/(m$^2 \cdot s$). To investigate the rate of erosion, a situation was modelled where the complete bed of the Oude Maas consists of clay. According to table 1.1 in chapter 1, the average degradation of the bed level in the middle part of the Oude Maas is equal to approximately 4.5 cm/year, of which 3.3 cm/year is covered by the erosion of clay layers. The goal of this simulation is to come up with a value for M that causes the model to approach this rate of erosion. Figure 4.2 shows the result of this 4 year simulation, where the average erosion is indeed somewhere between 10 and 15 cm, coinciding with a rate of 3.3 cm/year.

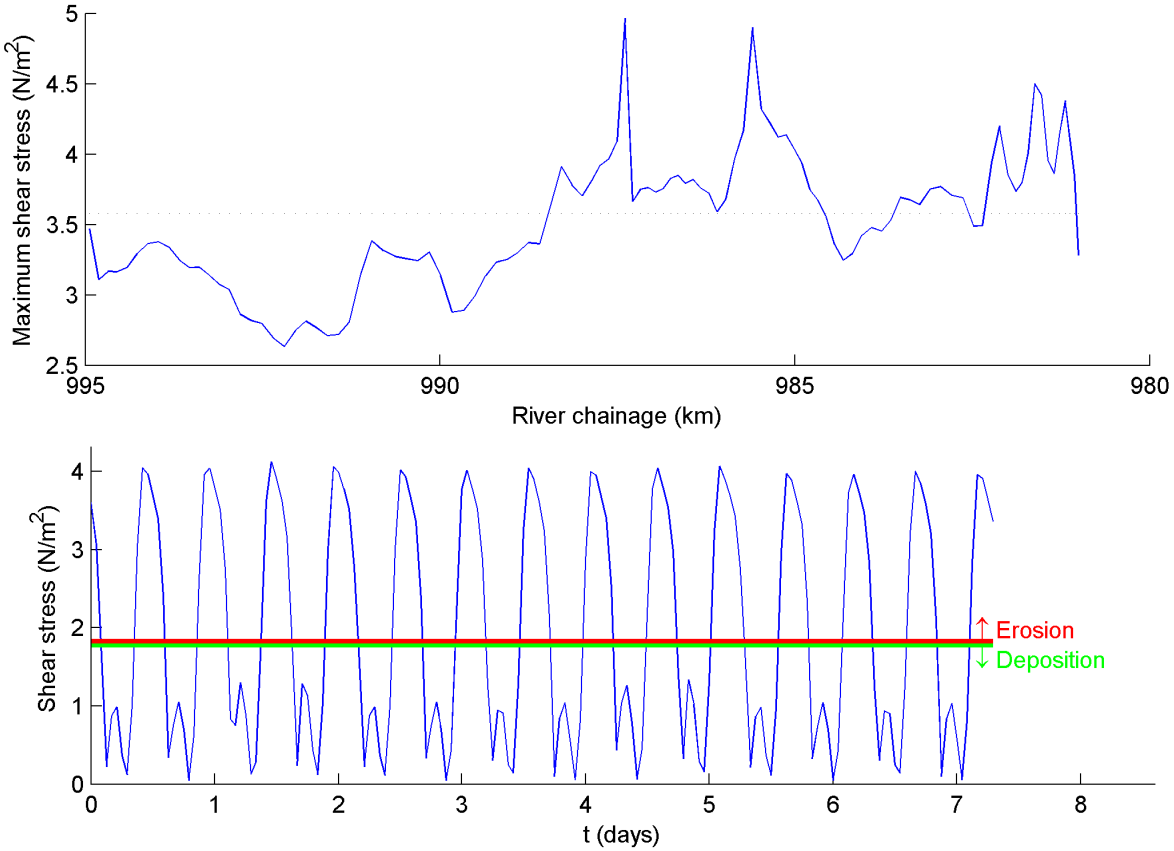

Figure 4.1: Maximum shear stress over the river (top) and time series of shear stress on an arbitrary location in the river (bottom).

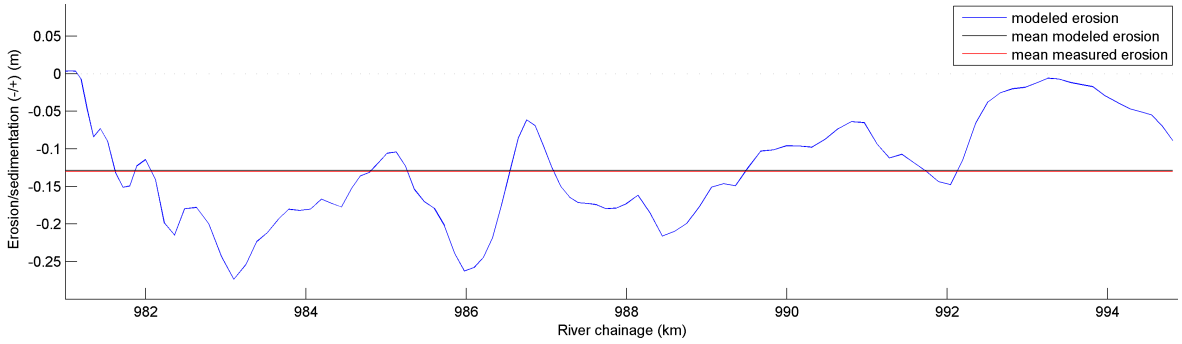

Figure 4.2: Modelled erosion rate of the Oude Maas compared to the measured rate for $3 \cdot 10^{-6}$ kg/(m^2·s)

4.2.2 Non-cohesive sediment transport

For non-cohesive (loose) sediment, flowing water will exert forces on the grains. When these forces exceed a certain critical value the grains will begin to move. With sediment transport a distinction is made between bed load and suspended load. Bed load is defined as the transport of bed material by rolling, sliding and jumping. Suspended load is defined as the

transport of sediment that is suspended in the fluid for some time. Part of the suspended load in the river can be wash load. This involves fine sediment that is brought in suspension from the upstream area. Figure 4.3 shows the distinctions in sediment processes.

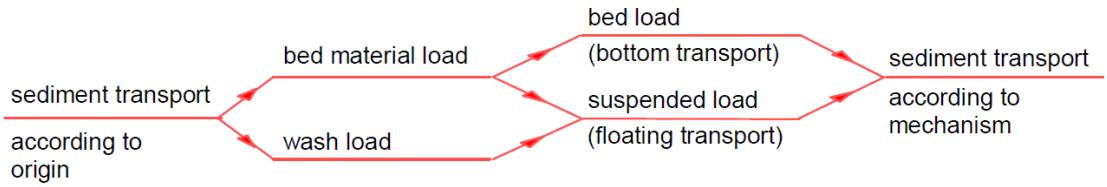

Figure 4.3: Classification of sediment transport (Jansen et al, 1994).

Delft3D offers a number of standard sediment transport formulations for non-cohesive sediment, which can be divided into different types:

- formulas for bed load
- formulas for suspended load
- formulas for total load

Several sediment transport formulas have been used for this research. The default sediment transport formula in Delft3D is the Van Rijn (1993) formula, which distinguishes between sediment transport below a reference height a which is treated as bed-load transport and that above the reference height which is treated as suspended-load. In the preliminary study by Giri (2010), the Van Rijn (2007a,b) transport formula has been used. Van Rijn (2007a,b) had been formulated to improve the influence of wind waves on sediment transport, and the presence of mud is also taken into account in this formulation. Just as in the Van Rijn (1993) formula, a distinction is drawn between bed transport and suspended transport. Because of the explicit distinction between bed load and suspended load, the area of application of this formula is quite large, so that both formulas can be considered for this research.

A frequently used sediment transport relation that is being considered as an alternative for this model is the Engelund-Hansen formula (1967). The Engelund-Hansen formula proves to be especially applicable for the total load of relatively fine material, in which the suspended load plays a vital role. However, unlike the Van Rijn 2007 formula, the Engelund-Hansen formula does not take into account the effect of a mud fraction and does not draw a distinction between bed load and suspended load. The following conditions must hold in order to apply the Engelund Hansen formula:

$$u_* > w_s \tag{4.3}$$

$$0.19 < D_{50} < 0.93 \text{ mm} \tag{4.4}$$

$$0.07 < \theta < 0.6 \tag{4.5}$$

To check this, the average of the magnitude of the flow velocity in the Dordtsche Kil is taken. For both rivers this is approximately 0.7 m/s. From this, shear velocity u_* and Shields

parameter θ can be determined:

$$u_* = \frac{\sqrt{g}}{C}u = \frac{\sqrt{9.81}}{50} \cdot 0.7 = 0.044 \text{ m/s} \quad (4.6)$$

$$\theta = \frac{u_*^2}{g\Delta D} = \frac{0.004}{9.81 \cdot 1.65 \cdot 2.5 \cdot 10^{-4}} = 0.48 \text{ for the Oude Maas, and} \quad (4.7)$$

$$= \frac{0.004}{9.81 \cdot 1.65 \cdot 4.5 \cdot 10^{-4}} = 0.27 \text{ for the Dordtsche Kil.}$$

The fall velocity, w_s, is equal to 0.025 m/s in the Delft3D model, so that all the conditions (4.3, 4.4 and 4.5) hold.[5] Another widely used transport formula is the Meyer-Peter-Müller formula (1948). This formula is however only applicable for rivers with coarse bed material, i.e. $D \geq 0.4$ mm. Therefore, this formula is not considered, leaving only the Van Rijn (1993), the Van Rijn (2007a,b) and the Engelund-Hansen formula.

4.2.3 Choice of formula

From the 3 formulas mentioned in the previous section, Van Rijn (1993) proves to be the best transport formulation for this case. That is to say, the Van Rijn (1993) formulation gives the least complications in calculating sedimentation and erosion. The Engelund-Hansen and the Van Rijn (2007a,b) formula both show some complications around erosion holes or in river bends, or tend to overestimate the sedimentation and erosion processes. Figure 4.4 and 4.5 compare a few locations for different transport formulas.

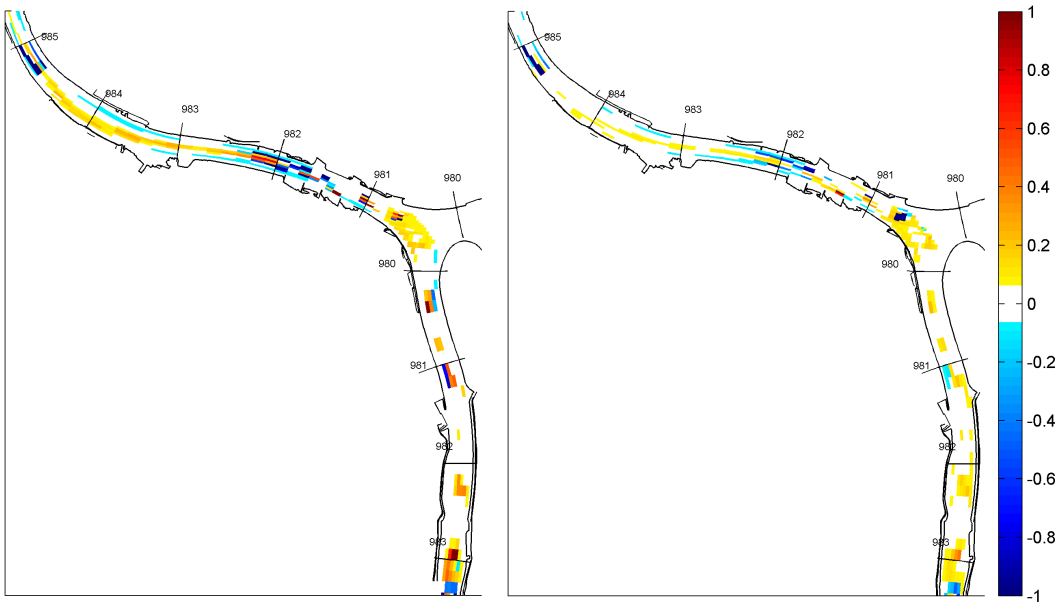

Figure 4.4: Cumulative erosion (-) and sedimentation (+) for Van Rijn 2007 (left) and Van Rijn 1993 (right).

[5]For particle size D in equation 4.7 an average of sediment fractions is taken. Section 3.4.2 shows that the sediment in the Dordtsche Kil and Oude Maas ia mostly in the range of $0.19 < D_{50} < 0.93$ mm.

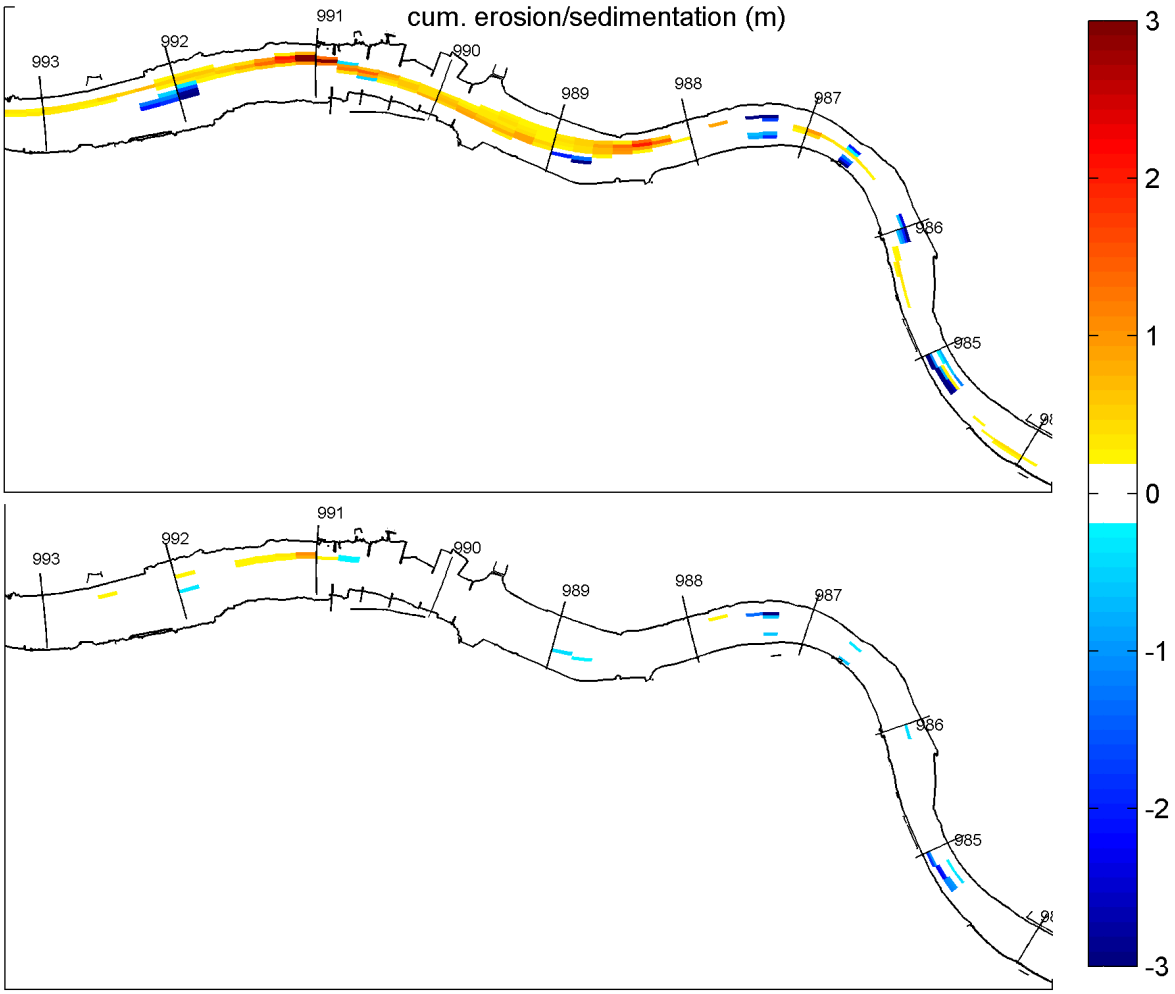

Figure 4.5: Cumulative erosion (-) and sedimentation (+) for Engelund Hansen (top) and Van Rijn 1993 (bottom).

Figure 4.4 shows that the Van Rijn (2007) transport formula causes a somewhat scattered erosion and sedimentation pattern, with a lot of strongly eroding and strongly aggrading cells adjacent to each other, whereas Van Rijn (1993) shows a smoother, more realistic erosion and sedimentation pattern. The Van Rijn (2007) formula should actually give similar results as the Van Rijn (1993) formula. Van Rijn (2007) had been formulated to improve the influence of wind waves on sediment transport and also takes into account the influence of a mud fraction. The influence of wind waves was not included in the model, so the only difference should be in the influence of mud (equation C.17). This causes the results of Van Rijn (1993) and Van Rijn (2007) to be of the same order of magnitude. The fact that the erosion and sedimentation pattern is still remarkably different in comparison to the Van Rijn (1993) formula could also be (partly) caused by a different implementation of the formula in Delft3D.

The Engelund Hansen formula in figure 4.5 gives a huge overestimation of erosion and sedimentation processes. The calibration coefficient α, which is now set to 1, would have to be decreased with at least a factor 10 to obtain a realistic pattern. The large deviation

of the results using the Engelund Hansen formula can be explained by the fact that the advection-diffusion equations for sediment concentration also become different when using the Engelund-Hansen formula. All in all, the default Van Rijn (1993) formula has proven to be the best formula to work with and is used for all other computations in this research.

4.3 Scour holes

4.3.1 Introduction

Apart from the general erosion processes, it is desirable to simulate the local erosion in the form of scour holes as well as possible. Since the model is a 2D model, however, this is only possible to some extent. Unlike a 3D model, it is not possible to take into account the vertical flow processes that occur, possibly detachment of flow or a vertically curved flow. There are however ways to model the effect of the bed slopes on sediment transport in a 2D model.

4.3.2 Transverse bed slope effects

Two effects cause deviations between the directions of bed load transport and depth averaged flow. The first effect is that curved flow induces a secondary helical water motion that leads to a difference between near-bed flow direction and depth averaged flow direction, The second effect is that sediment particles experience a downward acceleration along transverse bed slopes due to gravity (Mosselman, 2005). In the model these effects are modelled by the Koch and Flokstra (1980) formulation:

$$\tan \phi_{s_i} = \frac{\sin \phi_\tau + \frac{1}{f_i(\theta)} \frac{\partial z_b}{\partial y}}{\cos \phi_\tau + \frac{1}{f_i(\theta)} \frac{\partial z_b}{\partial x}} \tag{4.8}$$

in which ϕ_τ is the direction of bed shear stress and ϕ_{s_i} is the direction of sediment transport for fraction i, and where $f_i(\theta)$ equals:

$$f(\theta) = A_{sh} \theta_i^{B_{sh}} \left(\frac{D_i}{h} \right)^{C_{sh}} \left(\frac{D_i}{D_m} \right)^{D_{sh}} \tag{4.9}$$

where:

D_m = Median diameter of sediment grain size distribution;
D_i = Median diameter of sediment fraction i
h = Water depth
θ = Shields parameter

A_{sh}, B_{sh}, C_{sh} and D_{sh} are tuning coefficients, for which the values 9, 0.5, 0.3 and -0.3 have been chosen respectively to satisfy the empirical relation derived by Talmon et al. (1995):

$$f(\theta) = 9 \left(\frac{D_m}{h} \right)^{0.3} \sqrt{\theta} \tag{4.10}$$

This formulation, however, is not dependent on D_i, hence not dependent on the variation of sediment fractions in the model. By varying D_{sh}, the effect of the different sediment fractions can be investigated.

4.3.3 Effects of varying bed slope parameters

Varying the bed slope parameters seems to have a small impact on the general outcome of the model, but does effect the degree of erosion in the scour holes. One of the scour holes (figure 4.6) in the model is used here below to illustrate the effect of the bed slope parameters. Figure 4.7 shows the location of development of the cross section indicated in red in figure 4.6 for different bed slope parameters. Table 4.1 shows 5 different set of parameters for equation 4.9 that are used in this assessment.

	A_{sh}	B_{sh}	C_{sh}	D_{sh}
Option 1	9	0.5	0.3	-0.3
Option 2	9	0.5	0.3	2.7
Option 3	0.85	0.5	0	0
Option 4	0.4	0.5	0	0
Option 5	0.4	1	0	0

Table 4.1: Different sets of parameters corresponding to equation 4.9

The options in the table indicate the following:

1. Corresponds to equation 4.10, which is the one that is used in this model.
2. Takes an additional factor $\left(\frac{D_i}{D_m}\right)^3$ into account to simulate the effect of the different sediment sizes. Even with this large, arbitrarily chosen power of 3, the effect on the bed slope is minimal.
3. Corresponds to the default values in Delft 3D for these bed slope parameters.
4. The same reduced form as option 3, but with a lower value for A_{sh}. This value of 0.4 is based on an estimate of the value $A_{sh} = 9\left(\frac{D_m}{h}\right)^{0.3}$. The bed slopes in this case are almost exactly the same as in option 1.
5. The effect of choosing a linear relation between $f(\theta)$ and θ.

The figure shows that the development of the scour holes can be calibrated to a certain degree, although the differences between the different sets of parameters are not very large, which means that the model is not very sensitive to changes in the parameters. The rate of erosion can be calibrated by adjusting the different parameters in the Delft3D model and comparing the rate of erosion with measurements. Determining precise erosion rates for each erosion hole is however not a part of this study, so that the set of parameters representing equation 4.10 is used in this situation.

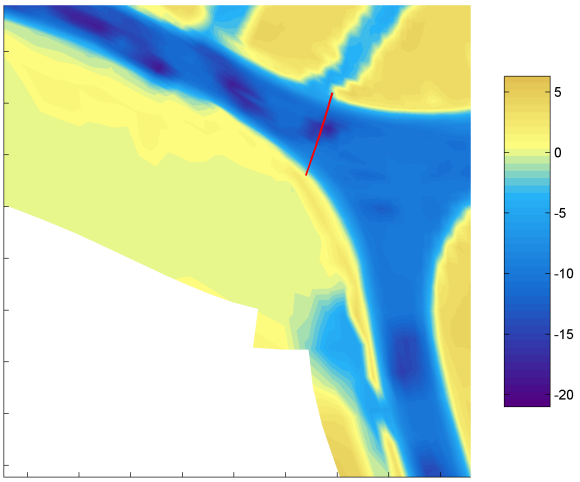

Figure 4.6: Scour hole near the junction of the Oude Maas and the Dordtsche Kil.

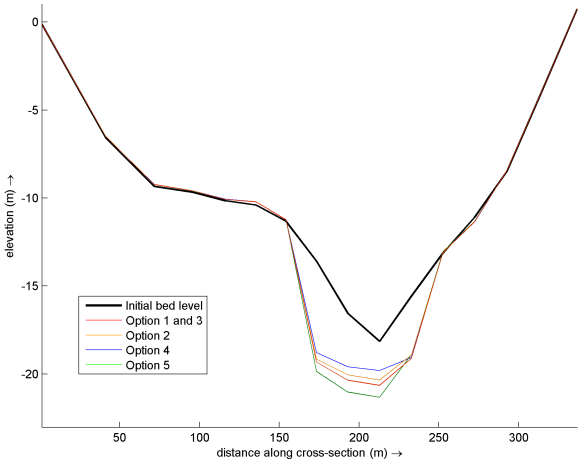

Figure 4.7: Four year development of the scour hole for different parameters.

4.4 Effect of higher and lower discharges

4.4.1 Introduction

Tidal influence is of great importance in this particular system of rivers. The influence of the tide changes for different upstream discharges, not only in magnitude but also in a way that the direction of flow and therefore the direction of sediment transport can change in some of the river branches. In this chapter, the effect of higher and lower upstream discharges on sediment transport are investigated. In addition to a better insight in the behaviour of this river system, it is a good way to assess whether the assumption of average upstream discharge is acceptable. Furthermore, a solution to the erosion problem in the Rhine-Meuse delta should be a sustainable one, so that the possible effects of future climate change should be investigated as well. Therefore, a simulation with sea level rise and a simulation with an upstream extreme discharge were carried out to investigate whether these changes have a large impact. A sea level rise is expected to have an additional negative effect on the erosion in the Rhine-Meuse delta due to the fact that a higher sea level causes the flow profile of the branches to increase, which could accelerate the erosion in the branches. The effects of the construction of the Haringvliet dam is also very important as pointed out earlier in this research. These effects however are discussed in the next chapter for the investigation of possible maintenance strategies.

4.4.2 High and low discharges

To gain insight in the effect of higher and lower discharges in the system, simulations with a lower and with a higher discharge are carried out, with the boundary conditions described in section 3.3.4. Regarding the varying of upstream discharge, two phenomena should be

looked at separately. A high discharge in a river should usually cause more erosion, which is why one can expect this to happen in this simulation. On the other hand it should be noted that, as discussed earlier in section 1.2, the increase in erosion in the last decade is caused by the increase in tidal intrusion. A higher discharge would cause a decrease in the tide's ability to intrude into the Rhine-Meuse delta, hence one would expect a decrease of erosion. Moreover, since the tidal influence is dominant in this area, it is highly questionable whether changing the discharge has a significant effect on the situation. The results of this simulation are shown in figures 4.8 and 4.9.

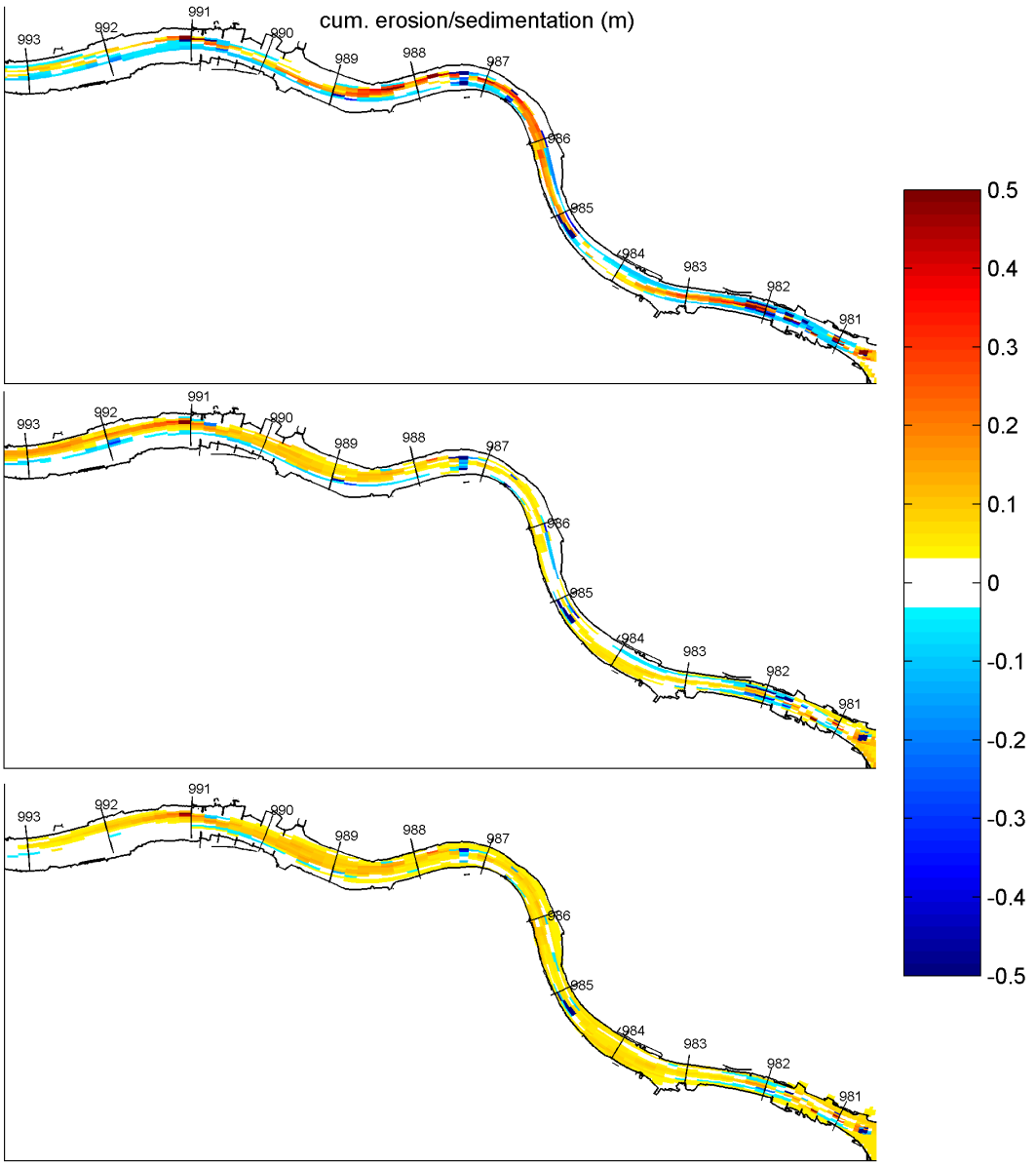

Figure 4.8: Cumulative erosion (-) and sedimentation (+) in the Oude Maas under low (top), average (centre) and high (bottom) discharge conditions.

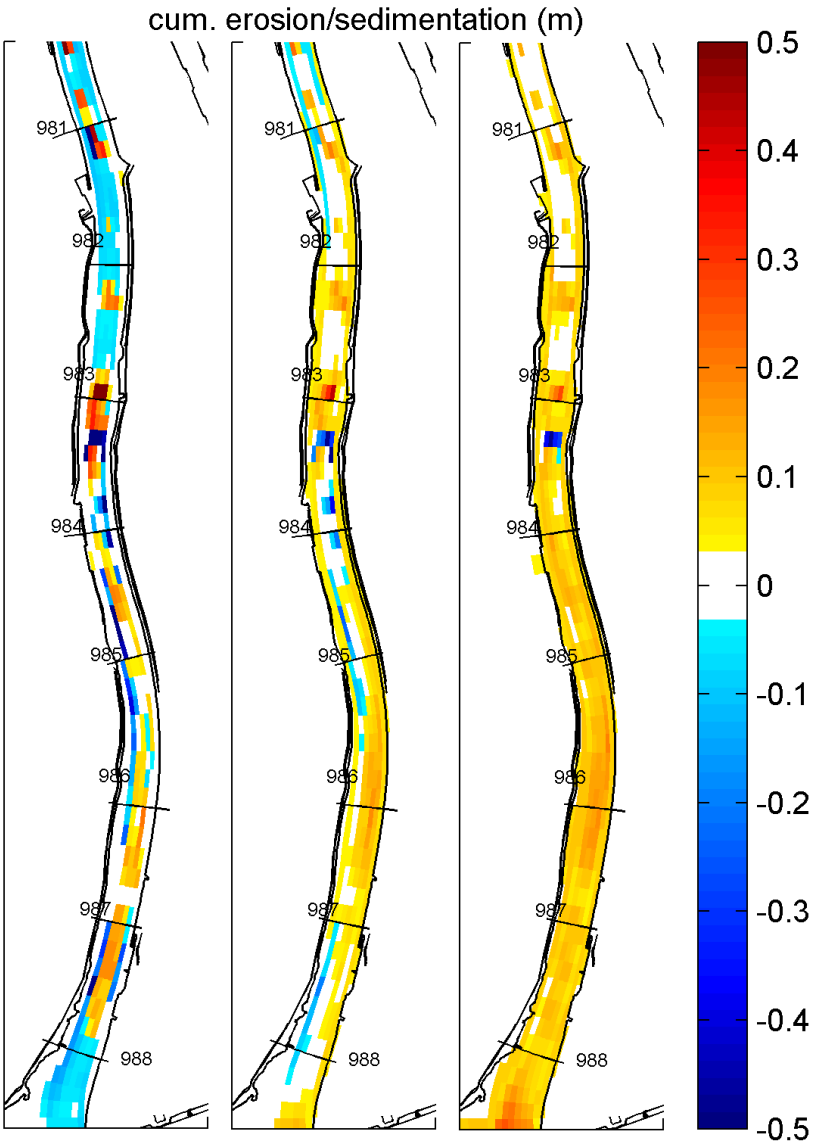

Figure 4.9: Cumulative erosion (-) and sedimentation (+) in the Dordtsche Kil under low (left), average (centre) and high (right) discharge conditions.

The first thing that stands is that in the case of a high upstream discharge, there is in general less erosion than in the other two cases, which is rather counterintuitive. An explanation for this effect is that the tide is not able to intrude far into the branches because of the high upstream discharge. Another explanation is that sediments that are usually deposited further upstream can now reach the Oude Maas and the Dordtsche Kil. In addition to the reduction of tidal intrusion an interesting side effect occurs: the high upstream discharge will cause the net sediment transport direction to change in the Dordtsche Kil. Whereas the transport of sediment is northwards in the averaged and low situation, the transport is southwards in times of a high river discharge. Figure 4.10 shows the difference in flow velocity, sediment transport and cumulative sediment transport due to varying discharges.

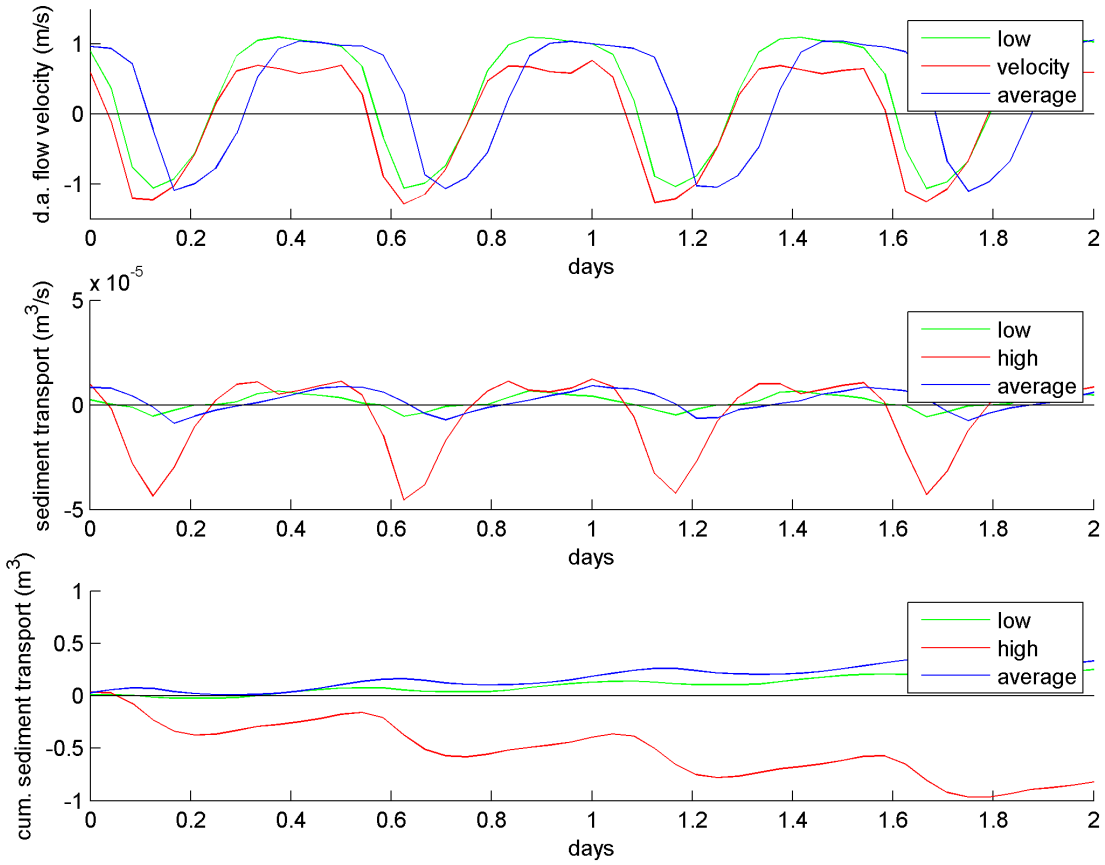

Figure 4.10: Flow velocity (top), sediment transport (centre) and cumulative sediment transport (bottom) in the Dordtsche Kil under low, average and high discharge conditions.

4.4.3 Effects of sea level rise

Another scenario that has to be accounted for is the expected future sea level rise. The sea level rise should have a certain influence on this tide-influenced area. A sea level rise of 1 metre is used in this scenario, which will influence the downstream conditions of the model. The downstream conditions are extracted from a new SOBEK calculation given the additional 1 metre at the downstream boundaries of the SOBEK model. The downstream boundary conditions extracted from this computation are included in appendix B.

The difference in terms of erosion and sedimentation in the model is not that obvious. Figure 4.11 shows the erosion and sedimentation pattern for the Dordtsche Kil, in which it can be seen that in case of a sea level rise the erosion hole in the Dordtsche Kil becomes larger. This might be caused again by the change of flow in this river branch. Figure 4.13 shows that there is no real net direction of sediment transport anymore in case of a sea level rise of 1 metre, where the net direction in the average situation is to the North. However, the overall outcome of change in sedimentation and erosion due to sea level rise is very small.

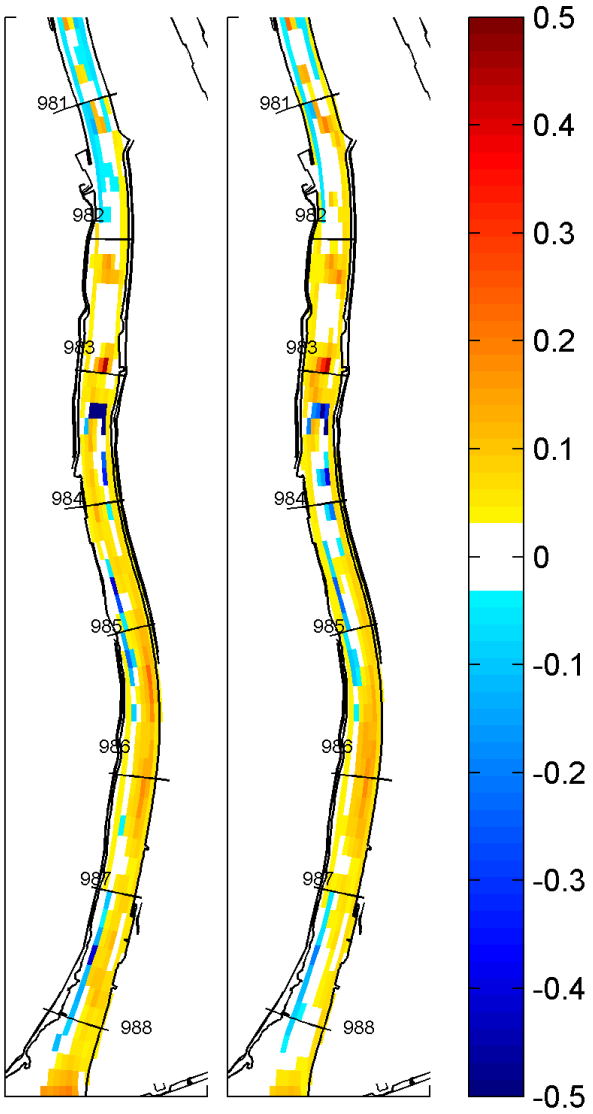

Figure 4.11: Cumulative erosion (-) and sedimentation (+) in the Dordtsche Kil for the case with one metre sea level rise (left) and the average case and (right).

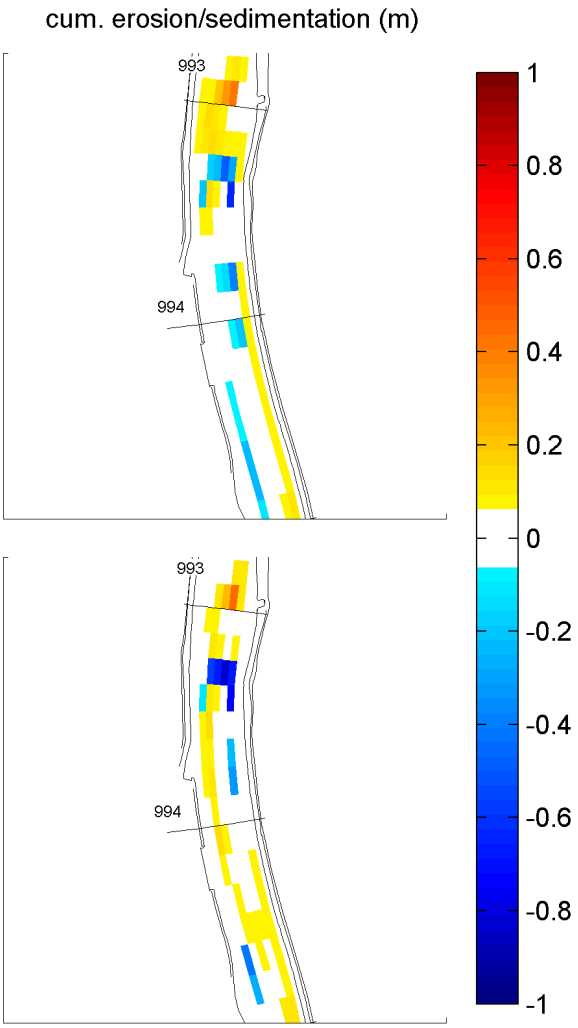

Figure 4.12: The biggest difference between normal situation (top) and the situation with sea level rise (bottom) is the larger scour hole in the situation with sea level rise.

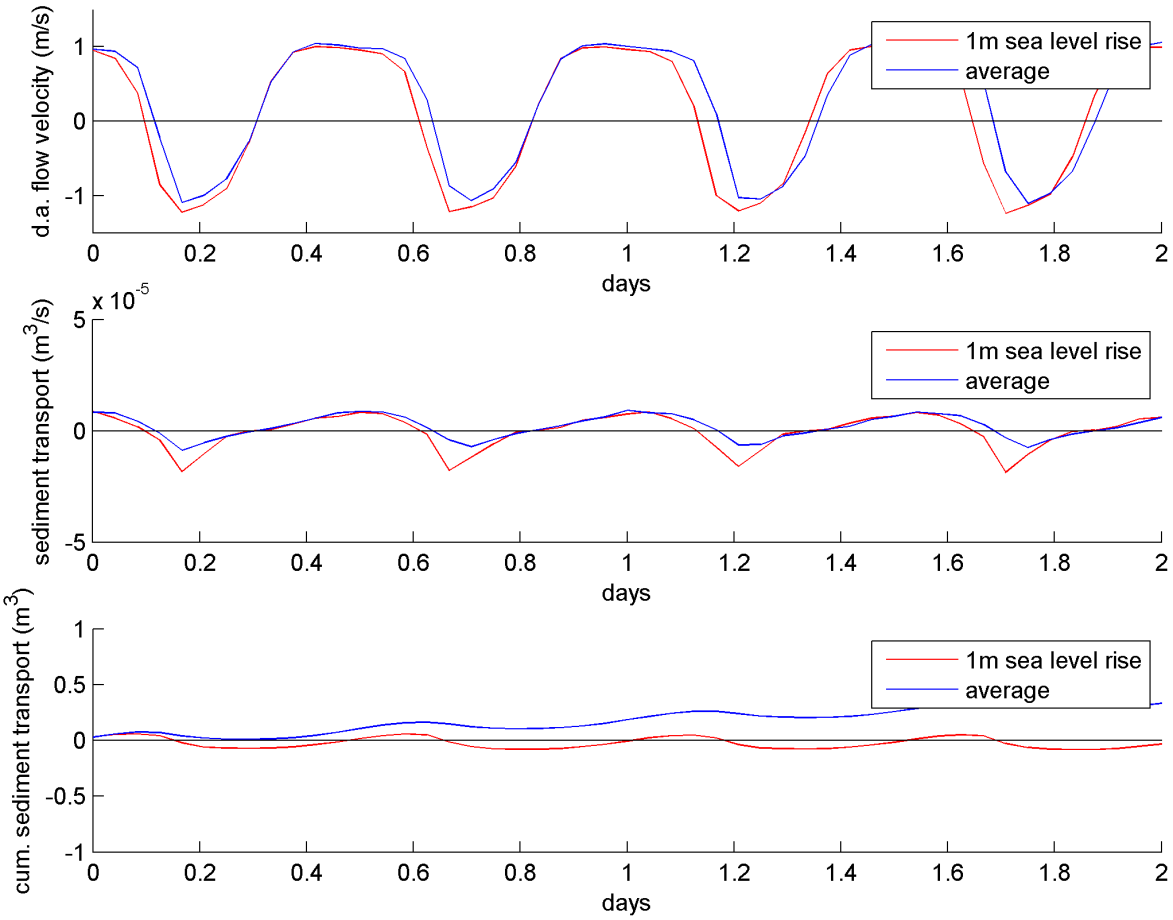

Figure 4.13: Flow velocity, sediment transport and cumulative sediment transport in the Dordtsche Kil for the average case and the case with one metre sea level rise.

4.4.4 Effects of an extreme flood wave

As a last scenario, the situation has been modelled under an unlikely flood wave with a peak discharge of 12.000 m^3/s. This corresponds to the expected future one-in-ten-thousand-years discharge of 18.000 m^3/s at Lobith. The upstream and downstream boundary conditions of this situation are included in appendix B. The computation for this situation has been carried out without morphological acceleration, since it involves the singly occurring event of a passing flood wave, for the period of one month. This results in an erosion and sedimentation pattern illustrated in figure 4.14. It shows that within a month of such an extremely high discharge, the same order of magnitude of erosion and sedimentation can occur as occurs in roughly four years under average conditions.

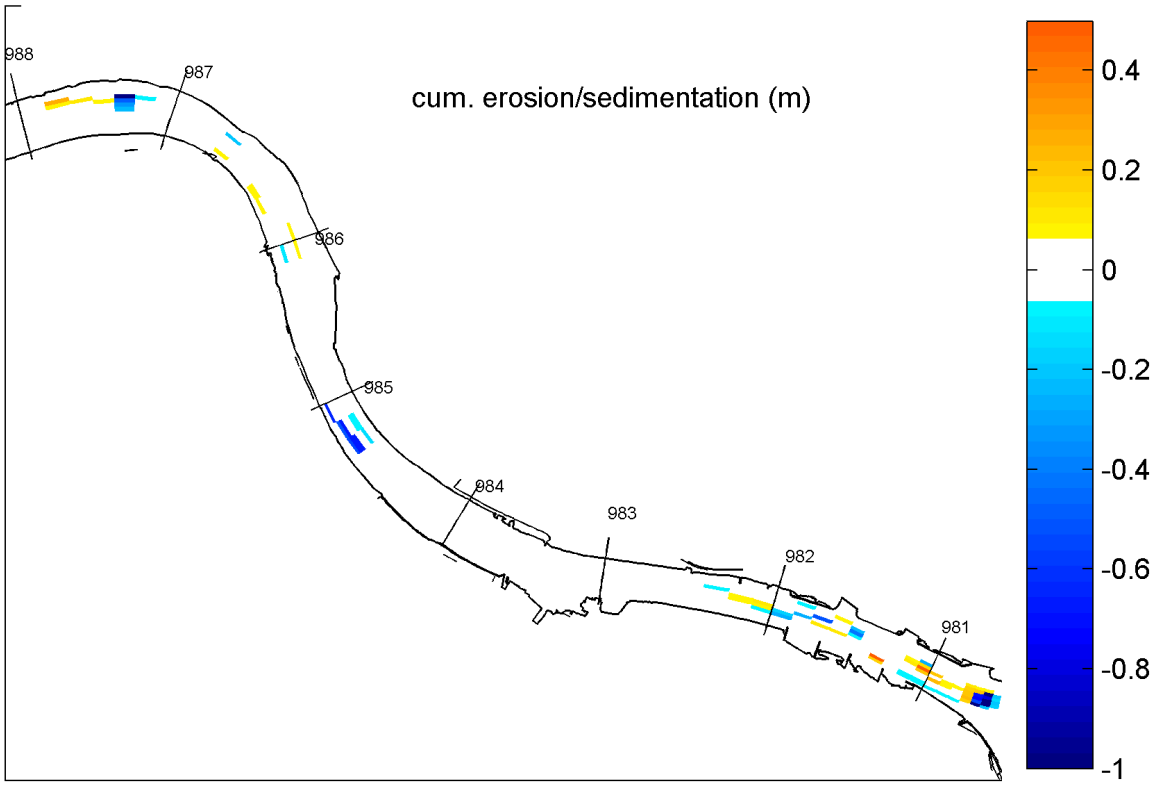

Figure 4.14: Scour hole development in case of an extreme flood wave.

4.5 Conclusion

The model has been improved in such a way that it quantitatively fits the existing situation. The clay layer in the model now erodes at the same order of magnitude as in reality as can be seen in the model results for the Oude Maas (figure 4.15) and the local scour seems to be modelled in the correct way as well. This means that an approach with a multi-layered morphodynamic model can work out rather well for problems with clay layers alternated with layers of sand.

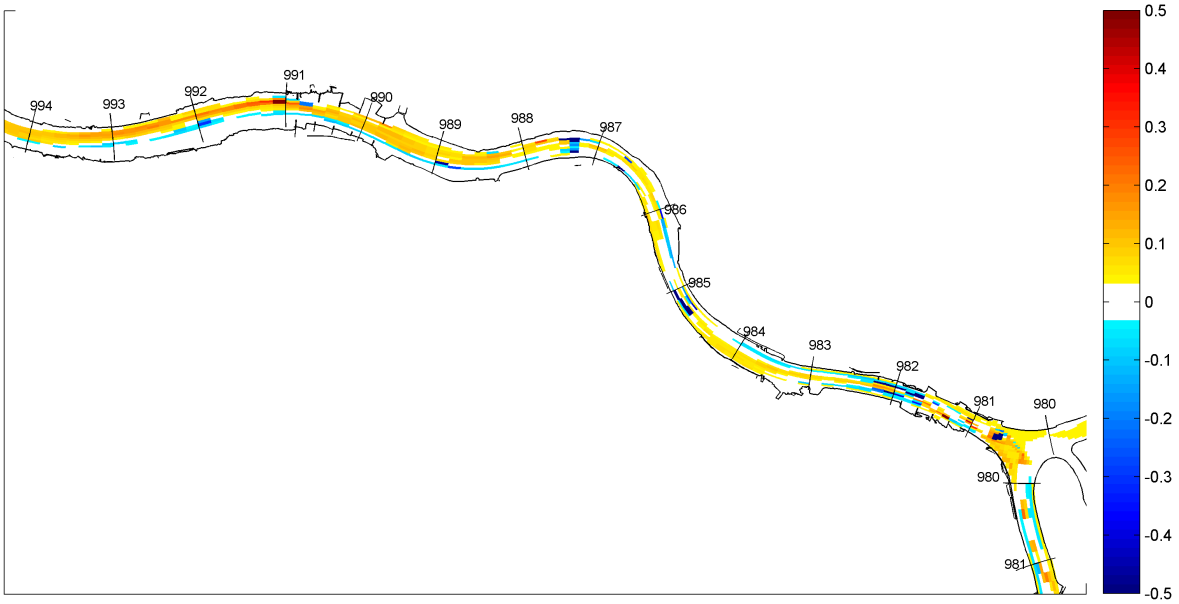

Figure 4.15: Cumulative sedimentation and erosion (m) in the Oude Maas.

Not only does the model reproduce the scour processes in the existing scour holes, it also produces scour holes at some other locations with underlying sand layers. These locations should be dealt with preventively in order to avert new deep scour holes.

Regarding the erosion holes, the model does reproduce the erosion correctly (in a qualitative way), but does not take into account possible three dimensional processes. An assessment is made in section 4.3 on using different parameters to model the erosion rate of the scour holes. The exact processes and rate of erosion are not particularly part of this study, but it is shown that the rate of erosion can be tweaked somewhat by adjusting bed slope parameters (see section 4.3).

For the Dordtsche Kil, the same kind of layered sediment fractions have been implemented. In this river branch the model also seems to work sufficiently. Figure 4.15 shows a comparison of the results of the model by Giri (2010), before implementing the multiple sediment layers, and the results for the Dordtsche Kil with multiple sediment layers, from which it can be seen that the erosion patterns in the new model are more smooth and also quantitatively closer to reality.

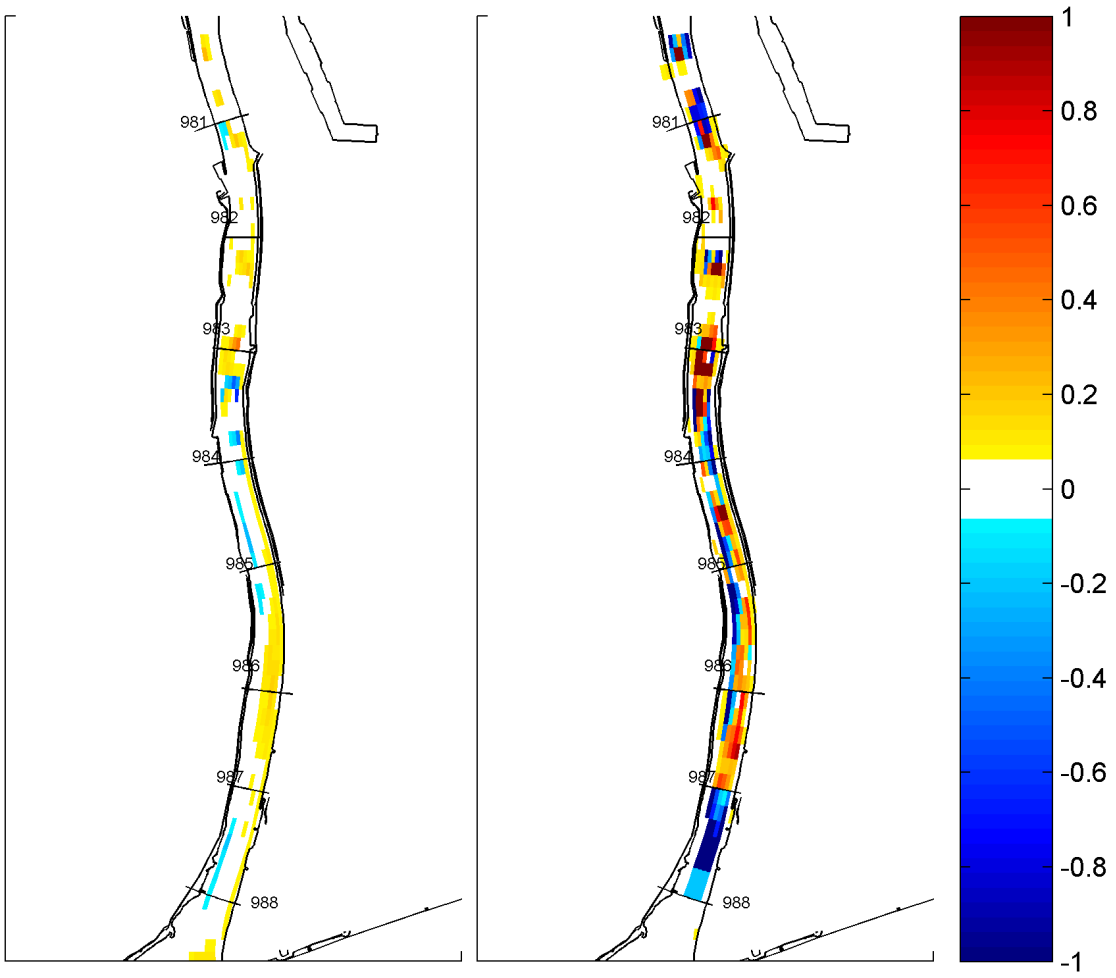

Figure 4.16: Cumulative sedimentation (+) and erosion (-) for the Dordtsche Kil before (left) and after (right) implementing multiple sediment layers.

Regarding the effects of different upstream and downstream discharges, the most important conclusion that can be made is that an average discharge situation seems to be a reasonable assumption for modelling the erosion and sedimentation. The low discharge case differs marginally from the average discharge case. All in all it seems that the interaction of a higher upstream discharge with the tidal intrusion has a positive influence on the model. However, a situation with a four year long constant high discharge is not a realistic case. The direction of transport in the Dordtsche Kil plays an important role in the distribution of sediments in this system and should be taken into account for possible maintenance strategies. The effects of sea level rise on the other hand are rather small and do not seem to have the significant negative influence on the system that was expected beforehand. An extreme upstream discharge causes a severe erosion in a short period of time, which shows that negligence of at least stabilising deep erosion holes can be dangerous if an extreme flood wave occurs. Though this occasion is unlikely (a one-in-10000-years flood wave), it should be accounted for.

5 Maintenance strategies

5.1 Introduction: Haringvliet sluices 'ajar'

As described in chapter 1, the main cause of the ongoing erosion in the Rhine-Meuse delta branches is the construction of the Haringvliet dam in 1970. The sluices operate in a way that water flows out of the Haringvliet towards the North sea during low-tide, that is, when the water level in the Haringvliet is higher than the water level at sea, and that the sluices are closed during high-tide, so that no salt water flows into the Haringvliet. Now, more than 40 years later, a governmental decision has been made than the sluices can also be slightly opened during high tide, in order to stimulate fish migration. The strong condition for this measure is to retain enough freshwater in the Haringvliet area, a politically sensitive issue, so that a lot of costly compensatory measures are an absolute necessity.

In this chapter, possible solutions for the problem are tested using the calibrated model, including the complete opening of the Haringvliet sluice, as to restore the tidal intrusion to the way it was before the Haringvliet dam was built. Now this may seem to be an infeasible solution considering the political issues outlined above, but the eventual costs of such a measure might be less than other possible solutions. The next sections elaborate on different solutions for both the local scour and long-term erosion problems, after which an economic consideration is made in section 5.5. Political issues are hereby left out of the equation in considering the optimal solution.

5.2 Important findings in the calibrated model

As concluded in the previous chapter, the model seems to qualitatively capture the processes that occur due to alternating sand and clay layers. Also, the rate of erosion of the clay layer is in the right order of magnitude. Regarding the scour holes, there are a few existing deep pits in the Oude Maas (all near the junction with the Dordtsche Kil) that erode and are still getting deeper according to the model, which is in line with the developments in reality. Furthermore, there are a few locations (further downstream) where the clay layer seems to be breached as well. It is important to take these locations into account in the solution for the scour holes. In the Dordtsche Kil, there is one scour hole that erodes further in the model.

5.3 Strategies for shortage of sediment

5.3.1 Filling erosion holes with sand

An interesting exercise is to look at the consequences of filling up the existing scour holes with sand. This is done for the set of scour holes in the Oude Maas just downstream of the

junction with the Dordtsche Kil. Figure 5.1 shows the bed topography of this area, where a depth of more than 14 m below NAP[6] is indicated with a darker blue color. These parts are filled with coarse sand from the Dordtsche Kil to a depth of 14 m below NAP. The total volume of sand needed for this is approximately 250.000 m^3.

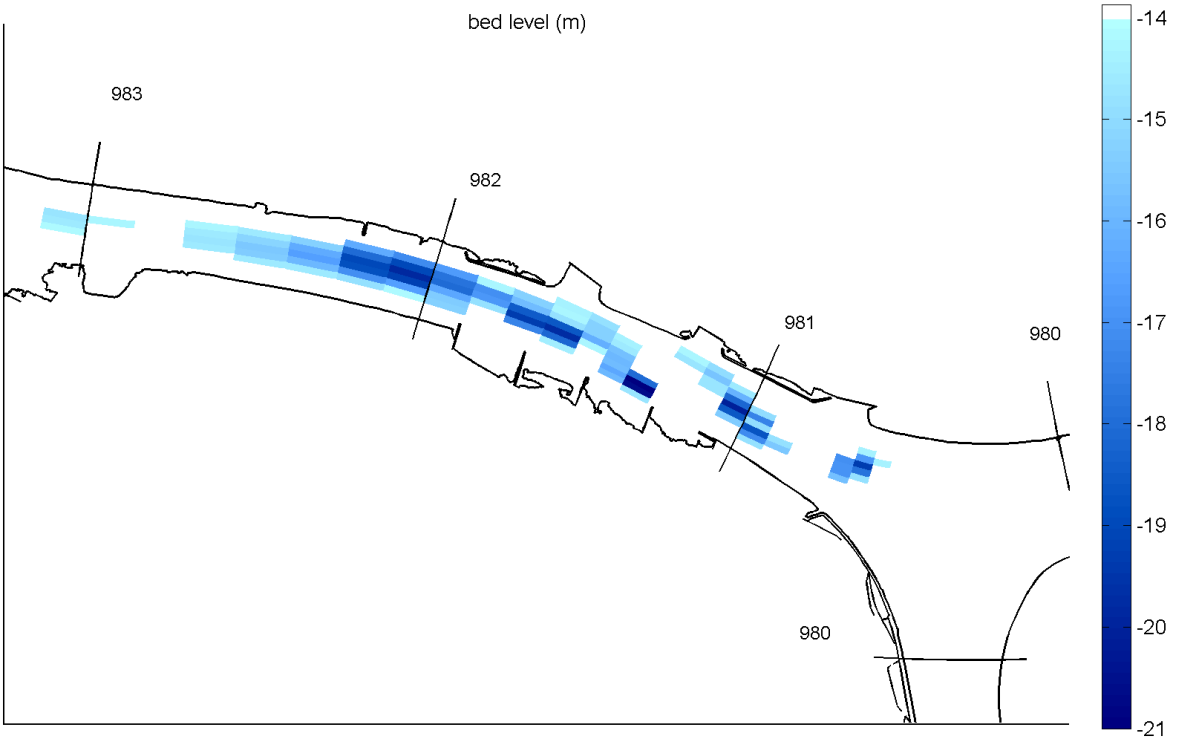

Figure 5.1: Depths larger than 14 m below NAP.

Figure 5.2 shows the amount of sediment needed to fill the erosion holes (figure 5.1), and how this nourishment migrates after one, two and three years[7]. It shows that the nourished sediment is already completely washed out from the scour holes after a year, moving towards the sea through the Oude Maas. Since this rather coarse sediment (with a mean diameter of 600 µm) spreads so quickly, such a nourishment operation does not seem to be a sustainable solution to the local scour problem. However, slow movement and spreading of the sediment is a property that might be useful for a long term nourishment strategy. The direction of the tide averaged sediment transport of the different river branches plays an important role in constructing such a strategy. Section 5.3.3 elaborates further on this particular strategy for a long-term solution.

[6]NAP is short for 'Nieuw Amsterdams Peil', the Dutch reference level for geographical height
[7]Note that the top image of figure 5.2 is essentially identical to figure 5.1

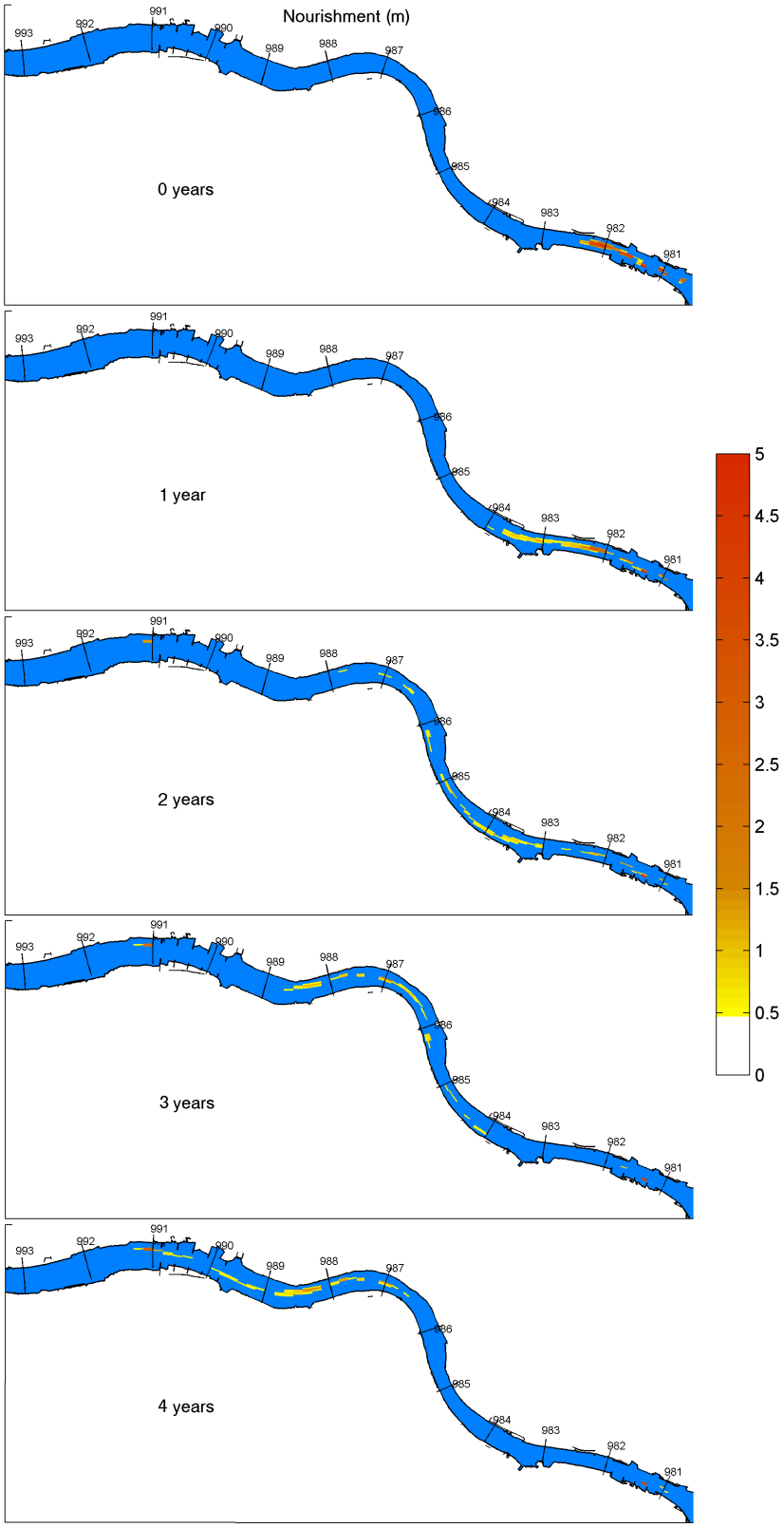

Figure 5.2: Initial nourishment, and the migration after 1, 2 and 3 years.

5.3.2 Fixed scour holes

An obvious solution for dealing with the scour holes is to fixate them with rubble. The weight, thus indirectly the diameter, of the protective material has to be able to withstand the forces that the flow exerts on it. An approximation for this diameter can be extracted from the relation for the Shields parameter ψ (equation 5.1), which should not exceed the value of roughly 0.03 in order to obtain bed stability. Parameter U is the maximum flow velocity in the Oude Maas. It is taken from the numerical model, approximately equal to 1.3 m/s.

$$\theta = \frac{U_*^2}{\Delta g D} \quad \text{with } U_* = \frac{\sqrt{g}}{C} U \tag{5.1}$$

$$\theta = \frac{U^2}{\Delta C^2 D}$$

$$D = \frac{U^2}{\psi \Delta C^2} = \frac{1.3^2}{0.03 \cdot 1.65 \cdot 50^2} \approx 0.014\,\text{m} = 14\,\text{mm}$$

In which:

θ	=	Shields parameter
u_*	=	Shear velocity
Δ	=	Relative density
g	=	Gravitational acceleration
D	=	Particle diameter
U	=	Depth averaged flow velocity

Placing this rubble as bed protection on the locations where a clay layer is not present or has been breached in both the Dordtsche Kil and the Oude Maas, results in the following distribution of protective material (figure 5.3, covering a total area of approximately 1.6 km^2. Figure 5.3 shows the sedimentation and erosion pattern after such an implementation. A logical consequence of this measure is that at the parts of the bed that are protected, no erosion takes place, but the unprotected clay layer still suffers from long term erosion.

5.3.3 Dredging and dumping strategically

Another solution to fight the slow erosion is to keep nourishing the river beds repeatedly (e.g. each year). As we saw in section 5.3.1, a concentrated amount of sediment dumped in the deep scour holes near the junction of the Dordtsche Kil and the Oude Maas has a tendency to migrate seaward (the tidal-average net flow direction) and to spread out over the river bed. Periodically dumping sediment in these pits will cause the outflowing sand to function as a continuous protection against erosion of the clay layer in the Oude Maas. The numerical model can simulate this effect and from this the yearly amount of sediment needed can be computed. It can also be checked whether the distribution of the sediment over the river bed is ideal.

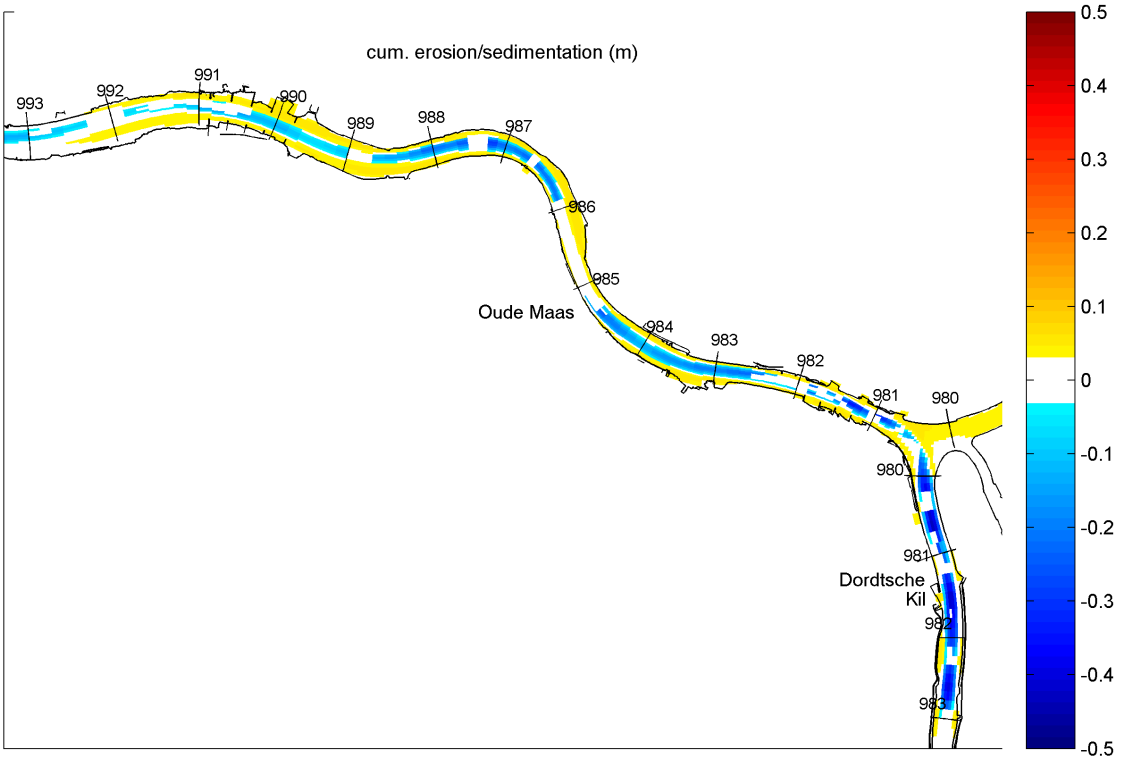

Figure 5.3: Erosion and sedimentation pattern for the situation where every breach in the clay layer is covered with riprap.

From the calculation in the previous section it can be concluded that an amount of 250.000 m^3 of sand will flow out in approximately one year and migrate downstream with the averaged rate of a few kilometres per year. Based on this order of magnitude, the yearly nourishment rate can be determined. The speed with which the sediment moves downstream will also depend on the particle size of the sediment used for nourishment. Varying this particle size in the numerical computation can also be effective in determining the optimal nourishment strategy.

Besides the necessary amount of sediment it is also important to think about the distribution of the nourishment over time. It is not possible to fill the holes with such a large amount of sediment in just one day, but spreading the nourishment evenly over a whole year can result in a different outcome. Both of these strategies are investigated. In the first case the scour holes in the Oude Maas near the junction of the Dordtsche Kil are filled up to a depth of 14 m below NAP; an initial nourishment of 250.000 m^3 just like in section 5.3.1. From here on there is a continuous nourishing of 250.000 m^3 per year in this area during the complete 4 year long morphodynamic simulation, to keep the sand here at approximately the same bed level. This nourishment rate is chosen because the initial nourishment of 250.000 m^3 was gone in about a year. This comes down to 1 cm nourishment per day in the designated area. Figure 5.4 shows the outcome of this simulation, and figure 5.5 shows the initially dumped sediment, followed by the migration in 1, 2 and 3 years.

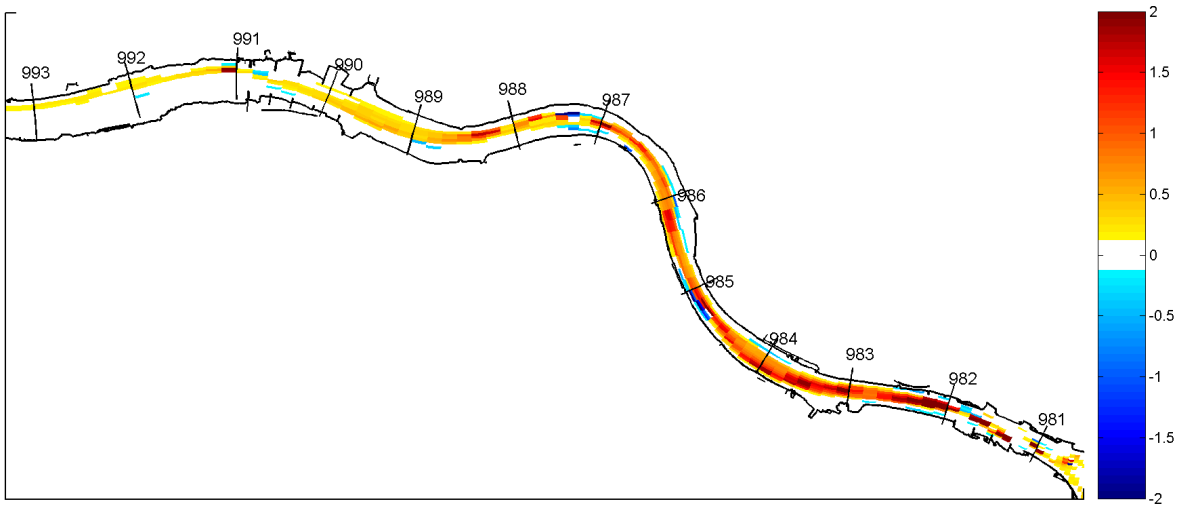

Figure 5.4: The 4 year simulation of continuously nourishing 250.000 m^3 of sediment.

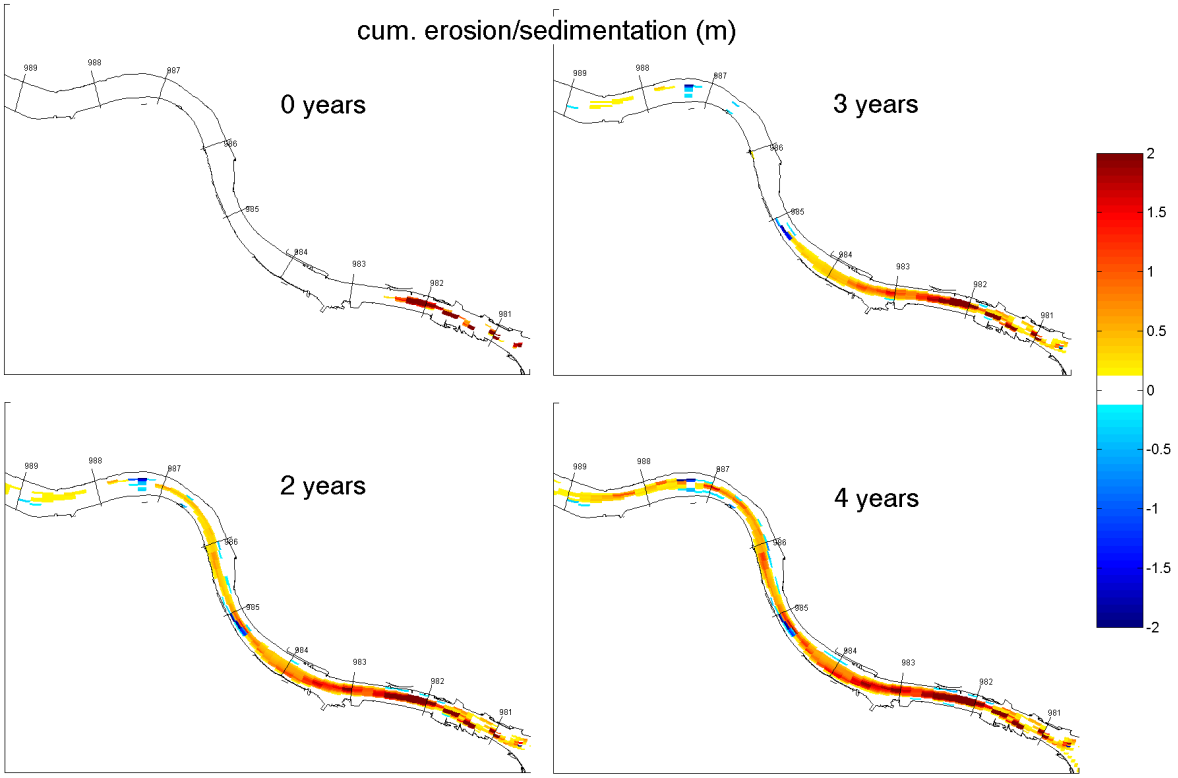

Figure 5.5: Initially dumped sediment and the migration after 1, 2 and 3 years for continuous nourishing.

In the other case, the nourishment that is initially carried out is repeated yearly. This is modelled as yearly filling up the erosion holes to a depth of -14 m below NAP. Because the erosion holes are not equally deep after each year, the amount of sediment needed for this operation will also vary yearly. The amount of sediment needed yearly decreases in time, and is indicated in table 5.1.

Table 5.1: Amount of sediment needed for a once-per-year nourishment

Year	0	1	2	3	4
Nourishment in 10^3 m^3	250	157	151	146	125

The total amount of sediment needed for this operation comes down to 830.000 m^3 from the model computations, a 34% decrease compared to the 1.250.000 m^3 in the case with constant nourishment. The erosion and sedimentation pattern after 4 years is shown in figure 5.6, whereas the initially dumped sediment and its migration after 1, 2 and 3 years are shown in figure 5.7. It can be seen that the largest difference between these two figures and the figures 5.4 and 5.5 is that the piling up of sediment just downstream of the scour holes where the nourishment takes place is reduced. It can therefore be concluded that the extra sediment used in the strategy of constant nourishment with respect to this strategy is not used effectively in the countering of bed erosion.

A major disadvantage of these nourishment strategies is that the sedimentation at several locations in the Oude Maas can become a few metres high in just four years (see figure 5.6). This can be troublesome for navigation in the Oude Maas. This uncontrolled way of nourishment could therefore lead to extra maintenance work .

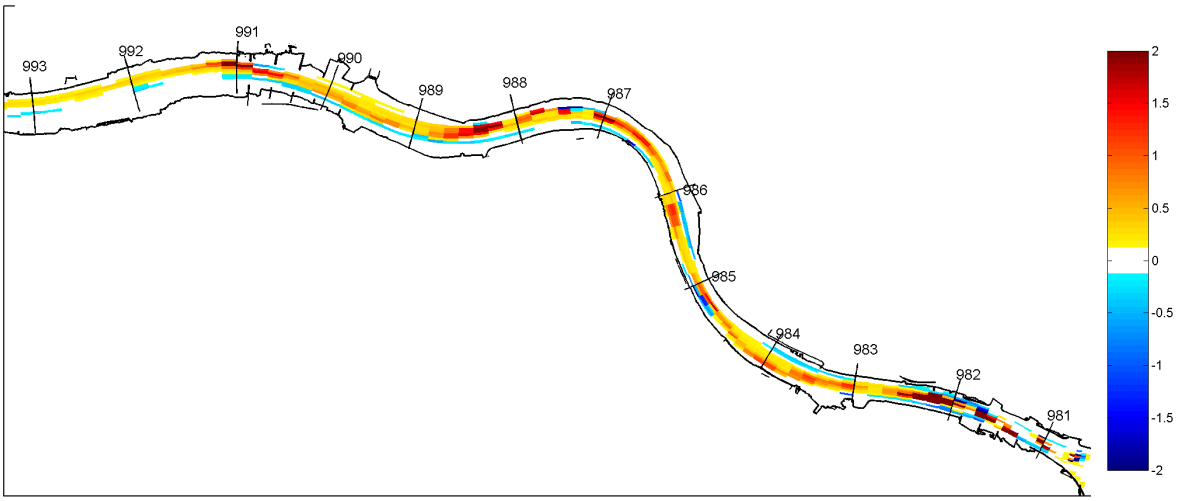

Figure 5.6: The results after a 4 year simulation of yearly nourishing in the Oude Maas up to 14 m below NAP.

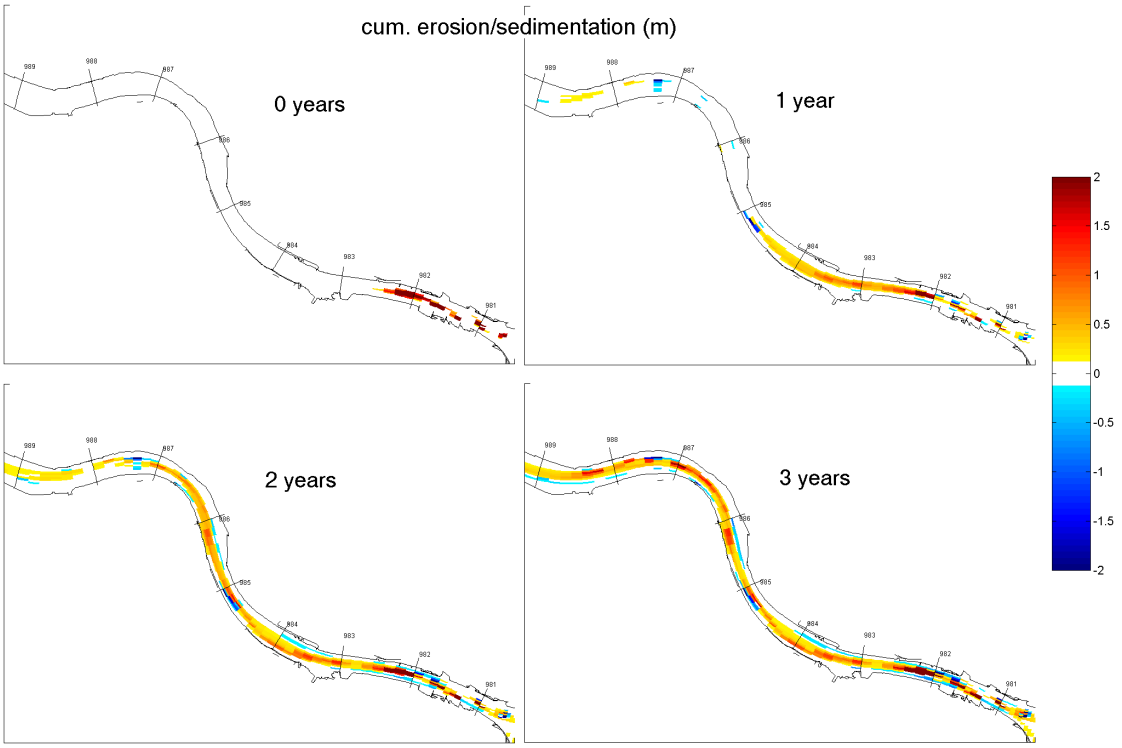

Figure 5.7: Initially dumped sediment and the migration after 1, 2 and 3 years for yearly nourishing up to 14 m below NAP.

With a simple calculation, the migration rate of the sediment can be determined roughly and compared to the results in figures 5.7 and 5.5. Such a simple approach may help to quickly assess the effect of various nourishment strategies on the downstream reach. The calculation is based on a simple relation for the celerity c of a bed perturbation (equation 5.2). The total length L over which the bed perturbation has moved in the complete 4 year simulation is calculated as the total sum (for $t = 0$ through $t = t_e$, the end of the simulation) of the celerities at time t multiplied with time step Δt (equation 5.3). The time step Δt is multiplied with the morphological acceleration factor, which also has to be taken into account. For this simple estimate, the sediment transport rate is based on the Engelund-Hansen formula (1967).

$$c = \frac{b \cdot q_s}{h} \tag{5.2}$$

$$L = \sum_{t=0}^{t_e} c(t) \cdot \Delta t \; = \sum_{t=0}^{t_e} \frac{b \cdot q_s(t)}{h} \cdot \Delta t \tag{5.3}$$

$$L = \frac{b \cdot \Delta t \cdot m}{h} \sum_{t=0}^{t_e} (u(t))^5 \text{, with } m = \frac{0.05}{\sqrt{g} C^2 \Delta^2 D_{50}}$$

$$L = \frac{5 \cdot 50 \cdot 600}{14} \frac{0.05}{\sqrt{9.81} \cdot 50^2 \cdot 1.65^2 \cdot 0.0006} \cdot 658$$

$$L = 1.07 \cdot 10^4 \cdot 3.91 \cdot 10^{-3} \cdot 658 = \boxed{27 \cdot 10^3 \text{ m}}$$

This estimate suggests that the nourished sediment moves at 6-7 kilometers per year, wheras the figures show a celerity of about 2-3 kilometers per year. Possible errors in the computation can be caused by rough estimates for e.g. water depth and roughness, but are most likely caused by inaccuracies in the flow profile over time. The fact that this calculation is based on a sum of both positive and negative values of flow velocity u to the power 5, makes the outcome of this estimate very sensitive to small errors in u. Simple analytical calculations may therefore be considered too inaccurate for designing the appropriate nourishment strategies.

5.4 Strategies to reduce erosive flow

5.4.1 Open the Haringvliet sluice gates

A rather rigorous solution is possibly to open the Haringvliet sluice gates, in order to let the tide flow freely in an out of the Haringvliet. Doing so should lead to a reduction of tidal intrusion in the Oude Maas, causing the erosion to reduce. Again, the downstream conditions for the Delft3D model are extracted from a SOBEK computation, in which the Haringvliet sluice gates are now removed from the model. The downstream boundary conditions extracted from this computation are included in appendix B.

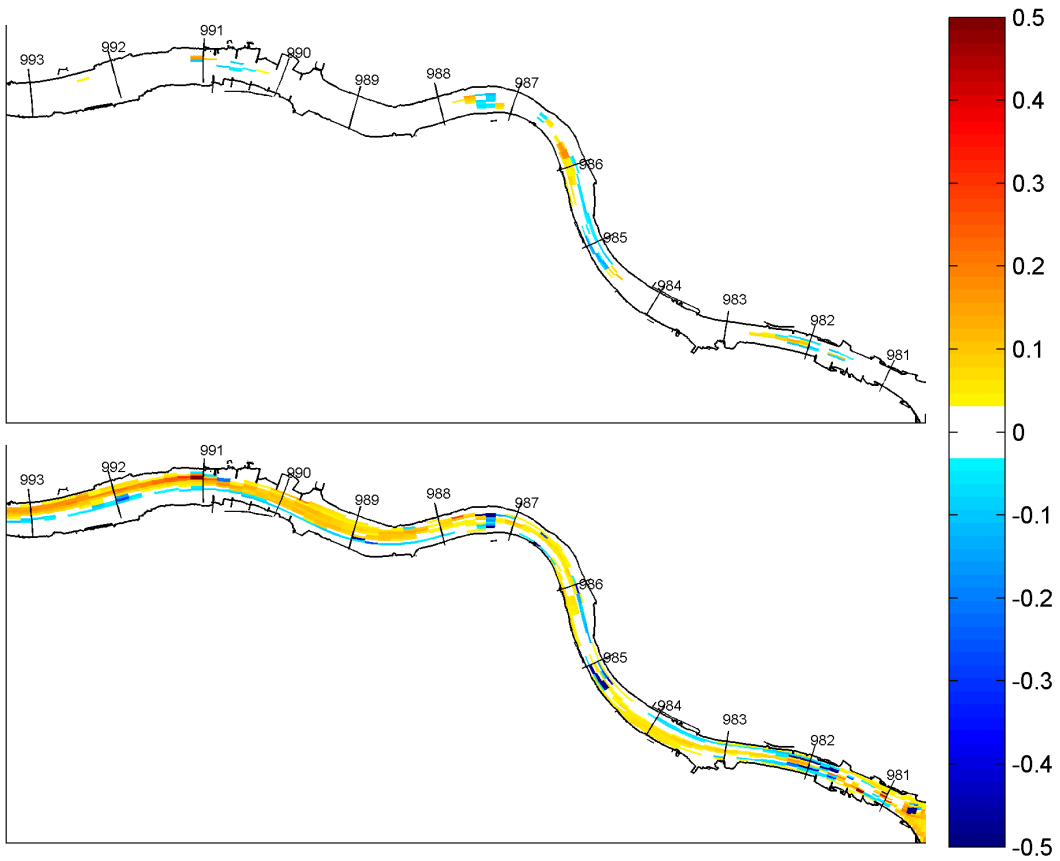

Figure 5.8: Comparison of the erosion and sedimentation for the situation when the Haringvliet gates are open (top) and the current situation (bottom).

5.4.2 Fixed scour holes and opened Haringvliet sluice gates

This strategy, which is a combination of strategy 1a and the fixation of the scour holes (section 5.3.2), results in the optimal, but a very expensive solution. Figure 5.9 shows the comparison of strategies 1a and 1b, where 1b proves to create a very stable situation for both the Oude Maas and the Dordtsche Kil. Note that the scale here is 10 times finer (from -0.1 m to 0.1 m) in order to illustrate the differences in more detail. The big difference in the two situations is that the scour holes do not erode anymore when they are protected. The sedimentation visible in the figure for the case without protection is caused by the sand that has eroded from the scour holes.

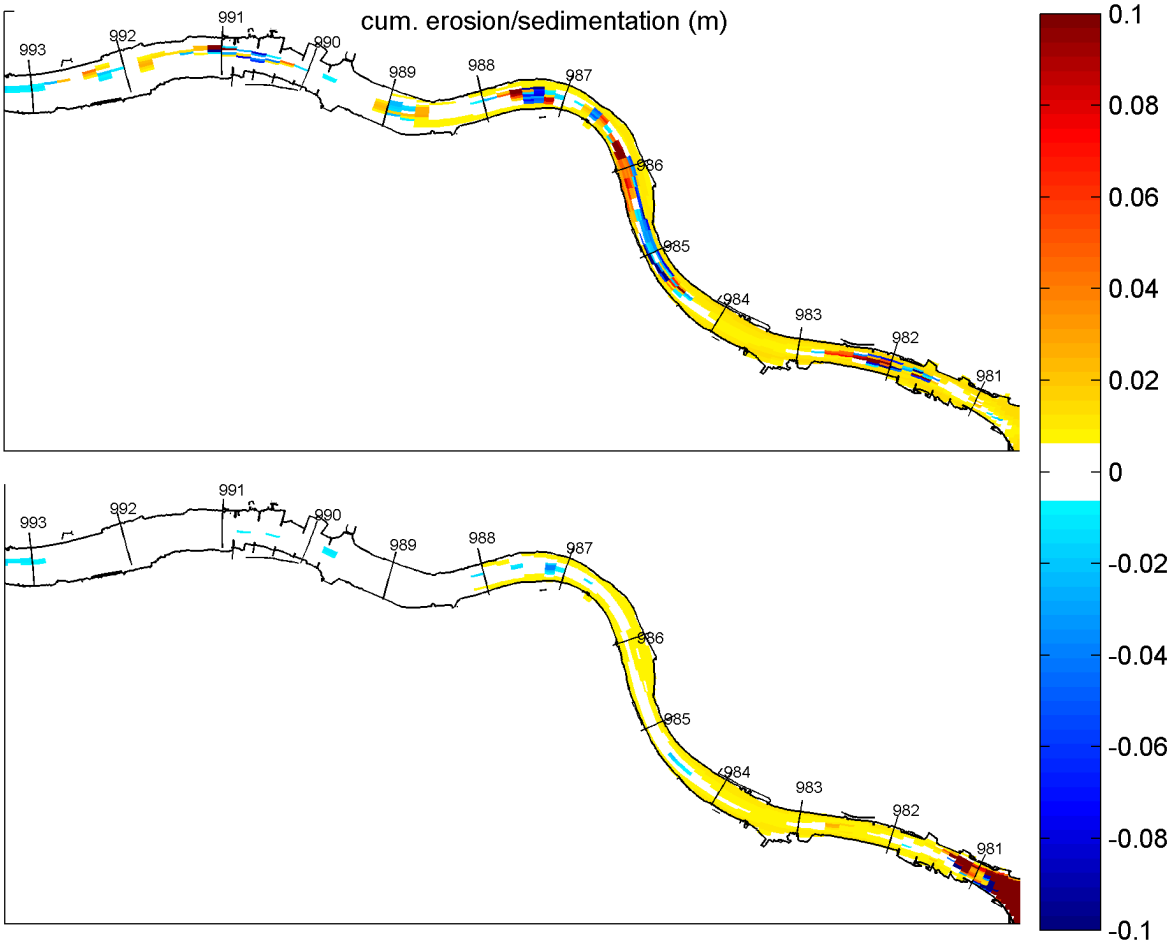

Figure 5.9: Comparison of the erosion and sedimentation for the situation when the Haringvliet gates are open, without fixating the scour holes (top) and with fixed scour holes (bottom)

5.4.3 Closing of the Spui branch

Besides the erosion in the Oude Maas, the erosion in the Spui branch is also alarmingly severe. In order to reduce erosion in this river branch, an option is to close it off. Doing so will cause more water to flow into the Oude Maas, but will keep the Spui from eroding any further. An additional advantage of this strategy is that the flow profile reduces in size, so that the tidal intrusion will reduce as well. The question is, however, if the flow velocity and with that the erosion in the Oude Maas will increase.

Figure 5.10 shows a comparison of erosion and sedimentation before and after the closing of the Spui branch. The maximum flow velocity in the Oude Maas increases by approximately 10%, which translates into slightly more erosion in the Oude Maas, especially for the scour holes. After all, a 10% increase causes the transport capacity to increase with a factor $1.1^5 \approx 1.6$. In the Spui branch, the flow velocity is reduced by more than half, since water can only flow in and out of the branch via the Haringvliet. The difference in maximum flow velocity is illustrated in figure 5.11.

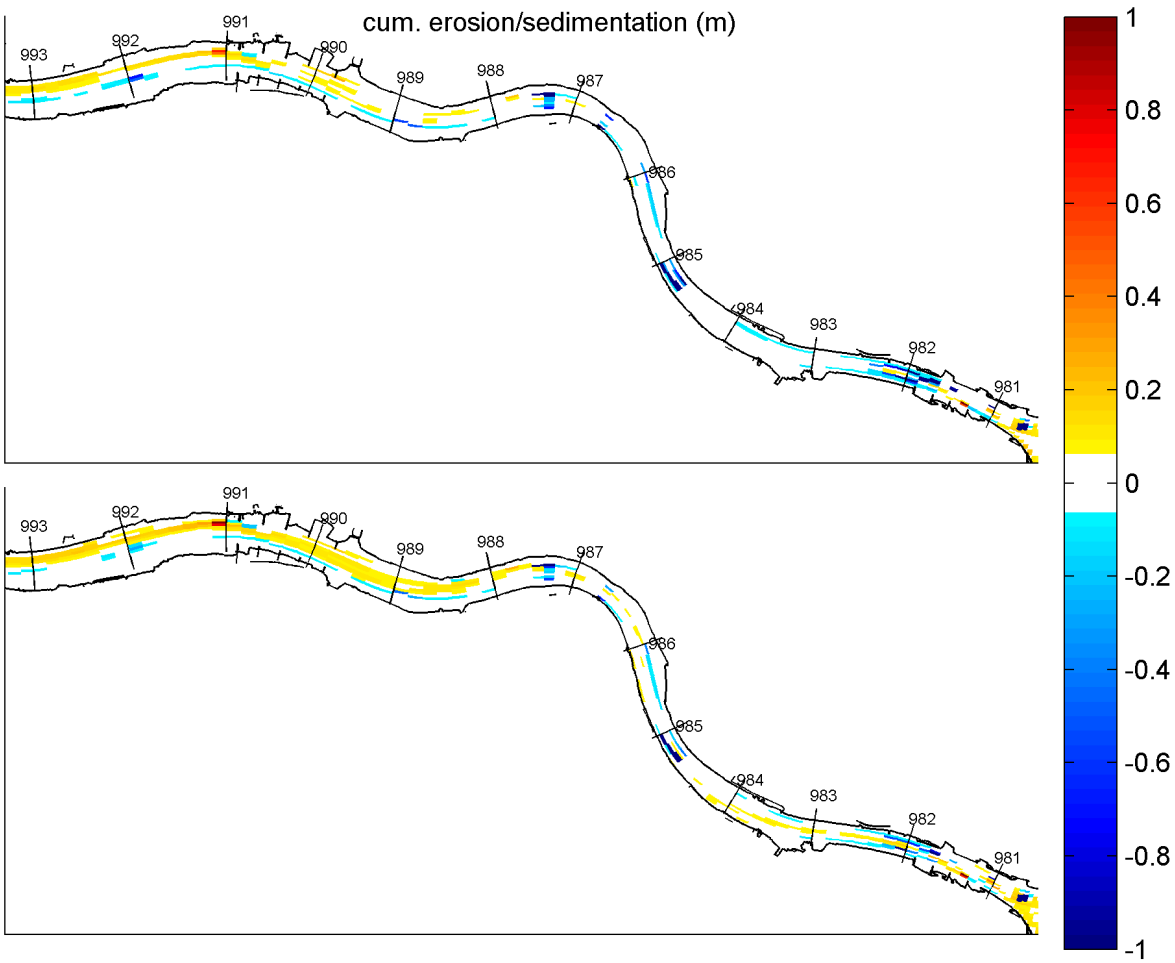

Figure 5.10: Comparison of the erosion and sedimentation for the situation when the river Spui is closed off (top) and the current situation (bottom).

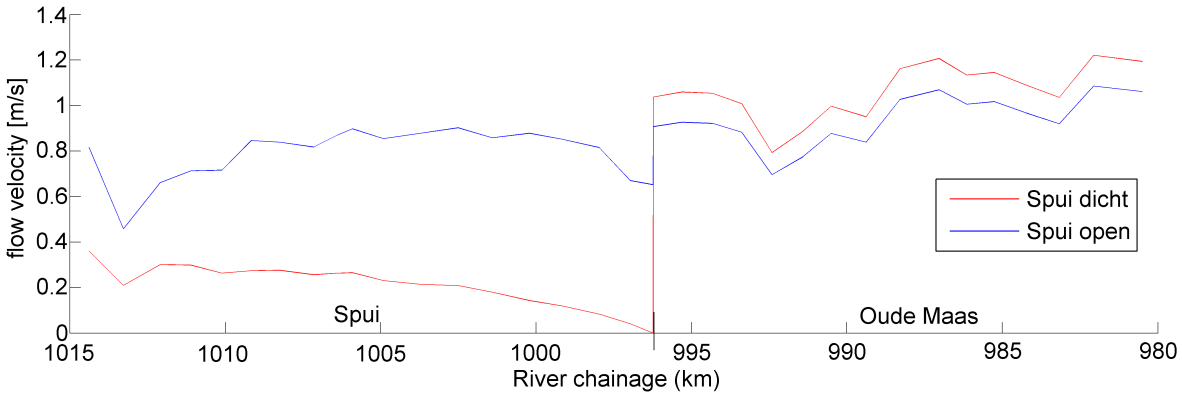

Figure 5.11: The impact on flow velocities due to the closure of the river Spui from the North side.

5.5 Economic consideration

From the analysis of the proposed strategies it becomes quite clear that some of the above strategies are more effective than others, but the costs of these strategies are also an important factor to take into account. The strategies involving nourishment and bed regulation are accurately quantifiable, but quantifying the costs of a new management for the Haringvliet gates is harder. The costs of such an alternative can only be estimated once there is a serious investigation on how to deal with tidal inflow through the Haringvliet river branch, which is unfortunate because the comparison between the opening of the Haringvliet gates and actual measures in the branches themselves can be considered (politically) as the most interesting.

For nourishing and bed regulation, a wide number of possible solutions has been discussed above. As for the nourishment strategy, the most promising solution is to yearly fill up the scour holes in the Oude Maas. A four-year simulation has shown a total amount of necessary sediment of 830.000 m^3, but this measure demands a continuous maintenance, also after these first four years. Under the assumption that the decreasing trend of the yearly amount of sediment needed stagnates (see table 5.1), this will come down to 125.000 m^3 per year after the first few years.

The cost of sand is estimated at $5 - 10$ € per m^3, including production costs, transport costs and actual costs of nourishing. The upper limit of 10 € in this estimation is high, but realistic for a situation where sediment is supplied each month, making transport more costly. Considering an average of 7.5 € per m^3 for the strategy in which nourishment is carried out yearly, the initial investment will be approximately 2 million €, followed by a yearly sum of over 1 million € for the following 3 years. After that, the costs will be about 900.000 € yearly according to this estimation. This solution is however only an effective one for the scour holes in the Oude Maas (the most severe scour), and provide a subsequent protection from clay erosion in this river branch.

The proposed bed regulation by fixating (parts of) the eroding river branches is estimated at a cost of 30 € per tonne. Under the assumption of a 30 cm thickness of the bed protection and a bulk density of 1.65 kg/m^3, this comes down to 15 € per m^2 bed protection. The sum of 30 € per tonne are the costs for the supply of the material and for the execution of the measure. Protecting only the parts in Oude Maas and Dordtsche Kil that are not protected by a clay layer, as simulated in section 5.3.2, demands a total area of 1.6 km^2 bed to be covered with rubble. The costs of such a measure would come down to an estimated 24 million €. Compared to the nourishment strategy, this solution is more durable. Costs of yearly nourishment will exceed the costs of bed protection in about 15 years[8]. An additional notion on the costs of different strategies is that solutions that include a one-time investment can be considered more attractive to the involved parties.

For the fixation of a local scour hole, the technique of using reinforced dredged material is an interesting one to consider, since sand in the scour holes has proven to wash out rapidly. The procedure of this technique is to sieve the coarse sediment particles out of the dredged material and to mix it directly with a hardener. The costs of such a measure are estimated at 30 − 50 € per m^3 (Van de Velde et al., 2009). Applying 30 cm of reinforced dredged material to the 1.6 km^2 of river bed that is not protected by a clay layer would cost 19.2 million €, assuming 40 € per m^3.

Just like the nourishment strategy, the above mentioned bed protection only provides a solution for the modelled parts of the problem area in the Rhine-Meuse delta: the Dordtsche Kil and a part of the Oude Maas. To be completely sure of a non-eroding Rhine-Meuse delta, one should fixate the branches of the Oude Maas, Noord, Spui and Dordtsche Kil completely. The total area of these river beds combined is estimated at 15 square kilometres, so that the costs of this rigorous measure would come down to roughly 225 million €.

The opening of the Haringvliet gates is also expected to provide a solution for all the river branches in the Rhine-Meuse delta affected by erosion. The costs of such a measure, however, are very hard to estimate, but there are known costs of the project 'Haringvliet gates ajar', which was described in section 5.1. The Dutch government invests 35 million € in this project, but also taking into account the contribution of the province, the water board and many others, the total investment comes down to 56 million (Burgers et al., 2004). However, the far-reaching measure of opening the Haringvliet gates further is expected to cost a multiple of this amount of money, and is therefore probably more expensive than the robust but less elegant solution of fixating all the branches subject to erosion.

[8]Not accounting for inflation or interest

5.6 Influence of sea level rise

Considering that a solution for this problem should be one that suffices for several decades, it is important to investigate the influence of sea level rise for the maintenance solutions as well. A particularly interesting case is the one where the Haringvliet gates are opened, since the sea level rise of 1 metre can change the distribution of tidal inflow with respect to the opened Haringvliet gates situation without the influence of sea level rise. Figures 5.12 and 5.13 compare these two cases, where the boundary condition for the case with sea level rise has again been deduced from a SOBEK computation (see Appendix B).

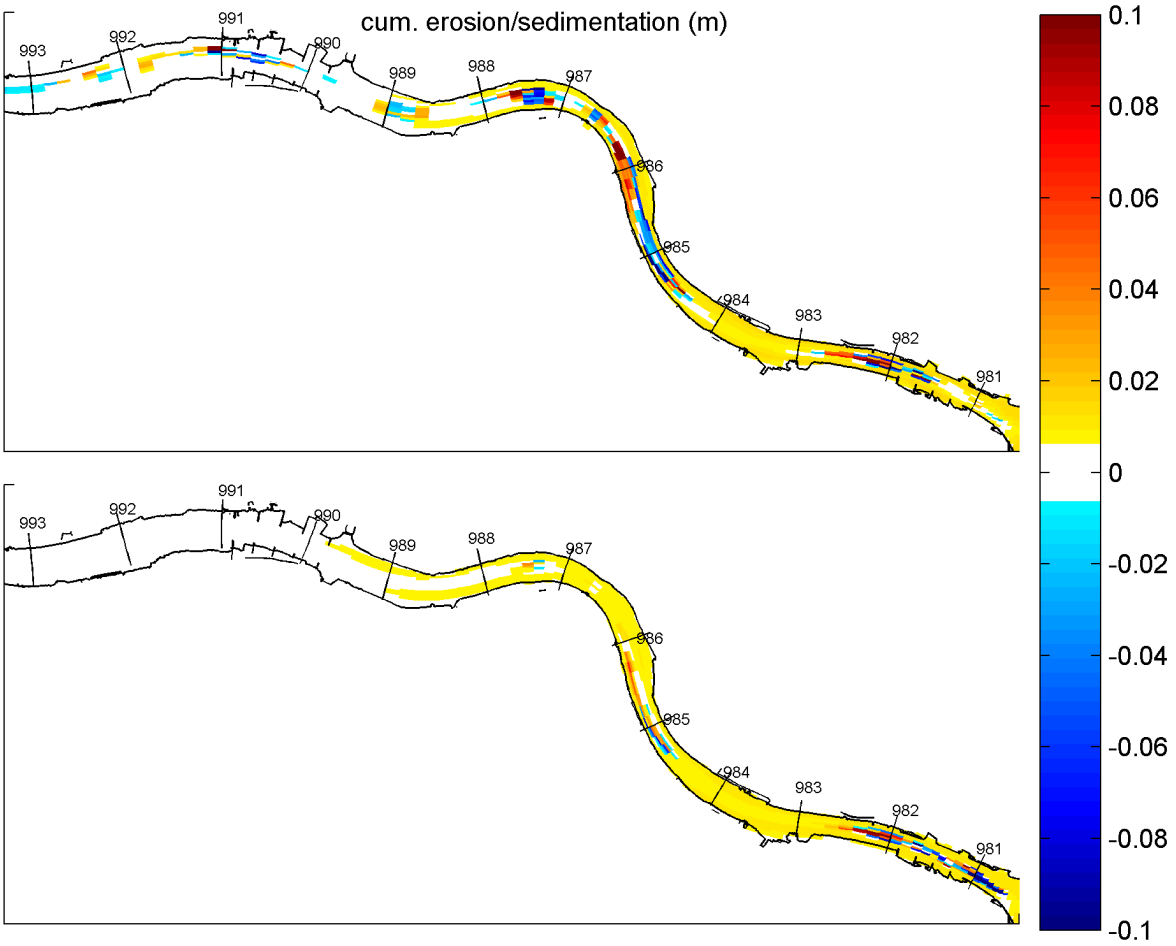

Figure 5.12: Cumulative sedimentation and erosion pattern in the Oude Maas in the situation where the Haringvliet gates are open, under the condition of a normal sea level (top) and 1 metre sea level rise (bottom).

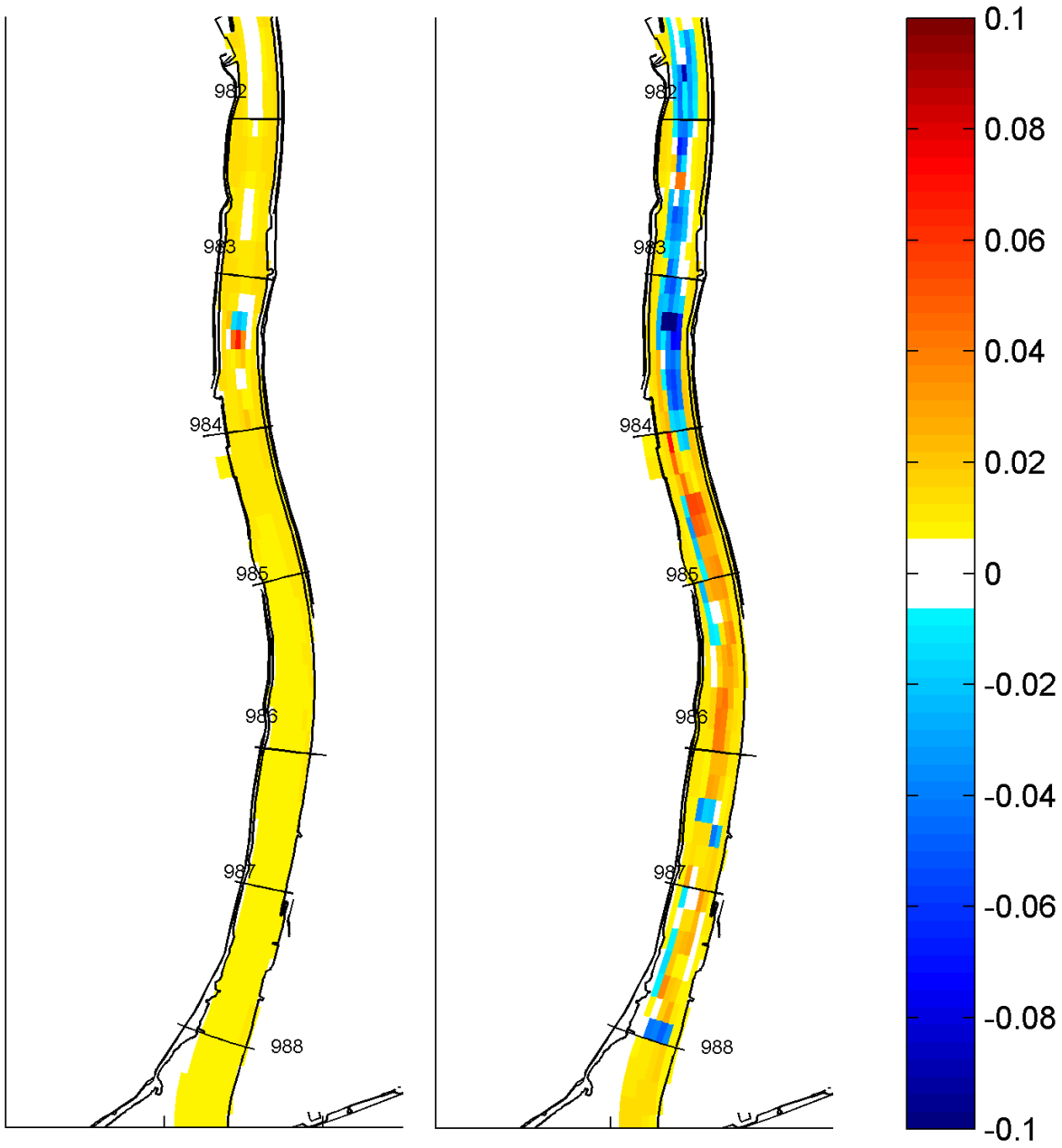

Figure 5.13: Cumulative sedimentation and erosion pattern in the Dordtsche Kil in the situation where the Haringvliet gates are open, under the condition of a normal sea level (left) and 1 metre sea level rise (right).

From the figure it can be seen that the differences in the Oude Maas are not substantial, but the effect on the Dordtsche Kil is notable. This is in line with the computations of sea level rise given the current management of the Haringvliet gates. Note that the scale of the figures goes from -0.1 to 0.1 metre, so that the magnitude of the erosion in the Dordtsche Kil is a few centimetres per year. Nevertheless, the change in erosion and sedimentation under influence of sea level rise is worth mentioning, and shows that the Dordtsche Kil is also sensitive to large-scale erosion, an outcome that the computations without sea level rise do not provide.

The extra reduction of erosion for the strategy where the Haringvliet gates are open, in combination with 1 metre sea level rise, can be considered an extra argument for this strategy. For the Dordtsche Kil however, more attention is needed when the sea level rises, just like in the current situation without the opening of the Haringvliet gates. An additional point of attention is that salt intrusion can increase heavily when the flow profile increases, which is an additional disadvantage of the strategy considering the fresh water supply in the Haringvliet.

5.7 Conclusions

The model outcomes are promising for both the long term and the short term solutions, in a sense that several effective strategies are available to deal with the erosion problems. The best way to deal with the local scour problems is to prevent further scouring of existing holes by fixation with rubble. Changing the flow by a change of management can reduce the speed at which the scour holes erode, but an eroding trend is, according to this model, still visible for these conditions.

Letting more sea water into the Haringvliet river by opening the gates during high tide leads to a remarkable reduction in erosion. The scour holes still undergo erosion, but at a slower rate, and the erosion of the clay layer decreases to a negligible amount. The alternative that results in the same outcome would be to apply bed protection for the Dordtsche Kil and Oude Maas, and possibly also for the rivers Noord and Spui, which suffer from similar erosion problems. An assessment of which solution should be implemented should be made in the future, in which a more detailed investigation of the costs and additional advantages or disadvantages is necessary. Economically it would probably be best to apply bed protection as opposed to opening the Haringvliet gates. The cost of the 'Haringvliet gates ajar' project are already over 50 million and the solution of completely opening the gates is considered to cost a multiple of that number. The following is an overview of the advantages and disadvantages of different solutions.

Nourishment strategies

Advantages	**Disadvantages**
The solution is cheap and easy to realise.	The strategy needs continuous attention. The project's costs are not one-off, instead costs are continiously increasing. The nourishment is uncontrolled and can hinder navigation.

Bed protection

Advantages	Disadvantages
Protection of the erosion holes with riprap or enforced dredged material provides direct protection against erosion.	The execution of fixating the erosion holes might be difficult, since sand tends to flow out rapidly. In order to provide full protection against erosion, all the branches that suffer from gradual erosion need to be protected, which is a costly operation

Open Haringvliet gates

Advantages	Disadvantages
Opening the Haringvliet gates leads to a remarkable reduction in erosion, without having to take measures in the area itself. This strategy reduces erosion by tackling the core cause of the eroding trend. An additional advantage of this strategy is the opportunity for ecological development due to salt intrusion.	Although the gradual eroding trend stops by opening the Haringvliet gates, this does not apply for the locations where the clay layer is locally breached. The salt intrusion caused by this strategy is also a problem for fresh water supply in the area near the Haringvliet gates.

Closure of the river Spui

Advantages	Disadvantages
Closing off the river Spui leads to a reduction of the flow profile through which the tide intrudes.	The flow velocities in the Oude Maas increase, leading to a slight increase in the rate at which the erosion holes erode. Closing of the Spui branch can be disadvantageous for navigation as well.

Open Haringvliet gates and bed protection

Advantages	Disadvantages
Opening the Haringlviet gates and locally protecting the erosion holes would be a complete solution to the problems described in this study. Bed protection is directly applicable and opening the Haringvliet gates tackles the gradual erosion problem at its cause.	The solution is expensive and the problem of salt intrusion also applies for this strategy.

As for the development under future conditions, opened Haringvliet gates with a condition of sea level rise cause no big change with respect to the current situation, which is in line with the computations made in chapter 4, where the difference between current and future conditions were rather small as well. The flow in the Dordtsche Kil seems more sensitive to sea level rise than the flow in the Oude Maas.

6 Discussion

This chapter discusses the numerical aspects and the simplification of hydrodynamics and morphodynamics in the numerical model.

Model boundaries

The numerical model has been decomposed into 5 different domains, each interacting with each other. A domain decomposition is very useful for a complex geometry like this part of the Rhine-Meuse delta, and has besides this flexibility several other advantages like local grid refinement and reduced memory demands. Another advantage is that the morphological updating can be switched on and off for all the upstream domains in the model that do not cover the area of interest in order to save computation time. Doing so, however, can have an effect on the interaction of sediment between the upstream domains and the domain that covers the Dordtsche Kil, Oude Maas and Hollandsch Diep.

Although this model now covers both the hydrodynamics and the morphodynamics of the river Dordtsche Kil and a part of the Oude Maas quite well, there are more rivers in the Rhine-Meuse delta that suffer from the same erosion problems, as already stated in section 1.2. For a better overall maintenance strategy, it is useful to include the whole Oude Maas, the Spui and the Noord as domains in the model, which Deltares is currently (November 2011) working on. Moreover, the interaction of sediment transport between these branches and the domain that is investigated in this research can be of influence on the results presented in this report.

Another point of discussion is that the boundary at the river Noord has now been implemented as a downstream boundary, whereas this river is actually an interconnection between the rivers Oude Maas − Boven Merwede and the rivers Nieuwe Maas − Lek. In the research by Giri (2010) this was already investigated, considering also the options of an (upstream) discharge boundary or a discharge extraction or insertion, like the implementation of the Amer river in this numerical model. A downstream water level boundary proved to be the best solution, but might also be more accurate when the domain of the river North is connected to the model. Another curiosity of this boundary is that it is quite close to the junction of the Dordtsche Kil and the Oude Maas, possibly resulting in some inaccuracies, which can also be solved by extending the model with (a part of) the river Noord. In any case, a new assessment of the type of boundary condition should be made when this river is connected to the model.

Computation time

Probably the most substantial limitation to this research is the computation time of the model. The current numerical model, with 5 domains and a 2DH grid simulates 30 days of hydrodynamics in approximately 20 hours. With a morphological factor of 50 for the average discharge situation this comes down to a 4 year morphological computation. Longer simulations would be preferable, but to be able to simulate 4 years within a day is already at the cost of a few simplifications.

The most severe but also most time saving simplification is the assumption of depth averaged flow velocity by modelling in 2D instead of 3D. Although a 2D model provides realistic morphodynamics results, a 3D model would capture a lot of local effects like vertical flow. These effects can play a substantial role for locations in the model with large local bed level variations like scour holes. The water around a scour hole has a tendency of flowing downwards into a hole, which is an effect of which the details cannot be captured with a 2D model.

The complete multi-domain model consists of several rivers, each with its own bed level characteristics. The sediment in the Dordtsche Kil for example is generally much coarser than the sediment in the Oude Maas and in the Hollandsch Diep, and over the length of each river the distribution of sediment also varies widely, as can be seen in figures A.2 and A.3 in Appendix A. The current numerical model, however, only provides 2 different sand fractions[9] and one mud fraction, since each additional fraction has a non-negligible impact on the computation time. With a wider variety of sediment fractions, results might be more accurately quantifiable.

Another time saving measure is that the multiple sediment layers have only been implemented in domain 5, which covers the area of interest. Applying multiple layers requires more computation time, and causes the data file to become very large. A possible disadvantage of this simplification is that the upstream domains can only be modelled as a fully mixed layer. The amount of inflow of sediment in domain 5 could deviate from reality, although this does not automatically mean that the erosion and sedimentation patterns in the Oude Maas and Dordtsche Kil are affected by this. Connecting new domains for which similar erosion problems like in the Oude Maas and Dordtsche Kil have to be computed can make computations quite cumbersome due to this extensiveness of multiple sediment layers.

[9]The two sand fractions in the model, a fine one and a coarse one, are described by a standard log-normal distribution with a mean particle diameter of 300 and 600 µm respectively. However, these two can be mixed to simulate fractions in between. This is described in section 3.4.2.

Sand-mud interaction

The morphodynamic model includes sediment fractions for both sand and mud. Delft3D takes interactions between different fractions into account, although especially in the field of sand-mud interactions still a couple of processes are lacking. Understanding the distribution and interaction of sand and mud in this area can be important for maintaining the river branches and for the sediment bed quality, and can be investigated with a large-scale model, as presented in the work by Van Ledden (2003). These processes might especially be of substantial importance in a scenario where the management of the Haringvliet gates is changed rigorously, since a change in tidal flow can have a lot of influence on the sand-mud interaction as well.

An additional effect that can have a great impact on the behaviour of suspended mud is the salinity of the water, which also changes with opening the Haringvliet gates. Salinity is not at all included in the numerical model and can play a role in processes like flocculation, especially in further investigations of a possible change in the management of the Haringvliet gates.

Economical and political feasibility

Economical and political consequences of a different management of the Haringvliet gates are discussed in chapter 5 but not carefully quantified. First of all, the feasibility of this measure is not certain without further investigation of the consequences for stakeholders and the economical consequences. Secondly, without a good estimate of the costs of a different Haringvliet strategy, it is hard to say whether this is really a good solution as opposed to the solution of nourishment or even fixing all the river branches with rubble.

On the other hand, other maintenance strategies can become quite costly as well. From a technical point of view it is obviously necessary to act immediately before the erosion, and especially local erosion, becomes a serious threat for the stability of dikes. The Dutch government can only spend its money once, and the question is whether this particular problem can get the appropriate political attention. Otherwise some of the strategies presented in chapter 5 will simply be to expensive and time-consuming.

7 Conclusions and Recommendations

7.1 Conclusions

On the basis of the goals of this research, some conclusion can be drawn. The goals with corresponding conclusions are stated here below.

Create a multi-layered model to capture the effects of sediment erosion between and under clay layers and determine whether a 2DH model with multiple sediment layers is sufficient for investigating local scour

The first main question at the start of this research is whether a 2DH model with multiple sediment layers is sufficient for investigating local scour, more specifically regarding a bed composition where clay layers and local sand packages alternate. More generally, this research has shown that a detailed chart of the river's subsoil can sometimes be a necessity in understanding the occurrence of erosion and sedimentation processes.

Calibrate the morphodynamics in an available Delft3D model in such a way that the erosion in the Oude Maas is of the right order of magnitude.

The initial model, with hardly any morphodynamic calibration, has been improved in such a way that it quantitatively fits the existing long term erosion trend, since the clay layer in the model now erodes at the same order of magnitude as in reality. Varying upstream discharge conditions did not have a strong impact on the long-term sedimentation and erosion patterns of the Oude Maas and Dordtsche Kil. Therefore, the assumption of an average upstream discharge is justifiable for investigating the erosion problems. Since this part of the Rhine-Meuse delta is a transition area between tidal influence and river influence, the direction of flow in the system is influenced by a change in upstream discharge. For example, the net sediment transport direction in the Dordtsche Kil changes from North to South for high upstream discharges. For future conditions, the flow in the Dordtsche Kil seems to be more sensitive to sea level rise than the flow in the Oude Maas, especially if the Haringvliet gates are open. The simulation with an extreme flood discharge shows that the scour holes are very vulnerable to high discharges, which can be considered an extra incentive to take action rapidly.

Investigate and possibly optimise the behaviour of the model around scour holes using this multi-layered model.
The accuracy of the erosion rate in scour holes is hard to determine, since some effects are not taken into account. However, the qualitative processes of scour in the model simulations

comply with the erosion occurring in reality. Not only does the model reproduce the scour processes in the existing scour holes, it also produces scour holes at some other locations with underlying sand layers. These locations should be dealt with preventively in order to avoid new deep scour holes.

Define and subsequently model suitable maintenance strategies for the project area in the Delft 3D model.

The model outcomes for different maintenance strategies are promising for both the long term and the short term solutions. Filling up scour holes with coarse sand has proved to be an non-durable solution for the local scour problem. However, continuous nourishment in scour holes in the Oude Maas near Zwijndrecht prevents the existing holes from scouring any further and provides sedimentation spread out over the Oude Maas. Although, this spreading sediment could lead to navigation problems. Another disadvantage of the nourishment strategy is the future obligation of continuous maintenance and monitoring for the whole Rhine-Meuse delta.

Letting more water into the Haringvliet river by opening the gates during flood leads to a remarkable reduction in erosion. The strategy that result in a total stable outcome would be to apply bed protection for the Dordtsche Kil and Oude Maas, and possibly also for the rivers Noord and Spui, which suffer from similar erosion problems. As for the development under future conditions, opened Haringvliet gates with a condition of sea level rise cause a big change with respect to the current situation, as opposed to the calculations made in chapter 4, where the difference between current and future conditions were rather small.

7.2 Recommendations

Given that the subsoil of the river was essential for this research, it is strongly recommended to have some database of detailed river subsoil charts, which can be used for monitoring and maintaining rivers. Deep scouring as in the Rhine-Meuse delta can be prevented if the lithological information is available beforehand.

A recommendation regarding the local scour problems is to further investigate the processes in and around a deep scour hole with a 3-dimensional model. The model that has been used now is a depth averaged model (2DH) and cannot capture all the effects that occur (as already mentioned in the discussion), while some of the occurring flow can be crucial for the severe ongoing scour. Research with a 3D-model could help to understand this problem better for possible similar situations in the future

For fixating the scour holes in order to prevent any further excavation, more research on flow around scour holes is not an absolute necessity. However, the process of fixation is a complicated one, so that it is recommended to look into possible ways to execute such a task. The previously mentioned technique of reinforced dredged material is a possible way of doing this.

It is strongly recommended to investigate the effects and possibilities of opening the Haringvliet sluices further. The effects of salt intrusion can be modelled with Delft3D as well, which is specifically recommended in further investigating this strategy. Also very important questions regarding this measure are to which extent it is politically possible to implement such a measure, and what the costs are of a change in operating the Haringvliet gates.

Given that the measure of keeping the Haringvliet gates ajar already costs 35 million €, of which 80% goes to the management of freshwater supply, a more detailed cost analysis of completely opening the gates should be done, which would logically cost a multiple of this 35 million. Is it feasible to keep implementing compensatory measures in the Haringvliet for freshwater supply when the gates will be opened further? Or should there be a change of mindset in the management of the Haringvliet area? These kinds of questions should be placed on a balance in a more detailed investigation regarding the Haringvliet gates management. Economically it would probably be best to apply bed protection as opposed to opening the Haringvliet gates. A nourishment approach can be less expensive, especially on the short term. However, a full assessment of a nourishment strategy cannot be carried out, since the model only covers a part of the total problem area. A more detailed economical analysis will also improve the possibility to make a decision on which long term maintenance strategy to apply in the Rhine-Meuse delta.

Also, further research should be done with the extension of the Delft3D model to the Spui river, the downstream part of the Oude Maas and the Noord. Since the numerical model can become (even more) extensive with the implementation of 3 more domains, much more insight in the problems can be obtained with the interaction of the different eroding branches in a Delft3D model. If the computation times of such a large model become unacceptably long, then of course these river branches should be investigated individually. A multi-bed-layer 2DH model as used in this study or a 3D model can be used to investigate the long term and local erosion in these branches as well, for which this study can be a useful start.

References

Burgers, M. et al. (2004) Realisatie de Kier: doordacht doen!: eindrapportage planstudie Haringvlietsluizen op een kier. Stuurgroep Realisatie de Kier.

Deltares (2010) Delft3D-FLOW User Manual; Simulation of multidimensional hydrodynamic flows and transport phenomena, including sediments. Version 3.14, Delft.

Engelund, F., Hansen, E. (1967) A monograph on Sediment Transport in Alluvial Streams. Teknisk Forlag, Copenhagen.

Giri, S. (2010) Study of Dordtsche Kil and Hollands Diep area using Delft3D. Deltares, memo 12002136-006.

Jansen, P. Ph. (Ed) (1994) Principles of river engineering: the non-tidal alluvial river. Delftse Uitgevers Maatschappij.

Klopstra, D., Barneveld, H.J., van Noortwijk, J.M. and van Velzen, E.H. (1997) Analytical model for hydraulic roughness of submerged vegetation. Proc. Managing Water: Coping with scarcity and abundance, San Francisco, pp 775-780.

Koch, F. G., Flokstra, C. (1980) Bed level computations for curved alluvial channels. In Proceedings of the XIXth congress of the International Association for Hydraulic Research.

Ledden, M. van (2003) Sand-mud segregation in estuaries and tidal basins. Dissertatie TU Delft.

Linden, M. van der, J.W. van Zetten (2001) Een SOBEK-model van het Noordelijk Deltabekken: bouw, kalibratie en verificatie. RIZA rapport; 2002.002. RIZA, Dordrecht.

Meyer-Peter, E., Müller, R. (1948) Formulas for bed load transport. In Proc. $2^n d$ Congr. IAHR, Stockholm, col. 2, paper 2, pp. 34-64.

Mosselman (2005) Basic equations for sediment transport in CFD for fluvial morphodynamics, In Computational Fluid Dynamics: Applications in Environmental Hydraulics, Bates, P.D., Ferguson, R.I. and Lane, S.N. (eds.). John Wiley and Sons.

Partheniades (1965) Erosion and Deposition of Cohesive Soils. Journal of the Hydraulics Division.

Rijn, L.C. van (1984c) Sediment transport, Part III: bed form and alluvial roughness. Journal of Hydraulic Engineering 110 (12): 1733-1754. 272, 365.

Rijn, L.C. van (1993) Principles of Sediment Transport in Rivers, Estuaries and Coastal Seas. Aqua Publications, The Netherlands.

Rijn, L.C. van (2007a) Unified view of sediment transport by currents and waves I: Initiation of motion, Bed roughness and Bed load transport, in: Journal of Hydraulic Engineering.

Rijn, L.C. van (2007b) Unified view of sediment transport by currents and waves II: Suspended transport, in: Journal of Hydraulic Engineering.

Sloff, C.J., Ham, G.A. van den,Stouthamer, E.,Zetten, J.W. van (2011) Visie Beheer bodemligging in Spui, Oude Maas en Noord.

Snippen, E., Fioole, A., Geelen, H., Kamsteeg, A., Van Spijk, A., Visser, T. (2005) Sediment in (be)weging: Sedimentbalans Rijn-Maasmonding periode 1990-2000. Rapport Rijkswaterstaat RIZA, afdeling WRE

Stouthamer,E., De Haas,T. (2011) Erodibiliteit en risico op zettingsvloeiing als maat voor stabiliteit van oevers, onderwatertaluds en rivierbodems van de Noord, de Oude Maas en het Spui. Universiteit Utrecht.

Talmon, A.M., Struiksma, N., Van der Meer, M.C.L.M (1995) Laboratory measuremens of the direction of sediment transport on transverse alluvial-bed slopes. Journal of hydraulic research.

Veen, J. A. van (1946) Electrische nabootsing van getijden, De Ingenieur 61.

Velde, J. L. van de, et al. (2009) Versterkte baggerspecie, een nieuwe innovatieve bouwstof. Bodem, nummer 1, februari 2009, p. 20-22.

Appendix

A Sediment data

A.1 Start-up

For the start-up of this research, a few data concerning the bed characteristics of the Rhine-Meuse delta have been used. Besides the data from the report of Stouthamer and De Haas (2011), a few charts from the report by Sloff et al. (2011) on the Rhine-Meuse delta have been used to get an idea of for example the variation in grain size and the variation in bed level change over the last couple of years. For the start-up of this research, figure A.1 taken from Giri (2010) was used for the sediment layers.

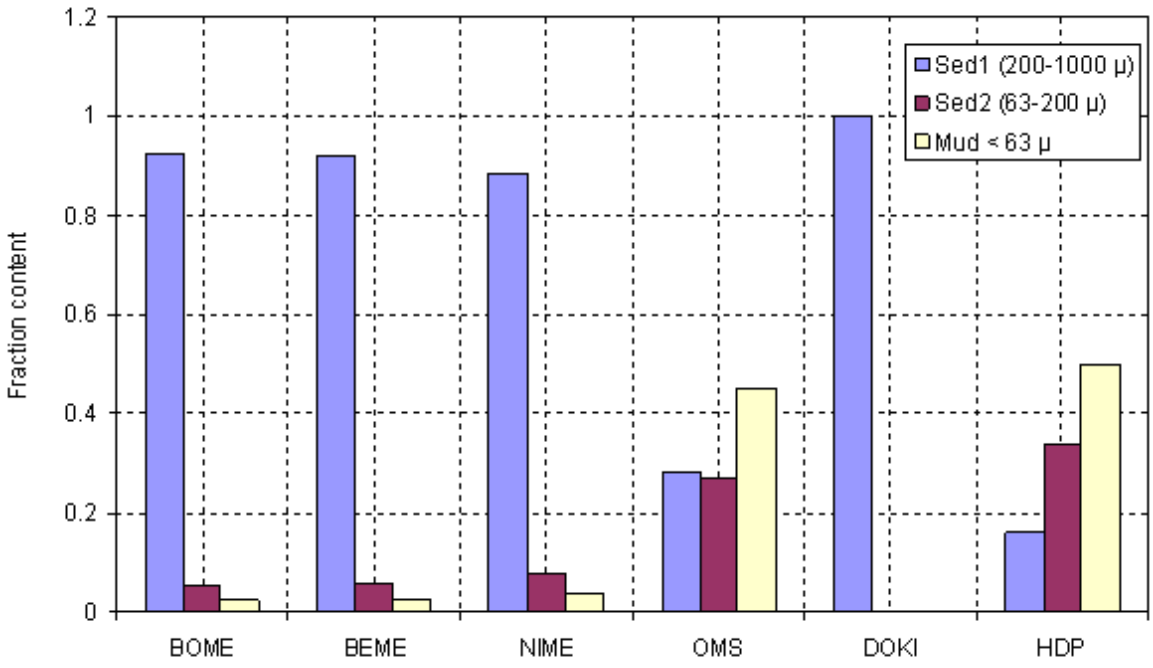

Figure A.1: Distribution of sediment fractions for the single mixed layer morphodynamic model.

A.2 Sediment distribution

Figure A.2 and A.3 were used for a first estimate of the mean particle diameter and variance for the sediment distribution. From here on out distributions for 3 different sediment fractions were specified and implemented in the morphodynamic model. Both figures show a wide variation in particle size for different locations along the rivers. Note that for the Oude Maas not all the data lies within the domain of the numerical model.

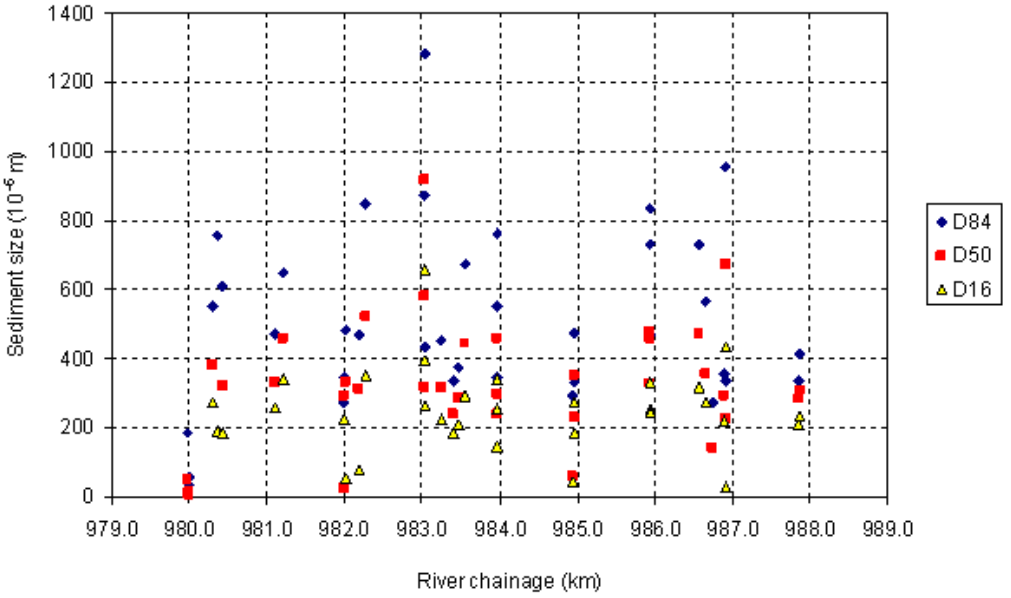

Figure A.2: Sediment distribution in the Dordsche Kil along the river axis.

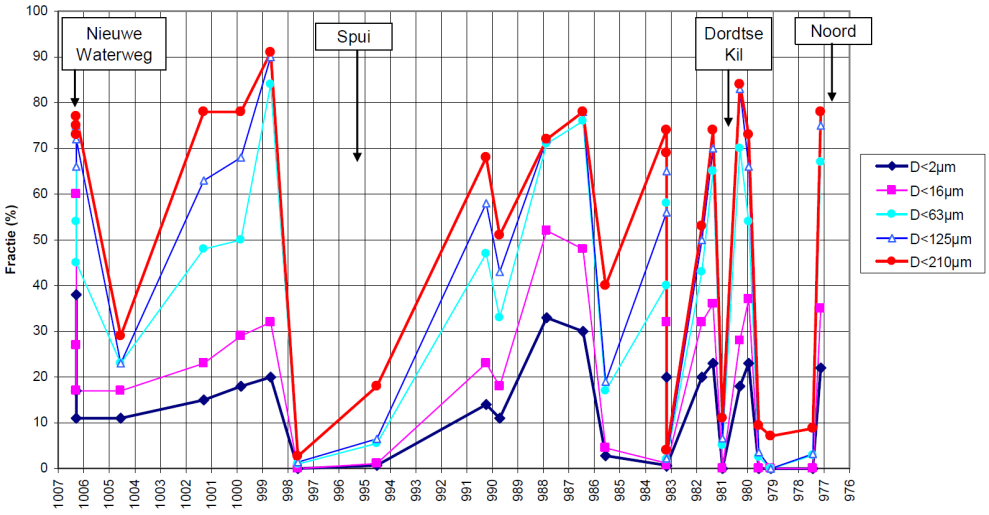

Figure A.3: Sediment distribution in the Dordsche Kil along the river axis.

A.3 Bed level development

Figure A.3 shows the development of the Oude Maas river for the past couple of years. The figure shows that bed level change is quite chaotic, forming a whimsical pattern over the years. Table 1.1 provides average data for bed level change, which is more useful for quantification, whereas this figure gives a better idea of the local behaviour of the river.

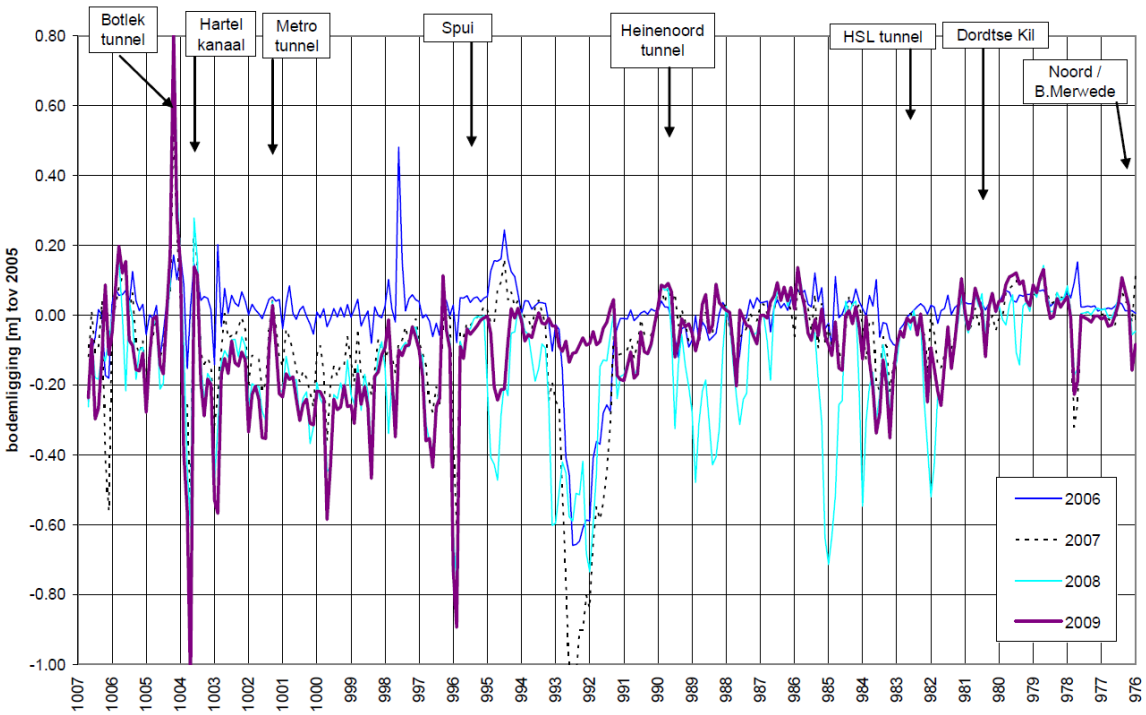

Figure A.4: Bed level development on the river axis of the Oude Maas from 2006-2009.

B Boundary conditions

B.1 Upstream boundaries

In this research, various boundary conditions have been used for the Delft3D model. All the boundary conditions have been extracted from the Sobek model.[10] The upstream boundaries in Delft3D are the same as the upstream boundary 'Tiel' in Sobek. Four different conditions have been applied in the model, which are shown in figure B.1. For the low, average and high discharge scenarios a constant discharge was used, whereas the extreme discharge scenario was modeled as a floodwave.

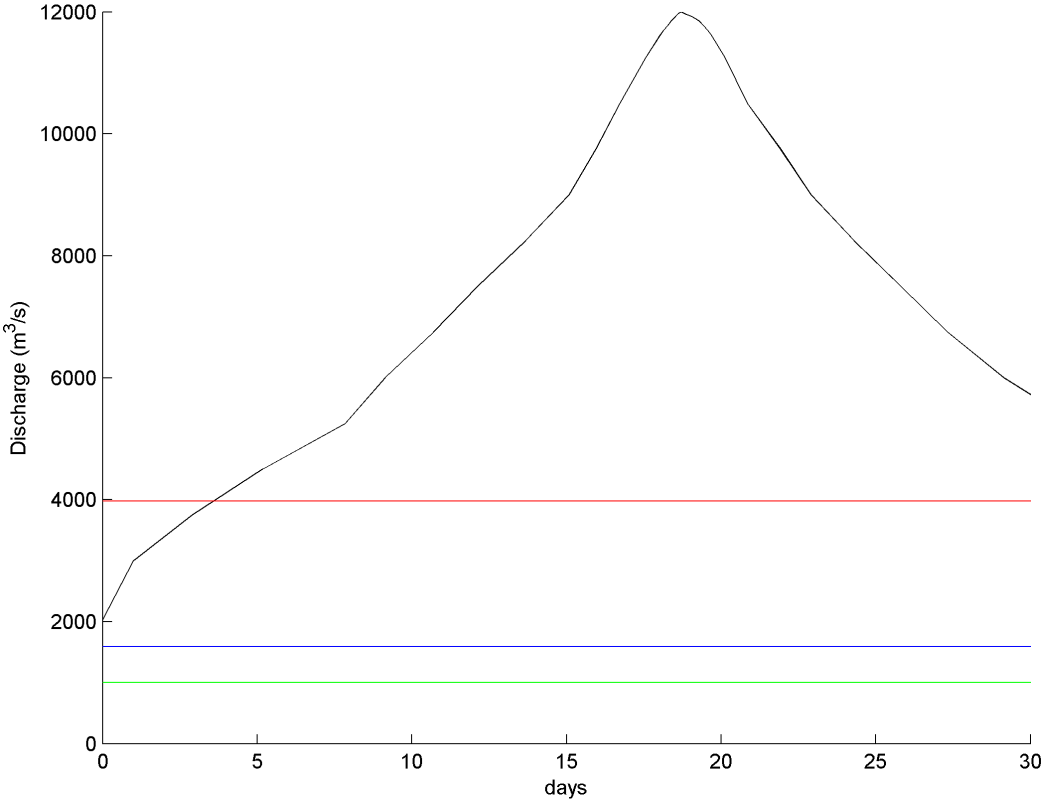

Figure B.1: Upstream boundary for the extreme situation, high discharge, average discharge and low discharge.

[10] More on this in section 3.2.1 and appendix D

B.2 Downstream boundaries for varying discharges

The downstream boundaries in the Delft3D model are extracted from the water level in the Sobek model on the corresponding locations. Different upstream conditions in the Sobek model result in different water levels at these locations so that the downstream boundary conditions in Delft3D are different for every flow scenario. Figure B.2 shows the downstream boundary conditions for the low, average and high discharge scenario on each of the three downstream boundaries and figure B.3 shows the downstream boundary condition for the extreme flood wave scenario as opposed to the average situation. A change the downstream Sobek boundary conditions also results in different downstream boundary conditions in the Delft3D model for the same reasons. Figure B.4 shows the diffence in boudary conditions for 1 meter sea level rise.

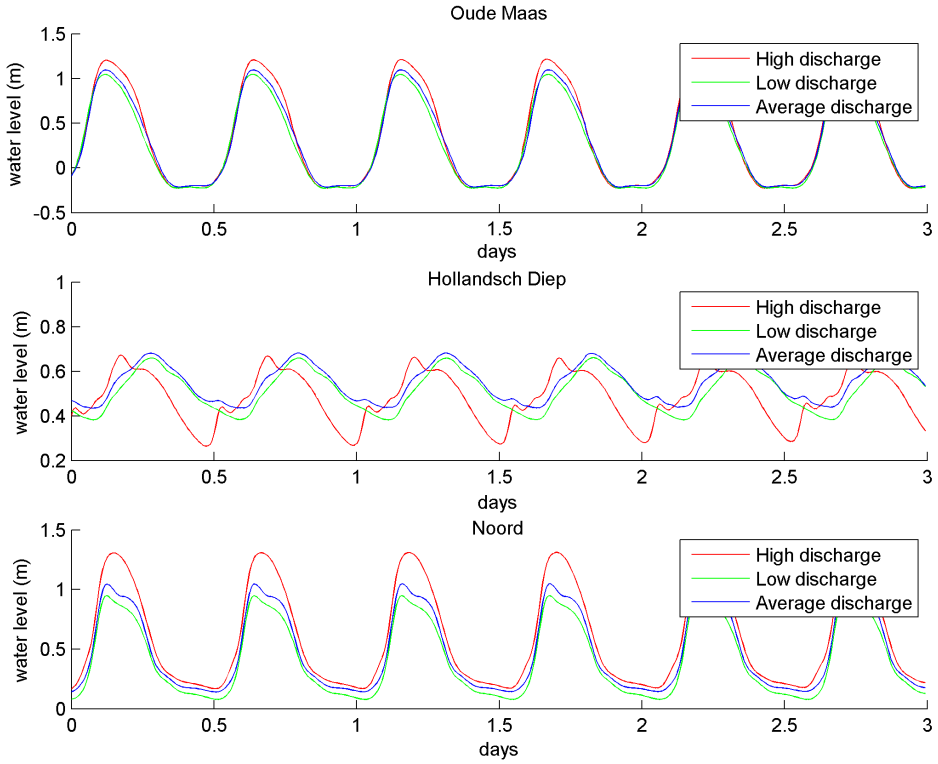

Figure B.2: Downstream boundary for the high discharge, average discharge and low discharge.

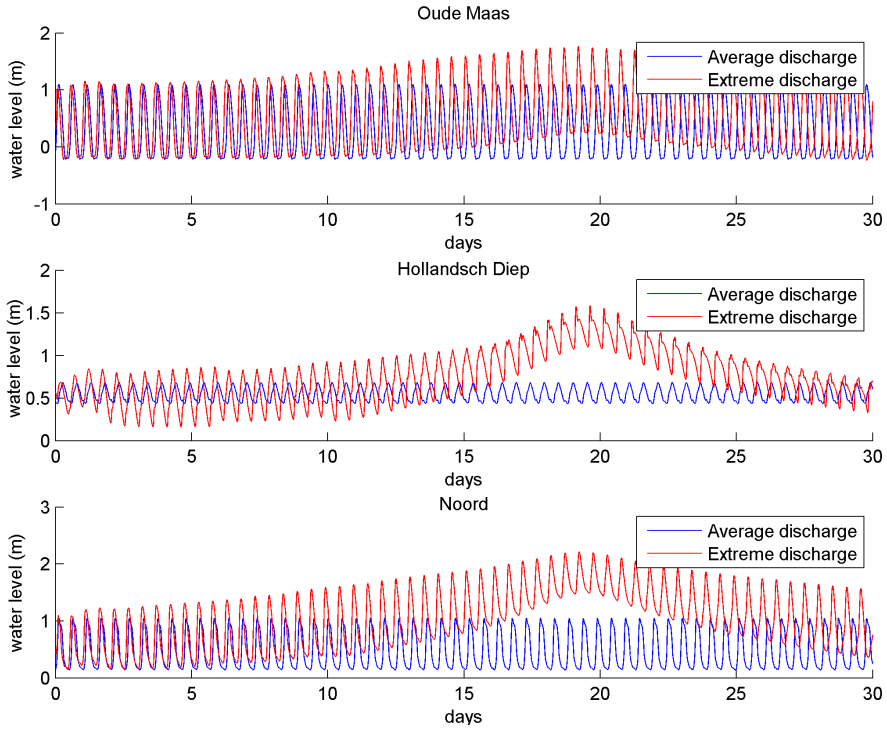

Figure B.3: Downstream boundary for the extreme situation and the average situation.

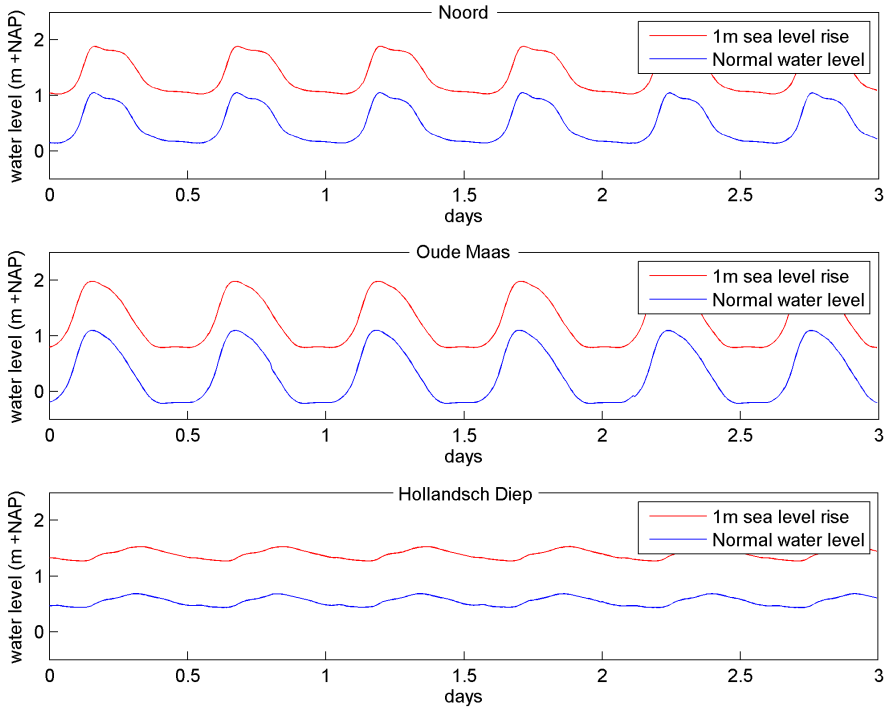

Figure B.4: Change in downstream boundary due to 1 meter sea level rise.

B.3 Downstream boundaries for different measures

As mentioned in the previous section, each different scenario in Sobek results in different boundary conditions in the Delft3D model. This also holds for some maintenance strategies. Figure B.5 and B.6 show the the boundary condtions for the situation with open Haringvliet gates (with and without the condition of sea level rise) and the situation where the Spui branch is closed off from the North East, compared to the normal situation.

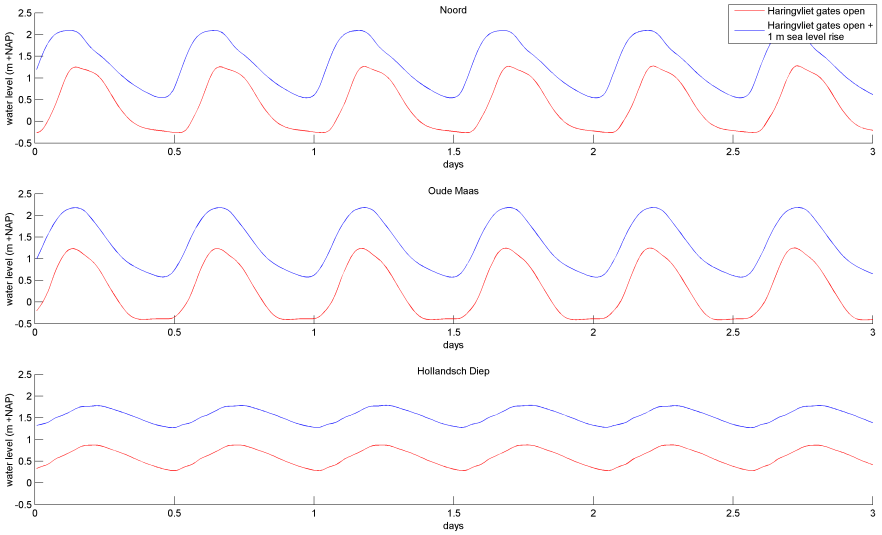

Figure B.5: Boundary conditions for opened Haringvliet gates.

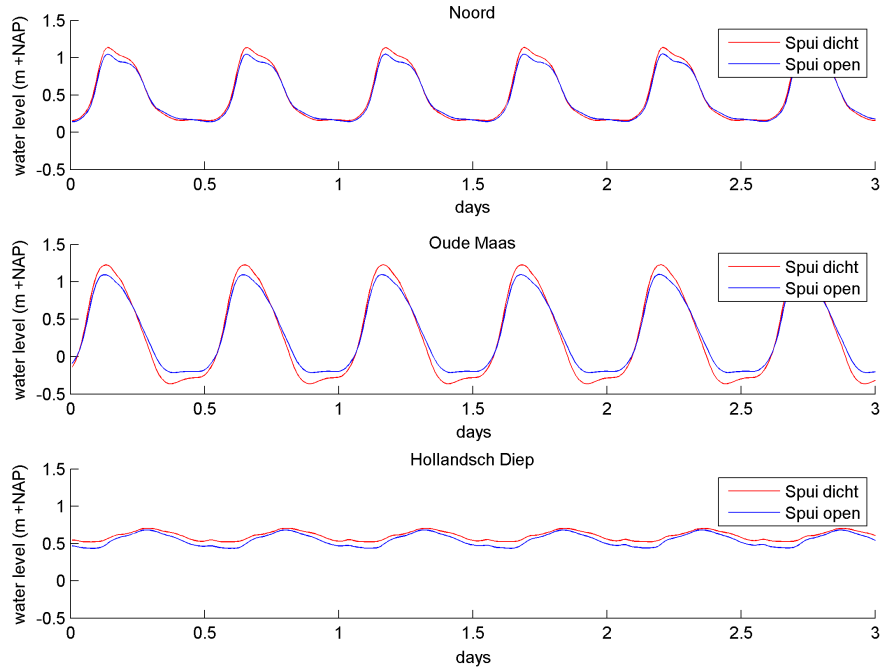

Figure B.6: Boundary conditions for a closed off Spui rive.r

C Delft3D Schematizations

C.1 Flow computations

C.1.1 Introduction

The Delft3D software package is a process based numerical model, which is under constant development adding new and improved capabilities of the software. Delft3D can predict the flow for rivers, coastal areas, estuaries, shallow seas and lakes in two-dimensional (i.e. depth averaged) or three-dimensional unsteady flow and transport phenomena. Starting point is computing the hydrodynamics, this is because every problem in river engineering concerns flows. For this study, a two-dimensional, depth-averaged approach is used. The RGFGRID module is used for creating a curvilinear orthogonal computational grid. QUICKIN is a component which appoints the bottom topography to this computational grid.

The modelling systems are based on a few assumptions. The relevant main assumptions and approximations for this study are that the flow is assumed to be incompressible and that the horizontal time and length scales are much larger than the vertical scales. In the vertical momentum equations, the vertical accelerations are now neglected, which leads to the hydrostatic pressure equation. A detailed list of assumptions and simplification are provided in the Delft3D-FLOW User Manual (Deltares, 2010).

C.1.2 Equations

The computations in Delft3D are based on the St. Venant equations described in section 3.3 (equations 3.1, 3.2 and 3.3). In these equations the density differences, the wind and the compressibility of the fluid are neglected. For 2−dimensional flow, the continuity equation and the momentum equation in x- and y-direction become:

$$\frac{\partial \zeta}{\partial t} + \frac{\partial [HU]}{\partial x} + \frac{\partial [HV]}{\partial y} = 0 \tag{C.1}$$

$$\frac{\partial U}{\partial t} + U\frac{\partial U}{\partial x} + V\frac{\partial U}{\partial y} = fV + \nu_H \left[\frac{\partial^2 U}{\partial x^2} + \frac{\partial^2 U}{\partial y^2}\right] - \frac{gU\sqrt{U^2+V^2}}{hC^2} \tag{C.2}$$

$$\frac{\partial V}{\partial t} + U\frac{\partial V}{\partial x} + V\frac{\partial V}{\partial y} = fU + \nu_H \left[\frac{\partial^2 V}{\partial x^2} + \frac{\partial^2 V}{\partial y^2}\right] - \frac{gV\sqrt{U^2+V^2}}{hC^2} \tag{C.3}$$

With:

h = Water level according to reference level
H = Total water depth
U = Depth-averaged velocity in x direction
V = Depth-averaged velocity in y direction
g = Gravitational acceleration
f = Coriolis parameter
ν_H = Horizontal eddy viscosity
C = Chézy coefficient

C.1.3 Numerical aspects

Delft3D is a numerical model based on finite differences. Therefore the shallow water equations have to be discretized. The shallow water equations are discretized via the staggered grid approach, where the water level points are defined in the cell centres and the velocity components perpendicular on the middle of the grid cell faces. An alternating direction implicit (ADI) method is used to solve the continuity and horizontal momentum equations. With the ADI method one time step is split into two stages in which all terms of the equations are solved with (at least) second-order accuracy in space. This method is denoted as the cyclic method, which is computationally efficient.

C.1.4 Grid

Delft3D is a numerical model based on finite differences, therefore the shallow water equations have to be discretized. The shallow water equations are discretized via the staggered grid approach. In a staggered grid not all parameters are defined at the same location in the numerical grid. The water level points are defined in the cell centre and the velocity components at the cell faces. It is important to understand the numbering of a staggered grid and the definition of a computational control volume. Figure C.1 shows the grid numbering and an example of a computational control volume.

This grid must fulfill several criteria, namely:

- The grid must fit the land-water boundaries of the area as close as possible, in order to exclude dry cells.
- The grid must be orthogonal, which means that the grid lines should intersect perpendicularly. By making the grid orthogonal, computational expensive transformations terms are left out. A measure for the orthogonality is the cosine of the angle between the grid lines. The cosine has to be smaller than 0.02.
- The grid spacing must be smooth in order to minimize inaccuracy errors in the finite difference operators. A measure for the grid smoothness is the aspect ratio of the grid

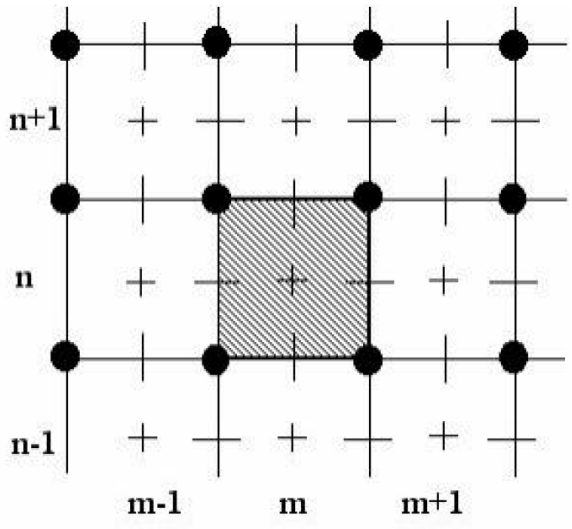

Figure C.1: Staggered grid with computational control volume.

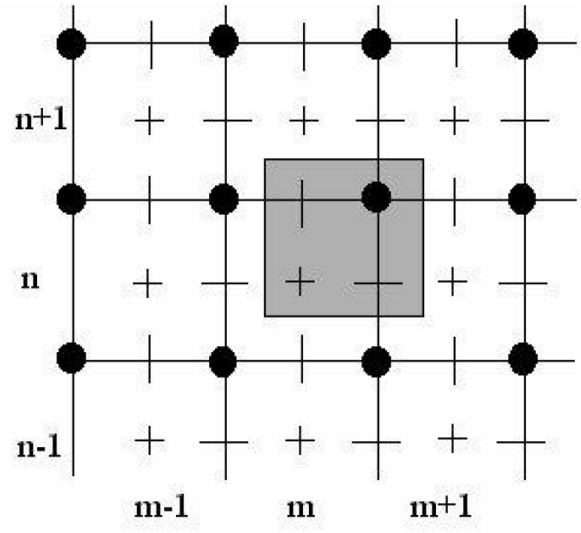

Figure C.2: Grid cell in the staggered grid.

cells [range 1 to 2] and the ratio of neighbouring grid cell dimensions, which should be less than 1.2 in the area of interest up to 1.4 far away.

An advantage of the staggered grid approach is that boundary conditions can be implemented on the grid in a rather simple way. Boundaries are defined on different locations, closed boundaries are defined through u- or v points, as are velocities, but water levels are defined at water level points (+ points). In Figure B.2 it is shown that the velocity points are on the closed boundary whereas the water level points for the boundary are defined outside the grid.

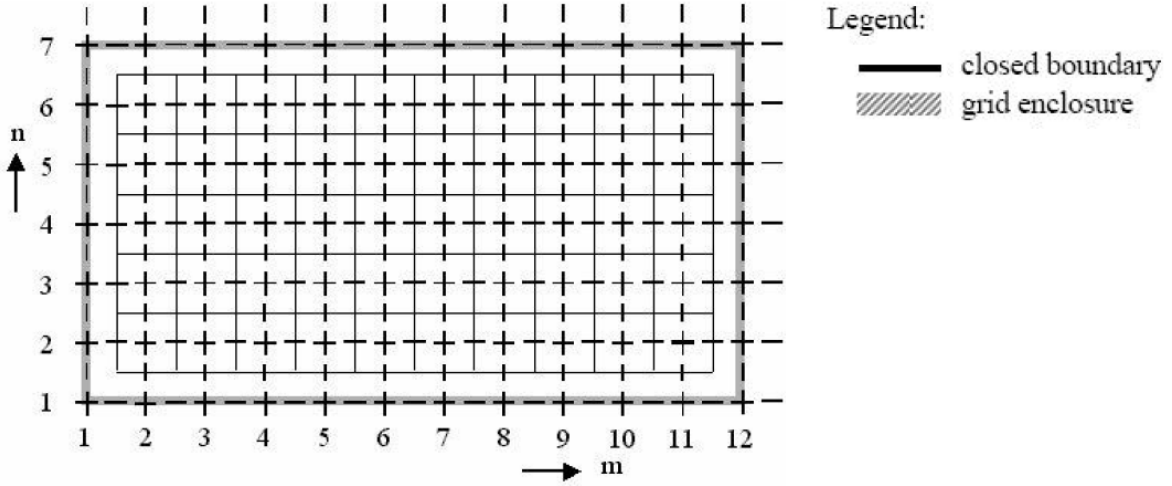

Figure C.3: Grid with grid enclosure and boundary location.

C.1.5 Domain and boundaries

In Delft3D, one can define the open boundaries, their location, type and all input data related to driving the simulation. At an open boundary the flow and transport boundary conditions are required. A conventional Delft3D model with only one domain has at least one upstream boundary containing a discharge boundary condition and at least one downstream boundary containing with a boundary condition that is water level forced. In this case, the model consists of multiple (5) domains. The model only contains a discharge forced boundary condition in domain 1 and 3 water level forced downstream boundary conditions in domain 5. The boundaries that provide the borders of the different domains describe themselves as domains decomposition boundaries.

Domain decomposition is a technique in which a model is divided into several smaller model domains. The subdivision is based on the horizontal and vertical model resolution required for adequately simulating physical processes. Then, the computations can be carried out separately on these domains. The communication between the domains takes place along internal boundaries, or so-called DD-boundaries. If these computations are carried out concurrently, we speak of parallel computing. Parallel computing will reduce the turn around time of multiple domain simulations.

The main motivation of decomposed boundaries is increasing the modelling flexibility of the system rather than focussing on increasing the effciency of the system by using many processors.The most well known example is the use of local grid refinement (see Figure C.2) and the use of domains with different dimensions. This is illustrated in Figure B.23, in which a 3D model is coupled to a 2DV (two-dimensional vertical), a 2DH (two-dimensional horizontal) and a 1D (one-dimensional) model. Less well known, but also quite important is the increased fexibility when modelling complex geometries. In practice, the model area can be quite complex due to, for example, irregular land boundaries and the existence of (a lot of) islands. This is also the case for the model used in this research, where there is a bifurcation and a interconnection (the Dordtsche Kil).

C.2 Morphology

C.2.1 Sediment fractions

The total sediment transport in Delft3D is determined by the sum of the sediment transport of multiple sediment fractions consisting of cohesive and non-cohesive sediments. Each sediment fraction must be classified as 'mud' (cohesive suspended load transport), 'sand' (non-cohesive bed-load and suspended load transport) or 'bed load' (non-cohesive bed load only).

C.2.2 Sedimentation and erosion

Regarding implementation of sedimentation and erosion in Delft3D, a distinction has been made between cohesive and non-cohesive sediment fractions. For cohesive sediment fractions the fluxes between the water phase and the bed are calculated with the Partheniades-Krone formulations, which are already described extensively in section 4.2.1. Non-cohesive sediment fractions are computed in a different way. The transfer of sediment between the bed and the flow is modelled using sink and source terms acting on the near-bottom layer that is entirely above Van Rijn's reference height a. Each half time-step the source and sink terms model the quantity of sediment entering the flow due to upward diffusion from the reference level and the quantity of sediment dropping out of the flow due to sediment settling. This process of sedimentation and erosion is shown in figure C.4. For more on the calculation of erosion and deposition fluxes for non-cohesive sediments is referred to the Delft3D-FLOW manual (Deltares, 2010).

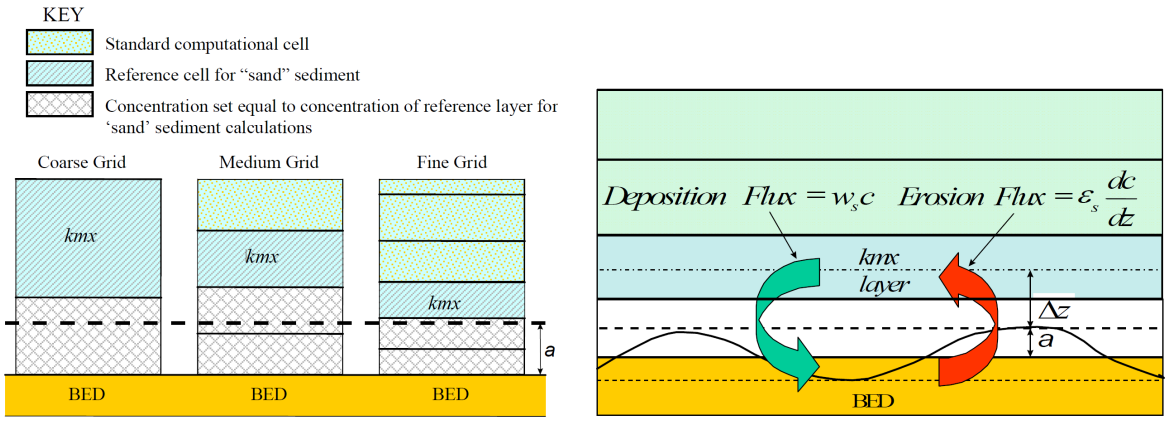

Figure C.4: Selection of the reference (kmx)layer (left) and schematic arrangement of flux bottom boundary condition (right).

C.2.3 Sediment transport formulas

The report describes three sediment transport formulas that have been used in this study for calibration. These formulas are described in this subsection.

Van Rijn (1993)
Van Rijn (1993) is the default transport formulation in Delft3D, and distinguishes between sediment transport below the reference height a which is treated as bed-load transport and that above the reference height which is treated as suspended-load.The total load is then calculated using:

$$S = S_b + S_s \tag{C.4}$$

The bed load transport formulation reads as follows:

$$S_b = \frac{1}{1-\epsilon_p} 0.005 U h M_e^{2.4} \frac{D_{50}}{h} \tag{C.5}$$

The suspended load transport formulation reads as follows:

$$S_s = \frac{1}{1-\epsilon_p} 0.012 U h M_e^{2.4} \frac{D_{50}}{h} D_*^{-0.6} \tag{C.6}$$

with:

$$D_* = D_{50} \left(\frac{\Delta g}{\nu^2} \right)^{\frac{1}{3}} \tag{C.7}$$

$$M_e = \frac{|U| - U_{cr}}{\sqrt{\Delta g D_{50}}} \qquad \text{if } |U| > U_{cr} \text{ , otherwise } M_e = 0 \tag{C.8}$$

ϵ_p = Porosity of the bed material
h = Water depth
U = Averaged flow velocity
U_{cr} = Averaged critical flow velocity
g = Gravitational acceleration
D_{50} = Median particle diameter
ν = Kinematic viscosity of water

If 100 µm $\leq D_{50} \leq$ 500 µm:

$$U_{cr} = 0.19 D_{50}^{0.1} \log \left(\frac{12h}{3D_{90}} \right) \tag{C.9}$$

If 500 µm $\leq D_{50} \leq$ 2 mm:

$$U_{cr} = 8.50 D_{50}^{0.6} \log \left(\frac{12h}{3D_{90}} \right) \tag{C.10}$$

In which,

D_{90} = Particle diameter such that 90% of the sample is finer

Van Rijn (2007)
In the preliminary study by Giri (2010), the Van Rijn (2007) transport formula has been used. Van Rijn (2007a,b) had been formulated to improve the influence of wind waves on sediment transport, and the presence of mud is also taken into account in this formulation. Just as in the Van Rijn 1993 formula, a distinction is drawn between bed transport and suspended transport:

$$S = S_b + S_s \tag{C.11}$$

The bed load transport formulation reads as follows:

$$S_b = \gamma \rho_s f_{silt} d_{50} D_*^{-0.3} \left(\frac{\tau_b'}{\rho} \right)^{0.5} T^{\eta} \tag{C.12}$$

with:

$$\tau_b' = 0.5 \rho_s f_c' U_\delta^2 \tag{C.13}$$

$$f_c' = 8g \left(18 log \left(\frac{12h}{k_s} \right) \right)^{-2} \tag{C.14}$$

$$D_* = d_{50} \left(\frac{(s-1)g}{v^2} \right)^{\frac{1}{3}} \tag{C.15}$$

$$T = \frac{\tau_b' - \tau_{b,cr}}{\tau_{b,cr}} \tag{C.16}$$

in which:

τ_b' = instantaneous grain-related bed-shear stress;
f_c' = grain friction coefficient due to current;
U_δ = instantaneous current velocity;
$\tau_{b,cr}$ = critical shear stress;
D_* = dimensionless particle size
f_{silt} = silt factor = d_{sand}/d_{50} ($f_{silt} = 1$ for $d_{50} > d_{sand}$)
γ = calibration coefficient (= 0.5)
η = exponent (= 1, calibrated value)

As mentioned above, an important new feature in the Van Rijn (2007) formula is the effect of the mud fraction on the critical shear stress of the sand particle that reads as follows, which should play a significant role in this system (Van Rijn, 2007a):

$$\tau_{b,cr} = (1 + p_{mud})^3 \, \tau_{b,cr,0} \tag{C.17}$$

in which, $\tau_{b,cr,0o}$ = critical bed shear stress for pure sand; p_{mud} = fraction of mud (≤ 0.3). In this formulation, however, the mud fraction does not interact with the bed, and only affects the mobility of sand. The suspended load can be calculated by:

$$S = Fuhc_a \tag{C.18}$$

in which,

u = depth average flow velocity;
h = water depth
F = integration factor;
c_a = sediment concentration at reference level a measured from the bottom

For the concentration c_a (excluding the pores), the following applies (Van Rijn, 2007b),:

$$c_a = 0.0015 \frac{D_{50}}{a} \frac{T^{1.5}}{D_*^{0.3}} \tag{C.19}$$

Engelund Hansen
A frequently used sediment transport relation that is being considered as an alternative for this model is the Engelund-Hansen formula (1967). The formula of Engelund and Hansen (1967) concerns the total load, and reads:

$$S = S_b + S_{s;eq} = \frac{0.05\alpha u^5}{\sqrt{q}\, C^3 \Delta^2 D_{50}} \tag{C.20}$$

In which:

u = depth average flow velocity;
Δ = water depth
C = Chézy
α = Calibration coefficient (O(1))

C.2.4 Morphological time scale factor

One of the complications inherent in carrying out morphological projections on the basis of hydrodynamic flows is that morphological developments take place on a time scale several times longer than typical flow changes (for example, tidal flows change significantly in a period of hours, whereas the morphology of a coastline will usually take weeks, months, or years to change significantly). One technique for approaching this problem is to use a 'morphological time scale factor' whereby the speed of the changes in the morphology is scaled up to a rate that it begins to have a significant impact on the hydrodynamic flows. This can be achieved by specifying a non-unity value for the variable MorFac in the morphology input file.

The implementation of the morphological time scale factor is achieved by simply multiplying

the erosion and deposition fluxes from the bed to the flow and vice-versa by the MorFac-factor, at each computational time-step. This allows accelerated bed-level changes to be incorporated dynamically into the hydrodynamic flow calculations (figure C.5).

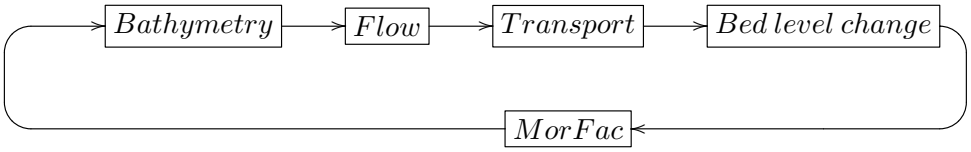

Figure C.5: Schematic representation of the implementation of the morphological factor in the Delft3D flow computations.

D SOBEK

D.1 SOBEK-RE

SOBEK-RE (Rivers and estuaries) is a one-dimensional open-channel dynamic numerical modelling system, capable of solving the equations that describe unsteady water flow, salt intrusion, sediment transport, morphology and water quality. For this research, the SOBEK model is used for the sole purpose of hydrodynamic modeling. The flow in the SOBEK model is described by the St. Venants equations[11]. Besides the limitations with respect to the 2D and 3D processes, SOBEK-RE cannot compute supercritical flow either so that the following restriction applies:

$$Fr = \frac{u}{\sqrt{gh}} < 1 \tag{D.1}$$

The topographic basis of each SOBEK model is the network of branches. Branches are connected to each other in nodes, forming the total domain of the model. Special nodes are the ones with only one connecting branch, located at the boundaries of the model. At those boundaries, boundary conditions must be specified. A SOBEK model can also contain contain structures, of which different types are available. In this model the structure representing the Haringvliet sluices is essential for the flow in the area of interest. The following sections elaborate on these three features - the domain (D.2), the boundaries (D.3) and the structures (D.4) - of the Rhine-Meuse delta SOBEK model.

[11] These are the same equations on which Delft3D bases its flow computations, equation 3.1, 3.2 and 3.3

D.2 Domain

Figure **??** shows the complete netwerk of branches and nodes in model forming the domain of the Rhine-Meuse delta SOBEK model. This model covers the Rhine-Meuse for the whole Western part of the Netherlands, with three boundaries at the coast (two at the Haringvliet and 1 at the Nieuwe Waterweg) and three upstream boundaries, in the river Lek, Meuse and Waal. In figure 3.1 in section 3.2.1 these boundaries are also indicated.

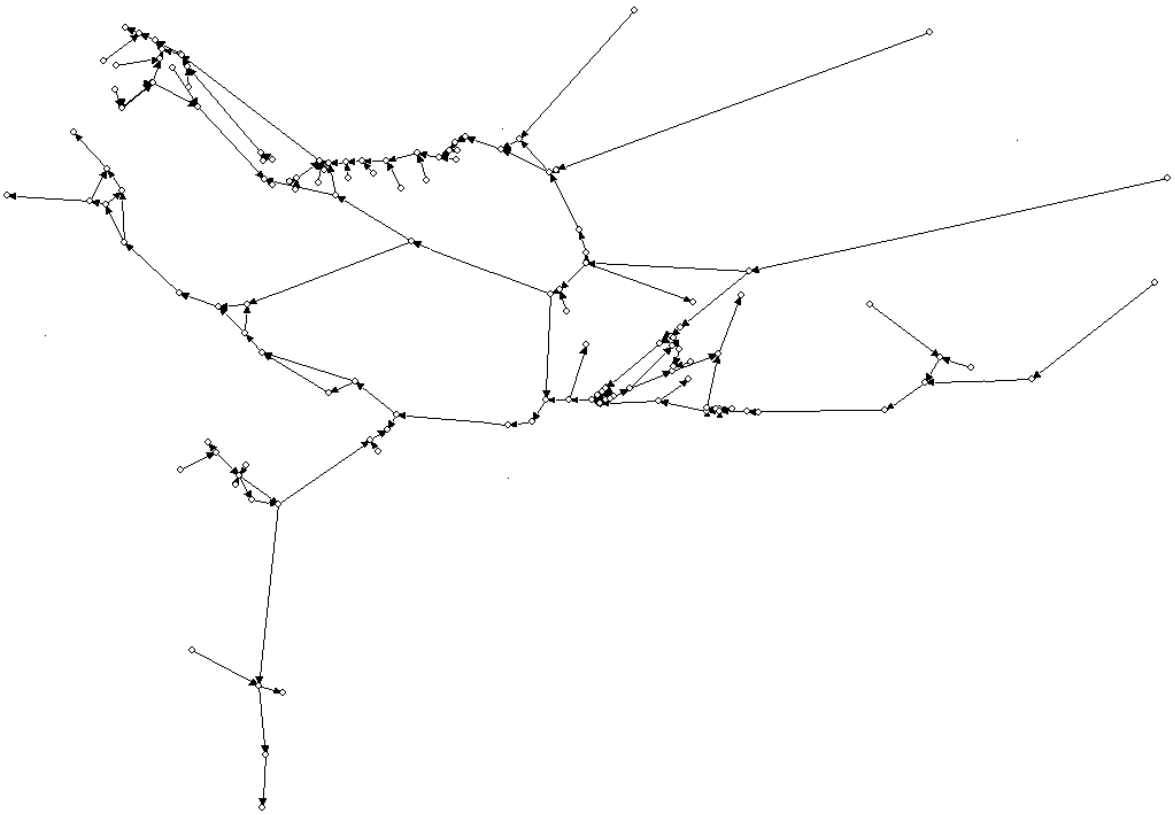

Figure D.1: Domain of the Rhine-Meuse delta SOBEK model.

D.3 Boundaries

Figure D.2 and D.3 show the upstream and downstream boundaries of the Sobek model. The boundary 'Tiel' in the river Waal is also the upstream boundary for the Delft3D model. In the scenario of sea level rise, one meter is added two both tidal time series.

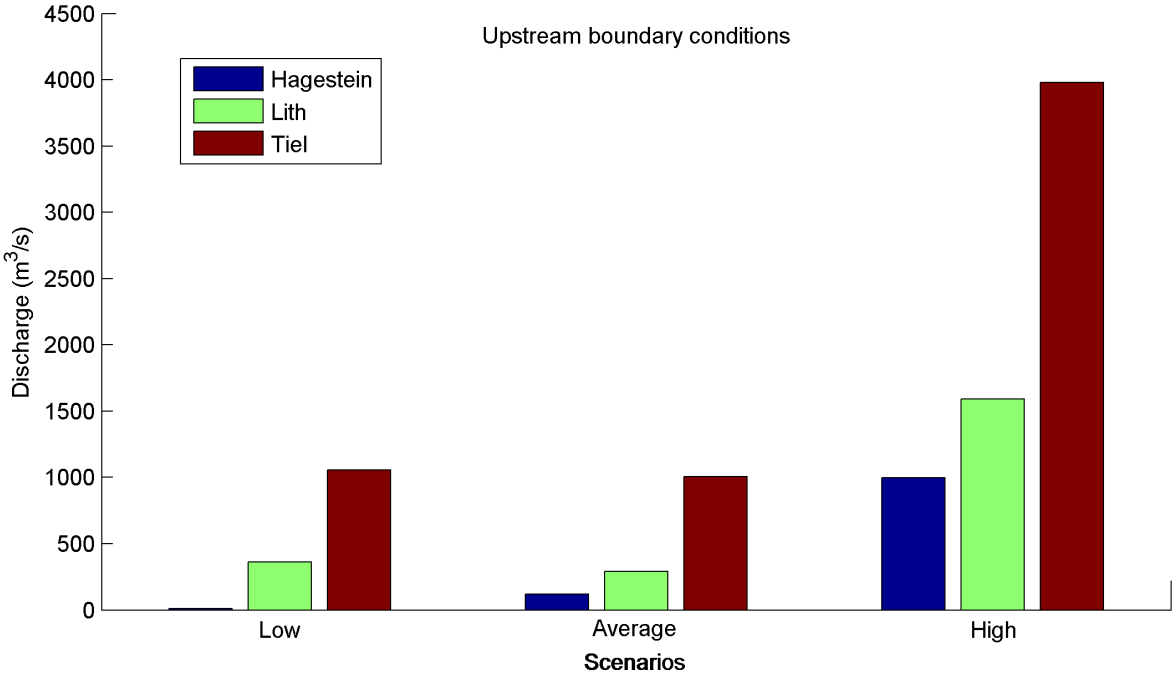

Figure D.2: Upstream discharges in the SOBEK model for the low, average and high discharge scenario.

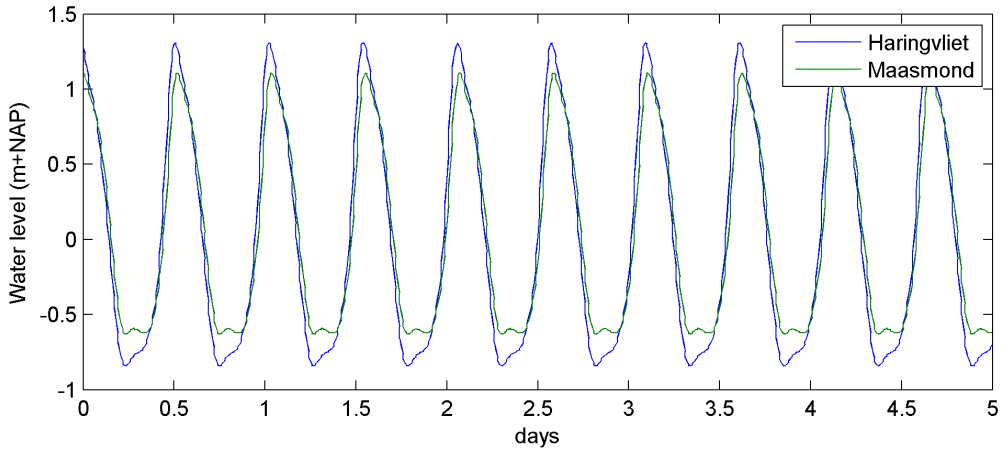

Figure D.3: Upstream discharges in the SOBEK model for the Haringvliet and the Nieuwe Waterweg boundary.

D.4 Structures

The Haringvliet gates, amongst other structures, are implemented in the SOBEK model as a structure. The Haringvliet structure is adjusted by a controller, which can be activated or de-activated by a trigger. For the Haringvliet, this particular trigger (a hydraulic trigger) is based on the head difference at a hydraulic structure: The gates are open when the water level on the inside is higher than the water level at sea and closed otherwise. In the model, this head difference is calculated each time step. For the case where the Haringvliet gates are always open, this trigger is simply left out of the model.